# CHAPTER FIVE

# *RESULTS ANDDISCUSSION*

## 5.1. Effect of aqueous surfactant solution on pool boiling data

In the present study, aqueous surfactant solutions of SDS, SLES and Triton X-100having different concentrations (measured as the wppm additive content) are prepared by dissolving weighed samples in distilled water. These solutions are used as the boiling fluids. The concentrations of the test surfactant solutions are 200, 500, 1000 and 1500 ppm.

The boiling data for pure distilled water is first established, to provide the baseline reference for the surfactant solution results are shown in Figure 5.1

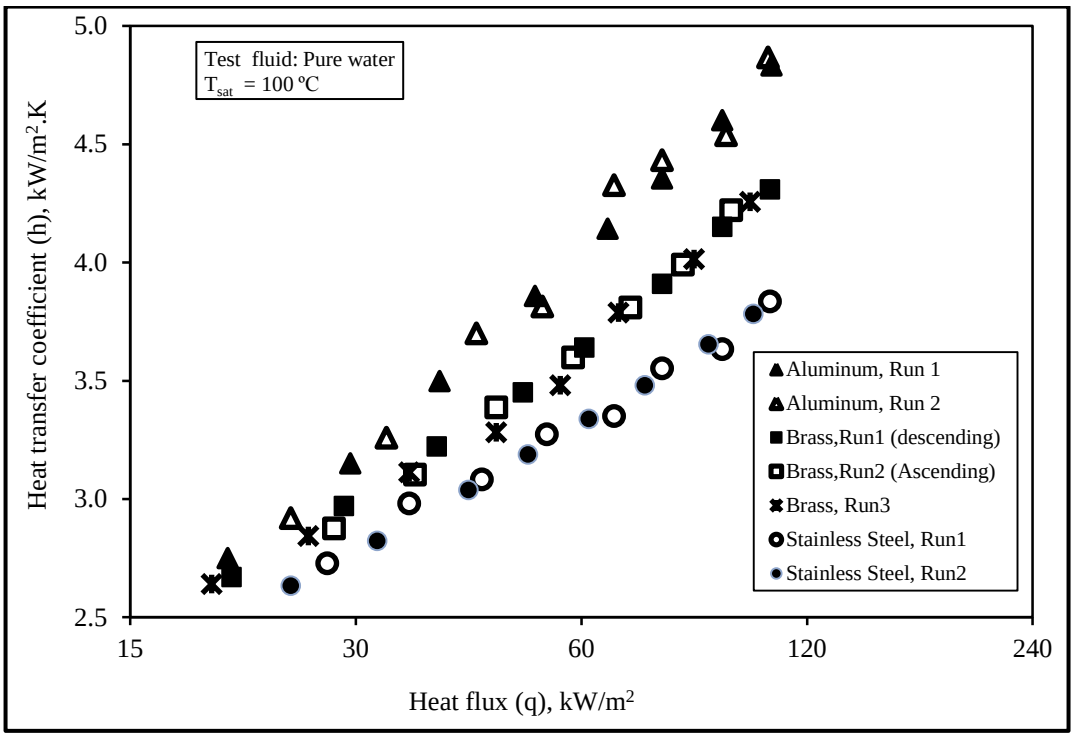


**Fig. 5.1: Variation of h with q for pure distilled water using brass, aluminum and stainless steel test tube**

Figures 5.2 and 5.3 show the comparative results of the variation of h with q using pure water, and different concentrations of aqueous surfactants solutions (SDS, SLES and Triton X-100). The comparison is made for the three test tubes S1, S2 and S3. It is realized that any increase in q causes a corresponding increase in h. This is attributed to the agitation effect resulted from the mobility of the vapor bubbles emitted form the tube wall nucleation sites, and then travel through the liquid pool. The increase in q activates greater number of nucleation sites.

It should also be noticed that for any level of q, increasing the concentration of aqueous surfactant solution causes appreciable increase in h. An explanation for observed enhancement in h could be given by considering the role of dynamic surface tension, and subsequent modification of bubble dynamics.

With the nucleation of a vapor bubble and during its subsequent growth, diffusion of surfactant molecules, and their adsorption / description rates at the interface govern the extent of dynamic surface tension. The dynamic surface tension is appreciably lower than solvent's surface tension, which helps promote large number of active nucleation sites. Lower values of dynamic surface tension also allow departure of smaller- sized bubbles because of the reduction in surface tension force at the heated tube wall that counters the bouncy force trying to pull the bubble away from the tube wall. The bubble growth time will consequently expect to be reduced, and lead to an increase in bubble departure frequency. Also, it is indicated that results for test tubes S1, S2 and S3 have the same trend with different slopes and absolute values.

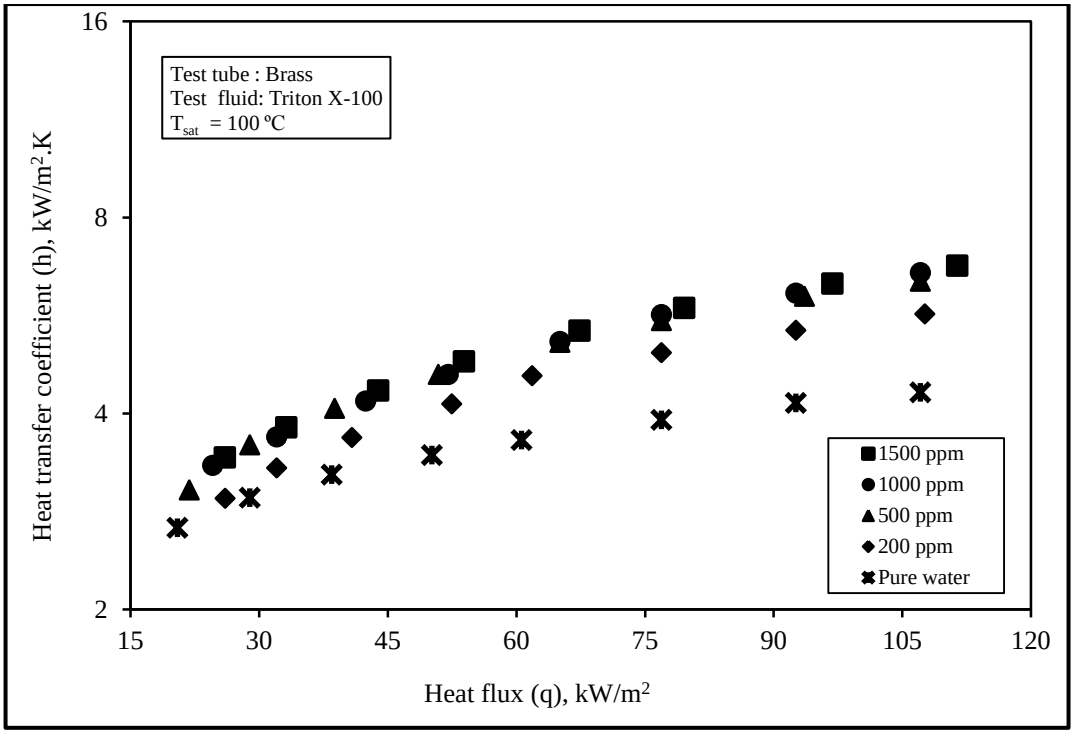


**Fig. 5.2a: Variation of h with q for different Triton X-100 concentrations using brass test tube**

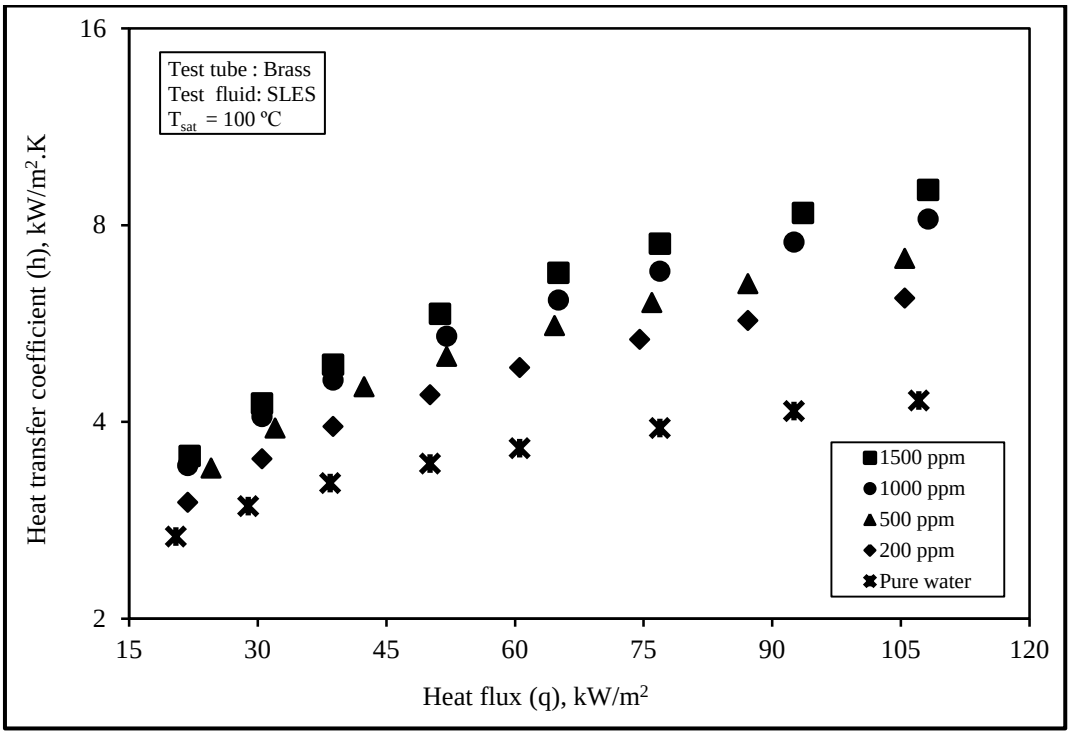


**Fig. 5.2b: Variation of h with q for different SLES concentrations using brass test tube**

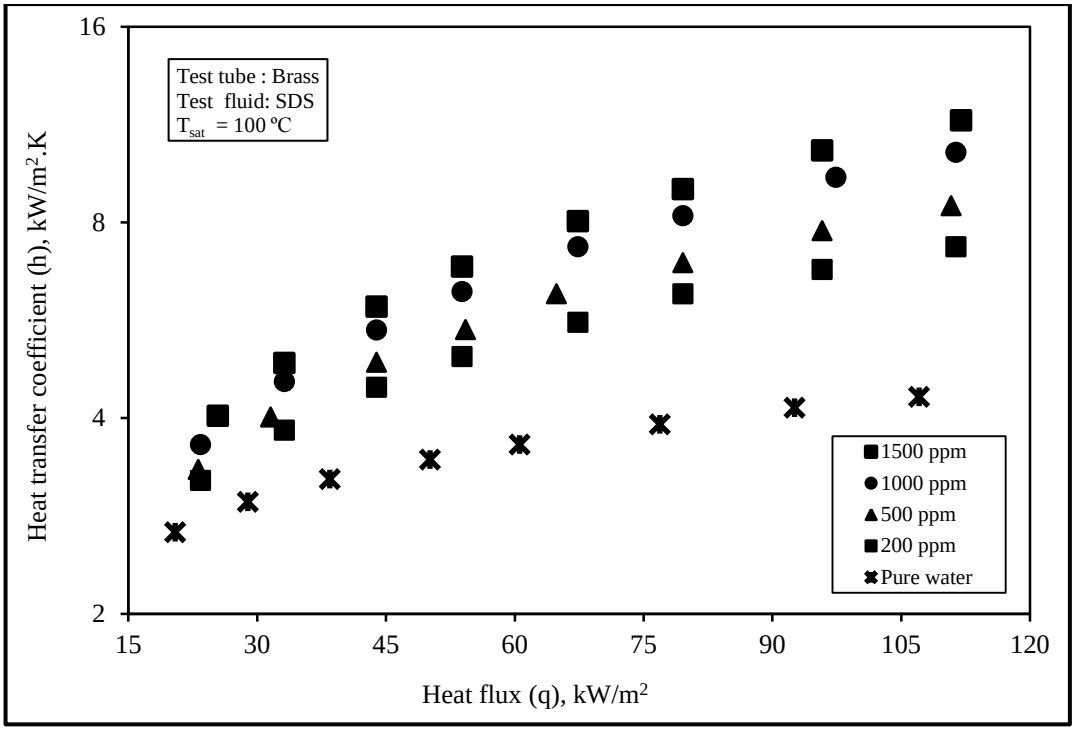


**Fig. 5.2c: Variation of h with q for different SDS concentrations using brass test tube**

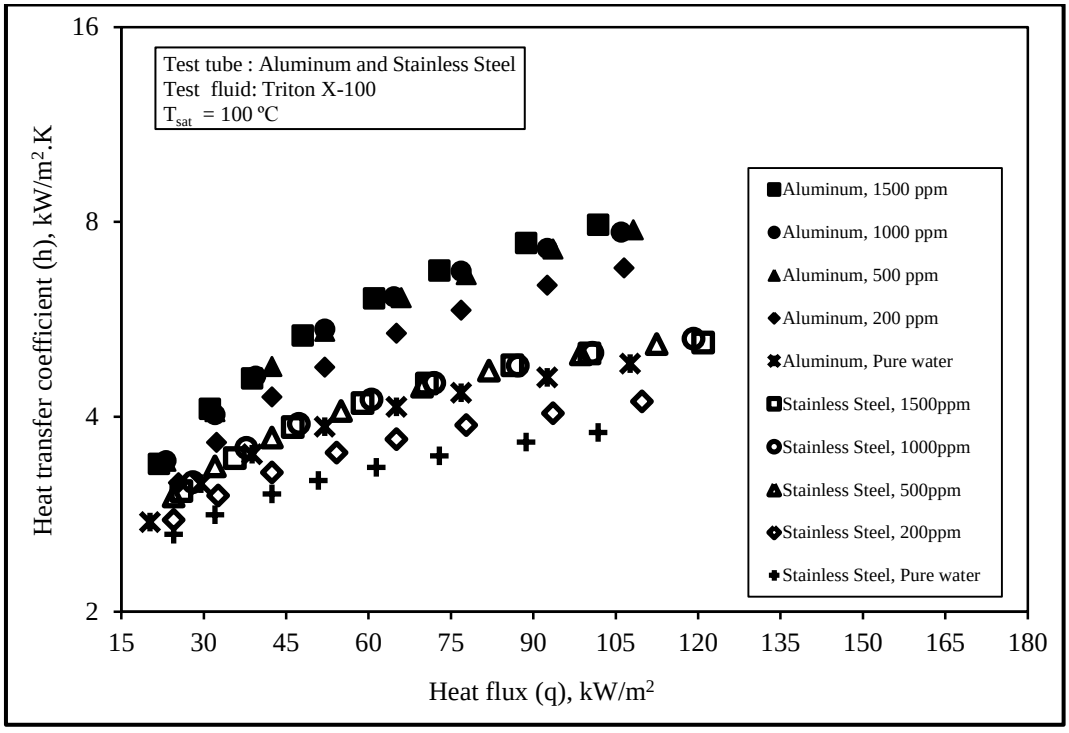


**Fig. 5.3a: Variation of h with q for different Triton X-100 concentrations using aluminum and stainless steel tubes**

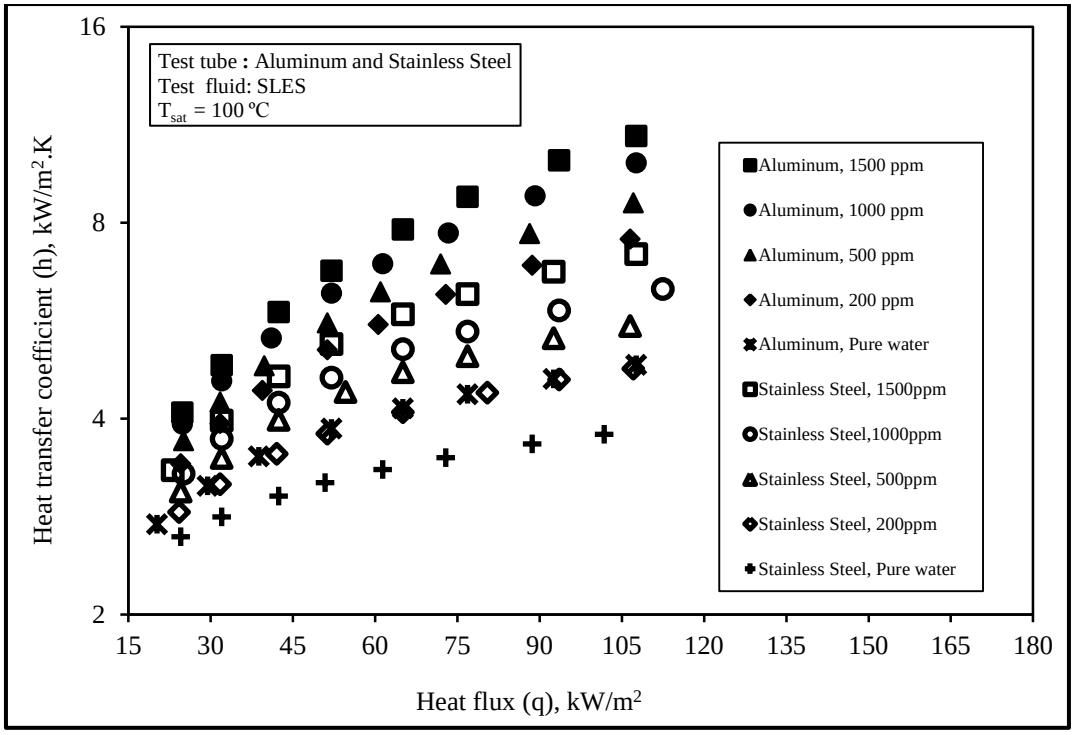


**Fig.5.3b: Variation of h with q for different SLES concentrations using aluminum and stainless steel tubes**

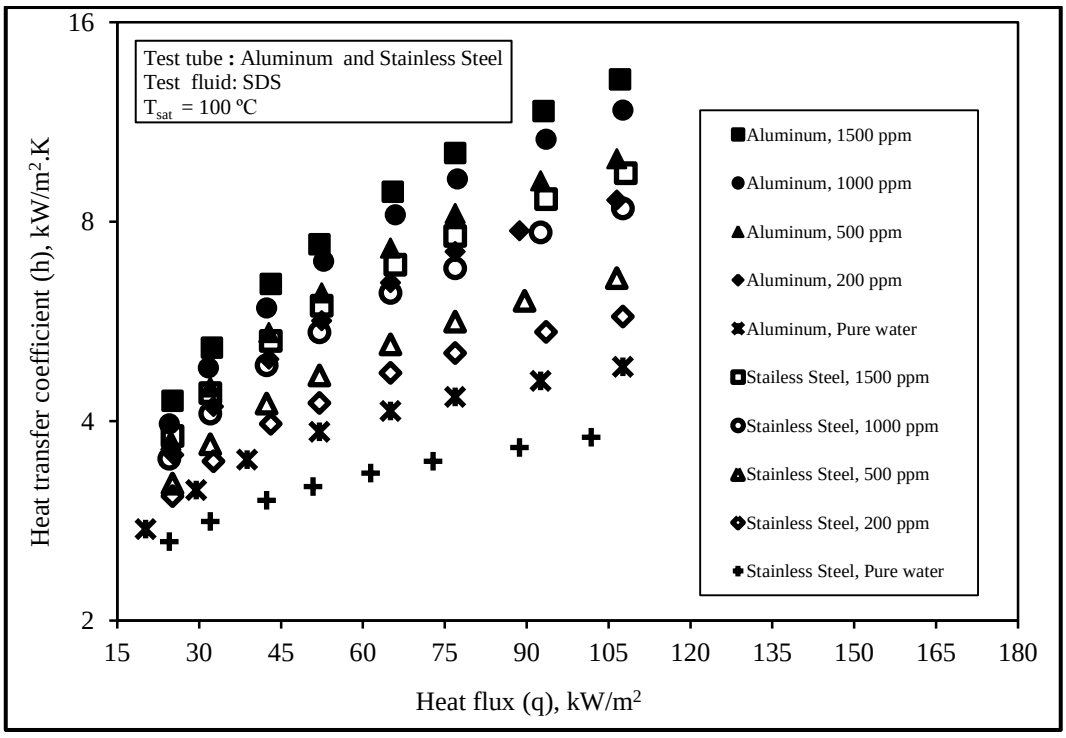


**Fig. 5.3c: Variation of h with q for different SDS concentrations using aluminum and stainless steel tubes**

The most surprising result is that there is no enhancement in h for any level of q when using aqueous Triton X-100 solutions with concentrations more than 500 ppm. This is true for the three test tubes. This is related to the fact that the variation of surface tension with concentration for Triton X-100 is constant above solution concentration of 500 ppm as shown in Figure 4.10.

To further explore, Figures 5.4 and 5.5 indicate the variation of h with q for specific concentration of aqueous surfactant solutions. A comparison is made for the results of SDS, SLES and Triton X-100 with pure water. It is realized that for a given q, and with any concentration of the aqueous surfactant solution, h is higher than that of pure water. This is due to the reduction in the dynamic surface tension associated with the aqueous surfactant solutions. This surface tension depression leads to promote the nucleation process, and the concomitant bubble dynamics. It should be also noted that for equal q and at any aqueous solution concentration, the surfactant SDS introduces the highest h, followed by SLES and then Triton X-100. This is believed to be due to the higher surface tension depression caused by SDS in its aqueous solutions which enhances the nucleation characteristics to greater extent rather than SLES and Triton X-100 aqueous solutions, in addition to the ionic nature of each surfactant, and its chemistry.

Figures 5.6 and 5.7 show the variation of the heat transfer coefficient, h with the concentration, C for specific constant wall heat flux of aqueous surfactant solutions. It can be seen that for a given wall heat flux, q, increasing the concentration of surfactant in its aqueous solution, increases the heat transfer coefficient. This is true for all test

tubes. It is also observed that for a given surfactant aqueous solution concentration and a given test tube, increasing wall heat flux q; increases the heat transfer coefficient, h.

Figures 5.8 and 5.9 show the variation of the heat transfer coefficient, h with aqueous surfactant solutions concentration at constant wall heat flux, q. A comparison is made between the results of SDS, SLES and Triton X-100 aqueous surfactant solutions. It is indicated that the boiling heat transfer characteristics of SDS is superior to that of SLES and Triton X-100 for all investigated aqueous surfactant solution concentrations.

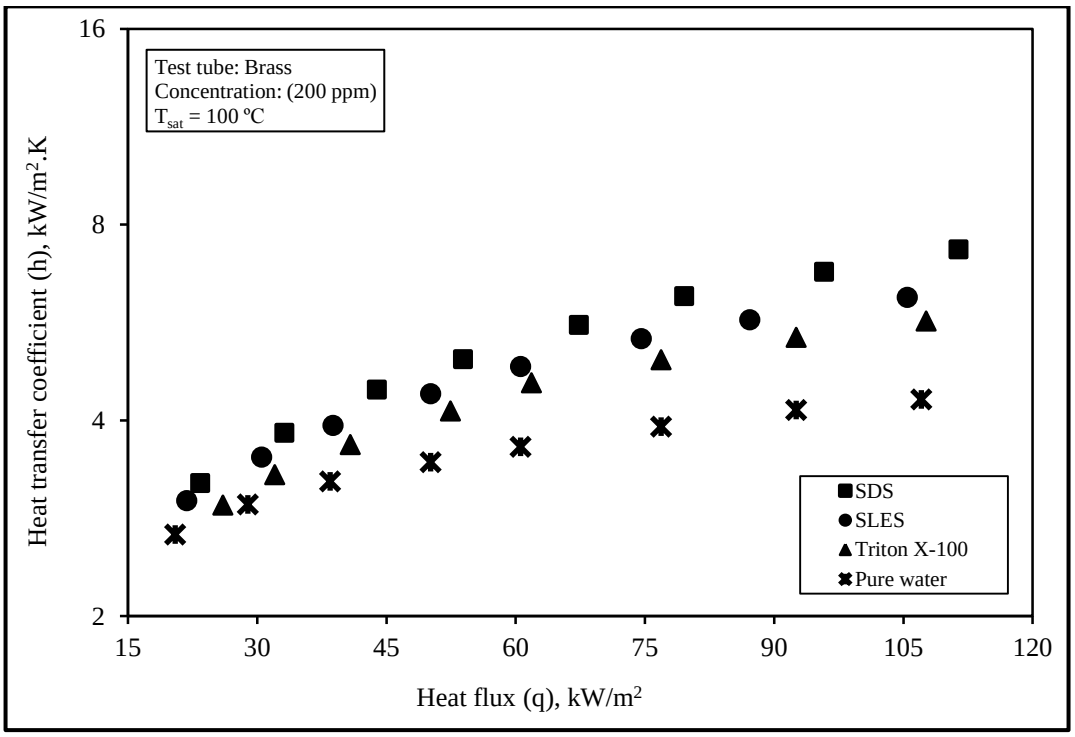


**Fig. 5.4a: Variation of h with q for aqueous solutions of SDS, SLES and Triton X-100 at concentration of 200 ppm using brass tube**

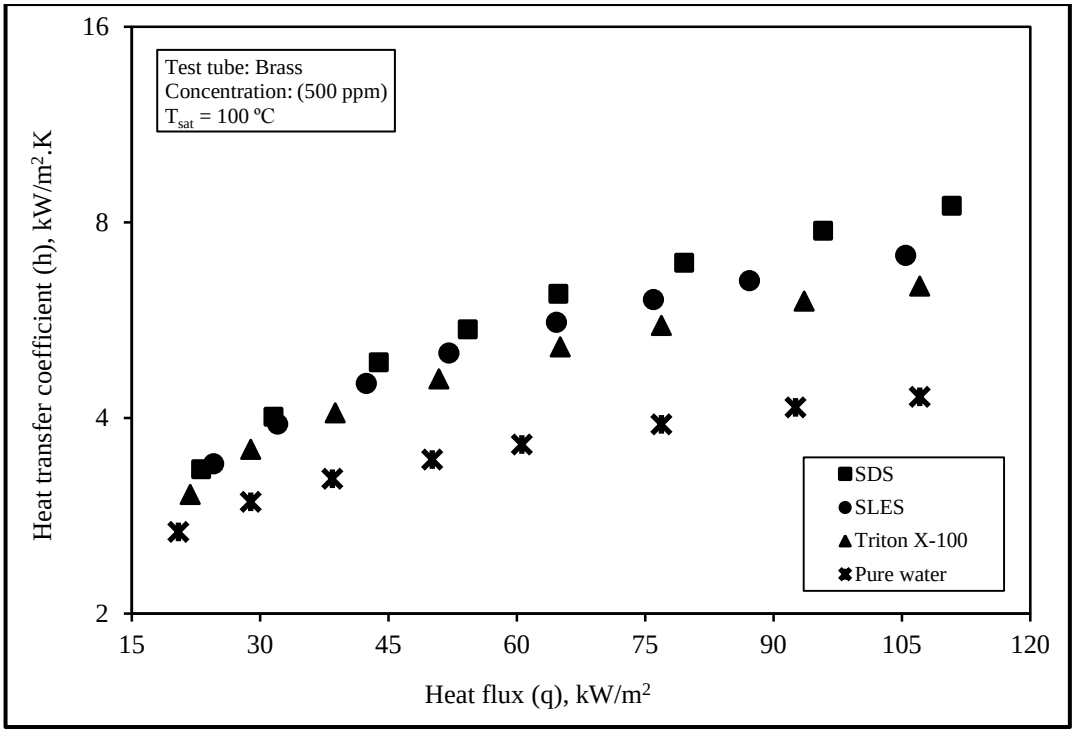


**Fig. 5.4b: Variation of h with q for aqueous solutions of SDS, SLES and Triton X-100 at concentration of 500 ppm using brass tube**

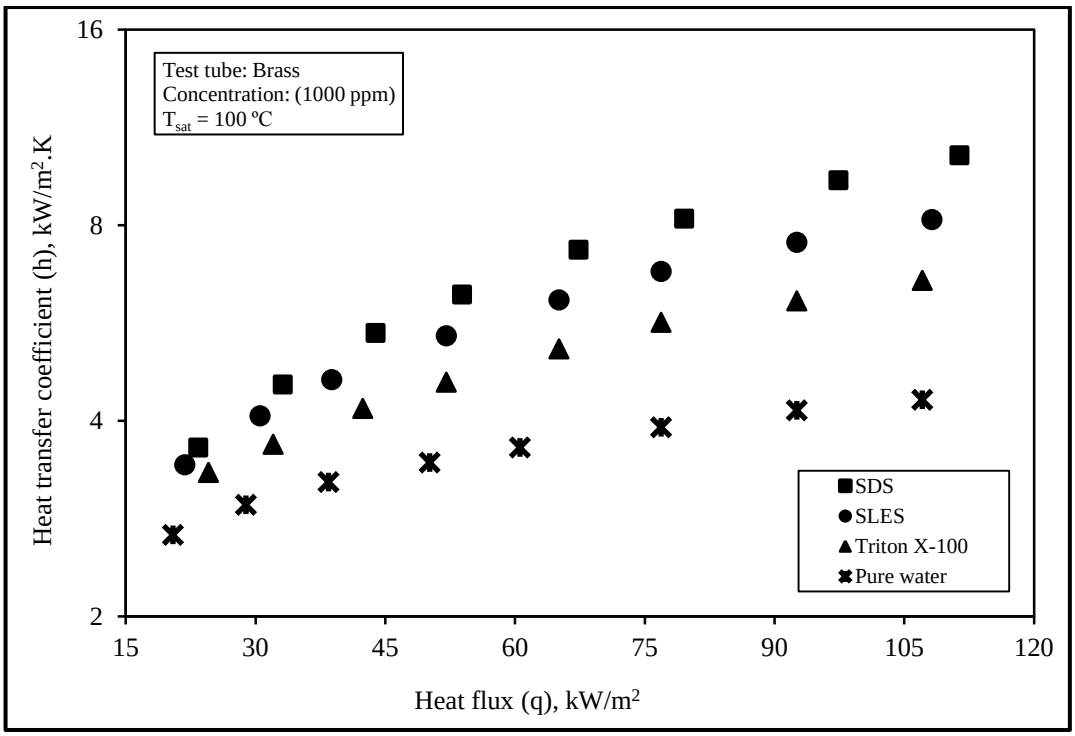


**Fig. 5.4c: Variation of h with q for aqueous solutions of SDS, SLES and Triton X-100 at concentration of 1000 ppm using brass tube**

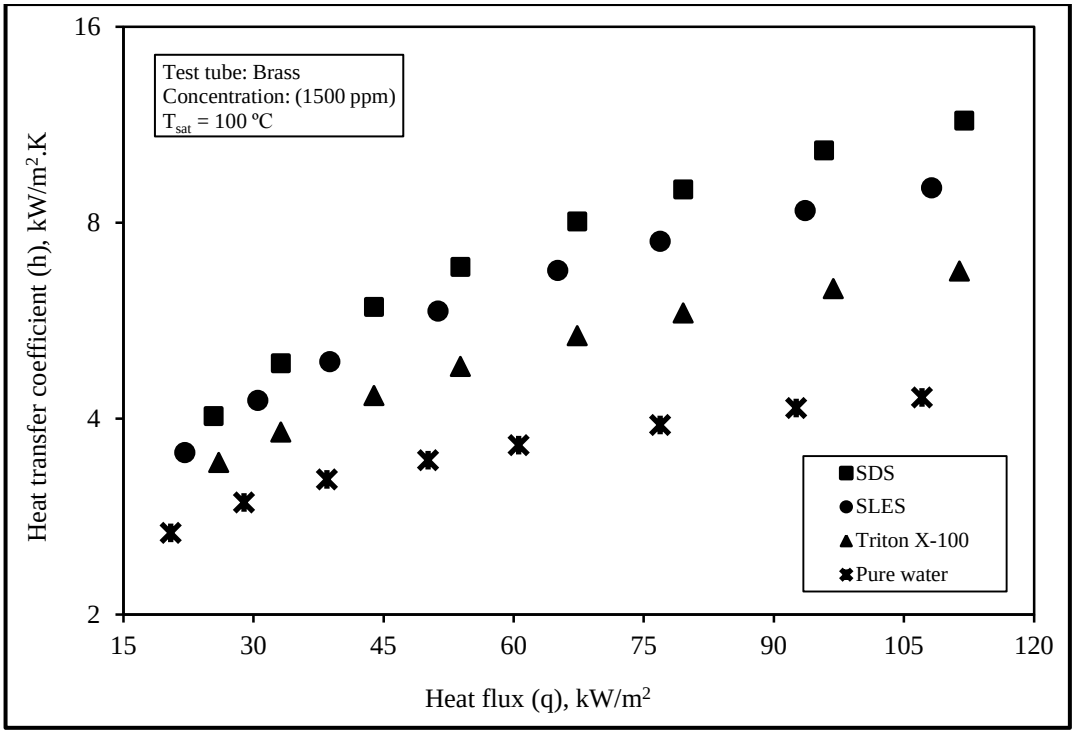


**Fig. 5.4d: Variation of h with q for aqueous solutions of SDS, SLES and Triton X-100 at concentration of 1500 ppm using brass tube**

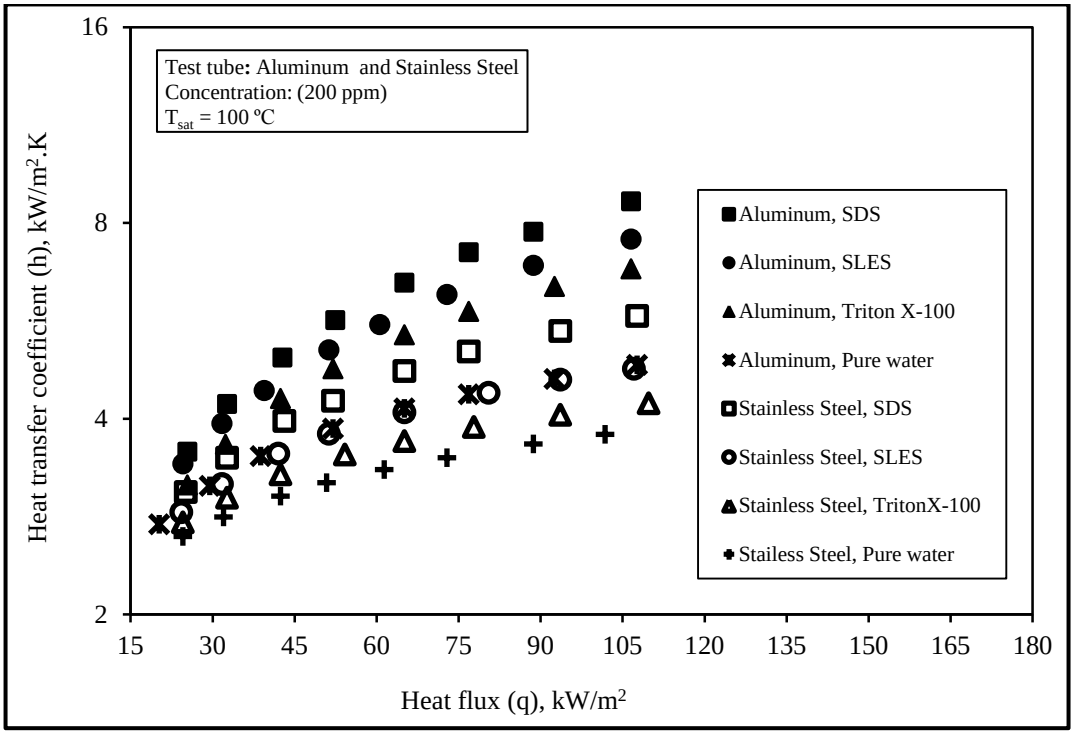


**Fig. 5.5a: Variation of h with q for aqueous solutions of SDS, SLES and Triton X-100 at concentration of 200 ppm using aluminum and stainless steel tubes**

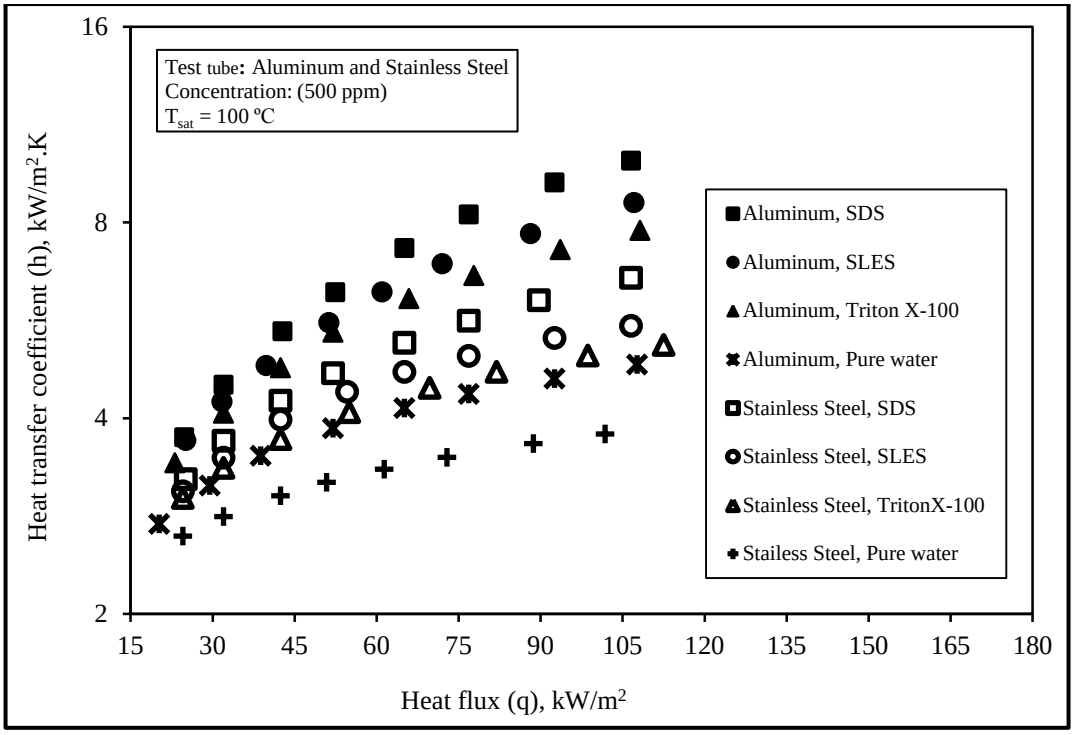


**Fig. 5.5b: Variation of h with q for aqueous solutions of SDS, SLES and Triton X-100 at concentration of 500 ppm using aluminum and stainless steel tubes**

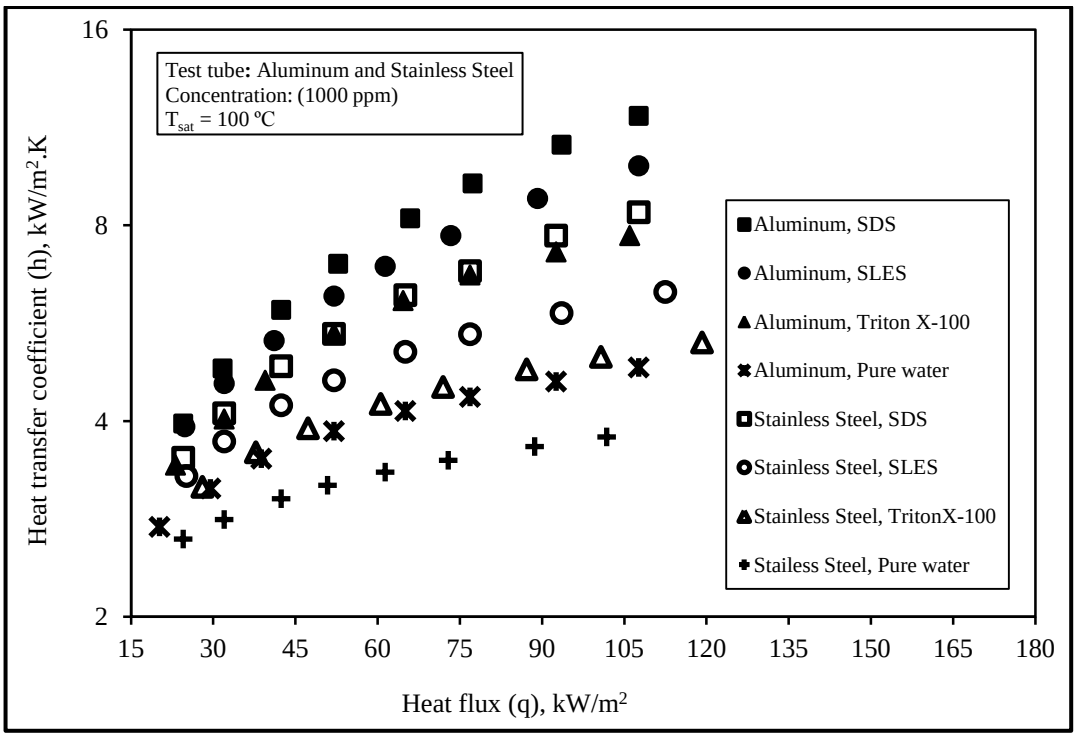


**Fig. 5.5c: Variation of h with q for aqueous solutions of SDS, SLES and Triton X-100 at concentration of 1000 ppm using aluminum and stainless steel tubes**

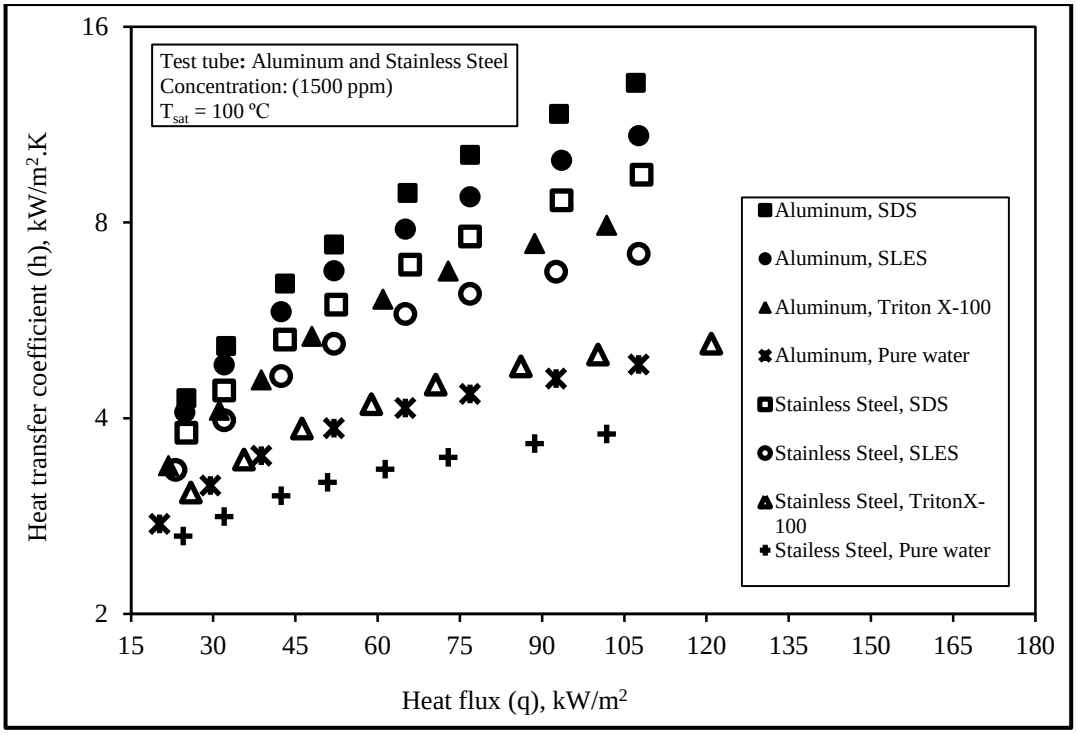


**Fig. 5.5d: Variation of h with q for aqueous solutions of SDS, SLES and Triton X-100 at concentration of 1500 ppm using aluminum and stainless steel tubes**

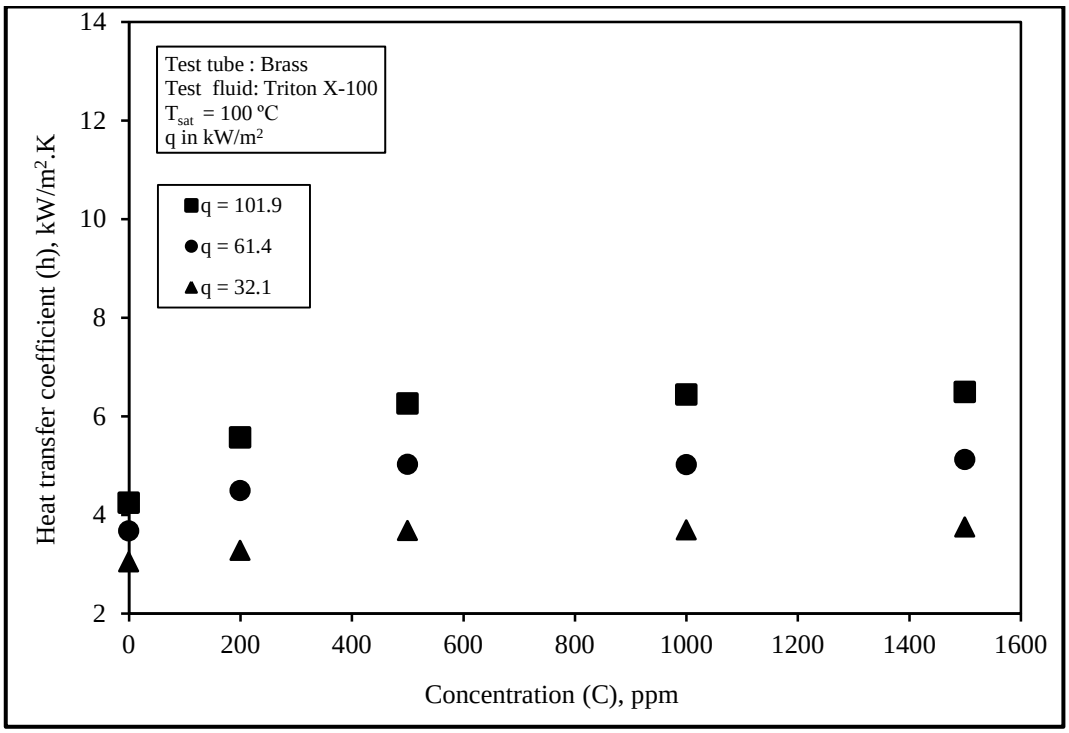


**Fig. 5.6a: Effect of the wall heat flux on the heat transfer coefficient for Triton X-100 aqueous solution concentration using brass test tube**

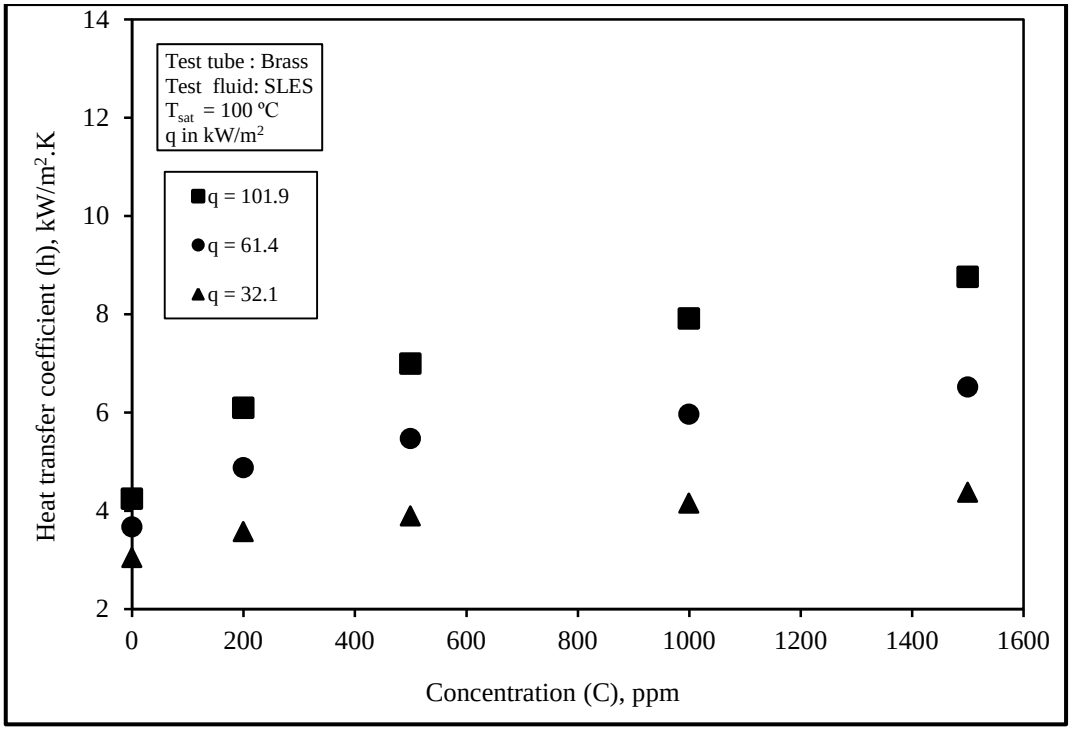


**Fig. 5.6b: Effect of the wall heat flux on the heat transfer coefficient for SLES aqueous solution concentration using brass test tube**

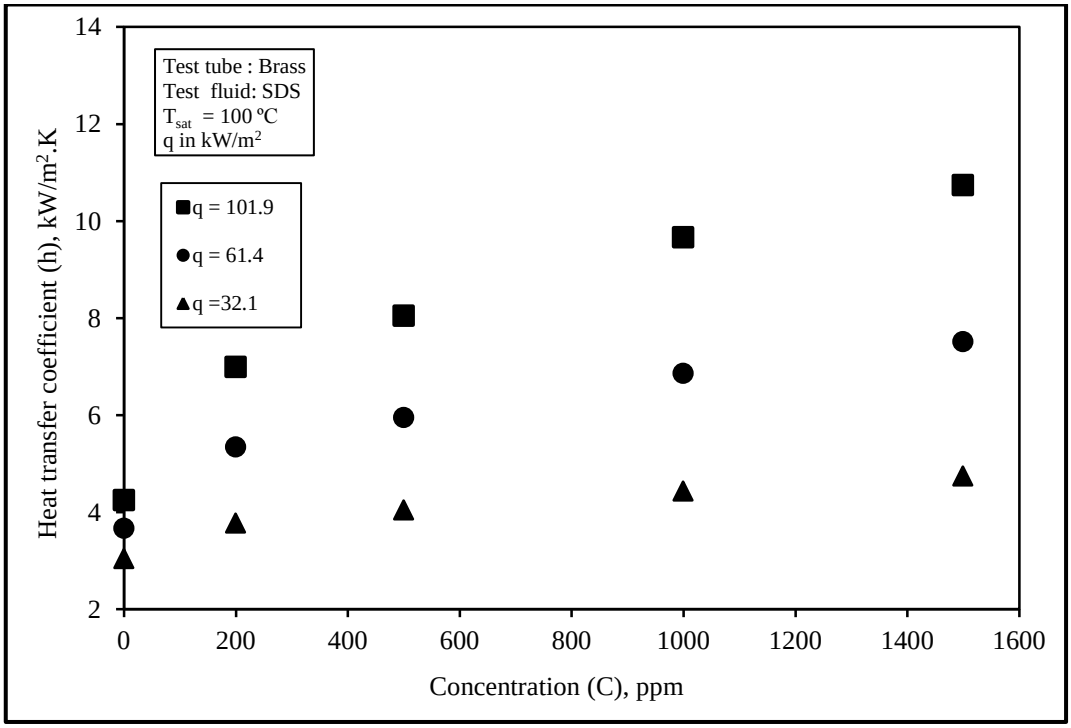


**Fig. 5.6c: Effect of the wall heat flux on the heat transfer coefficient for SDS aqueous solution concentration using brass test tube**

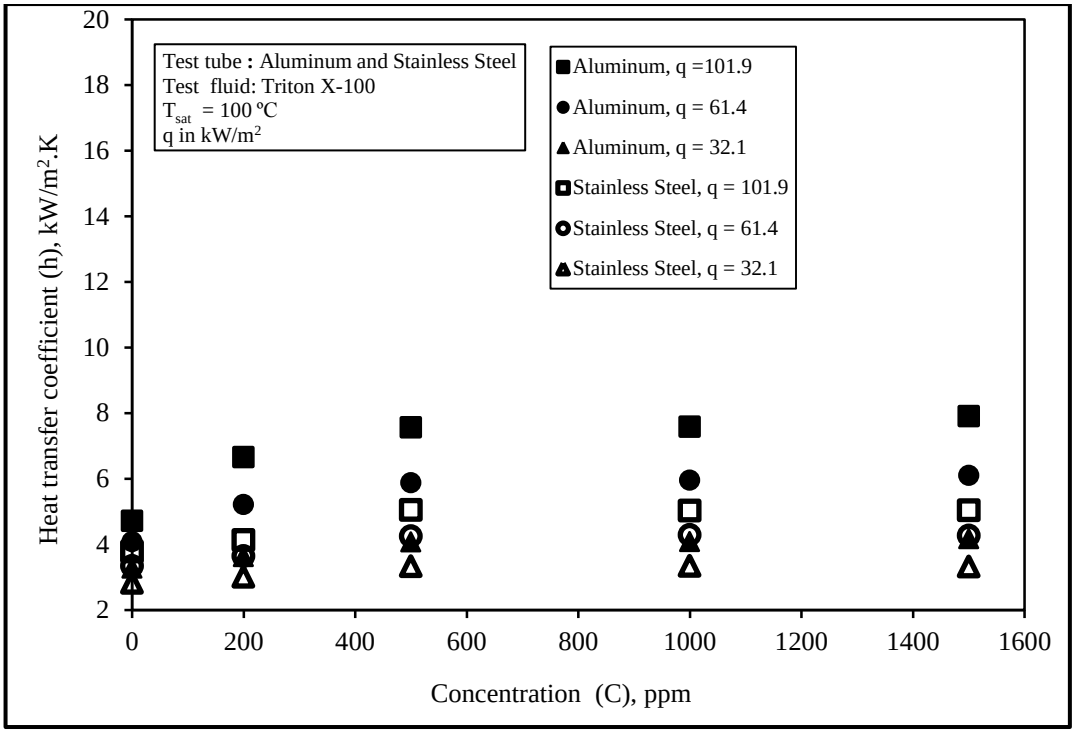


**Fig.5.7a: Effect of the wall heat flux on the heat transfer coefficient for Triton X-100 aqueous solution concentration using aluminum and stainless steel tubes**

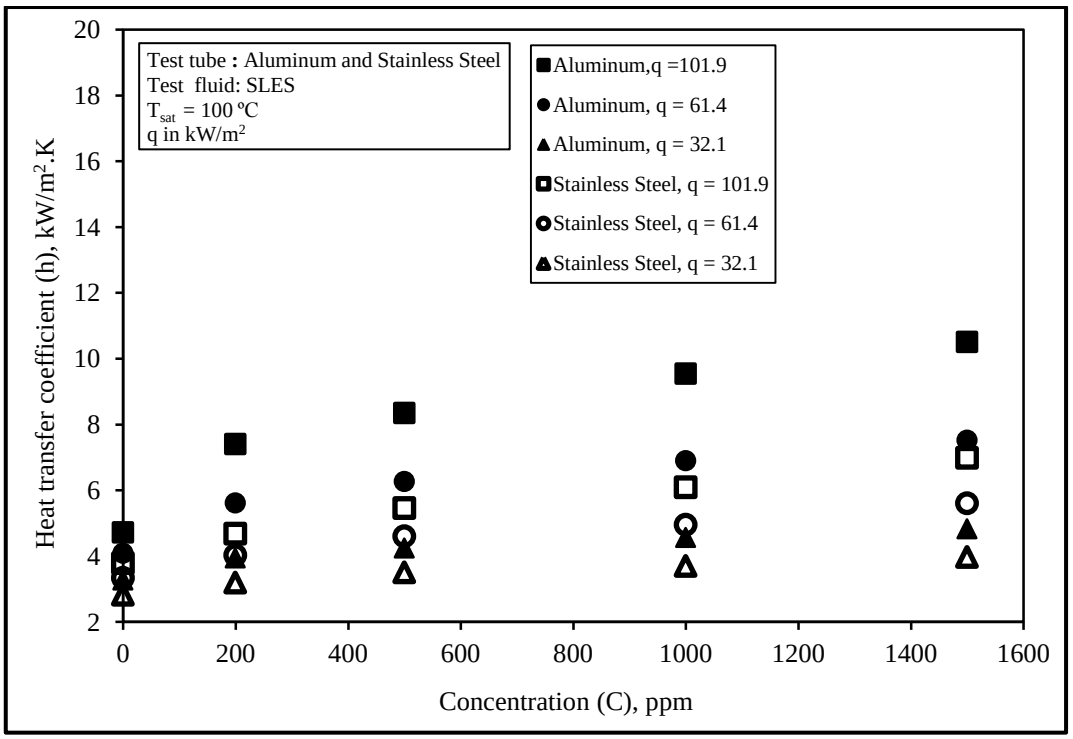


**Fig. 5.7b: Effect of the wall heat flux on the heat transfer coefficient for SLES aqueous solution concentration using aluminum and stainless steel test tubes**

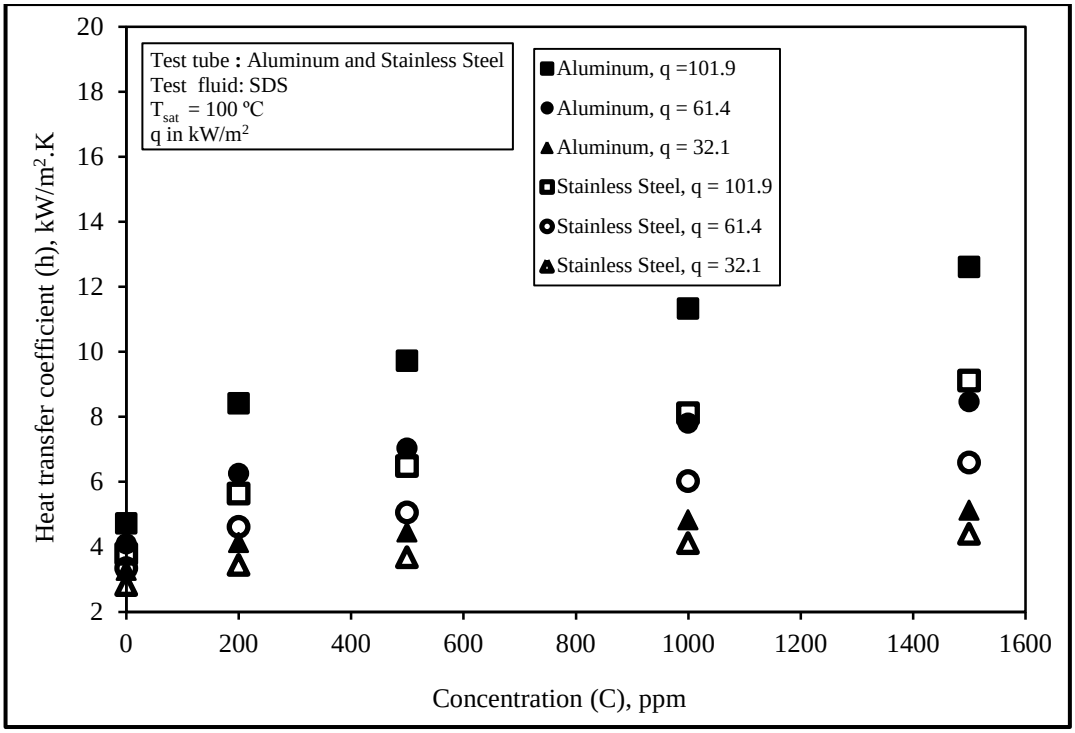


**Fig. 5.7c: Effect of the wall heat flux on the heat transfer coefficient for SDS aqueous solution concentration using aluminum and stainless steel test tubes**

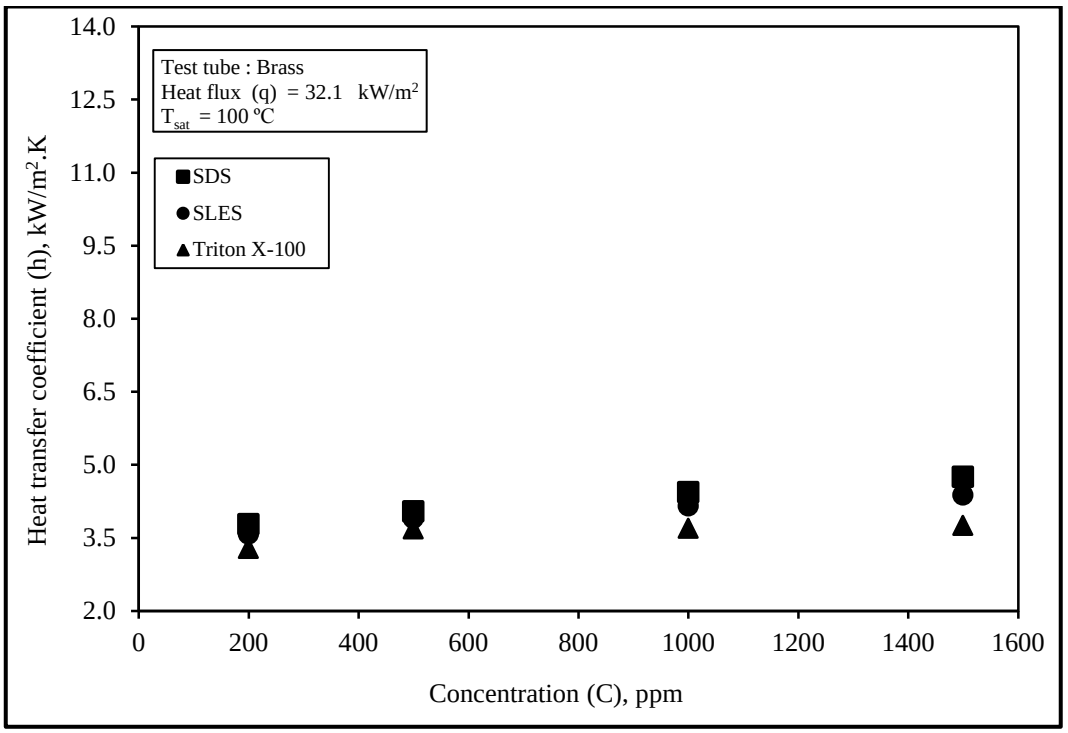


**Fig. 5.8a: Comparison between the three test surfactants for constant wall heat flux of 32.1 kW/m$^2$ using brass test tube**

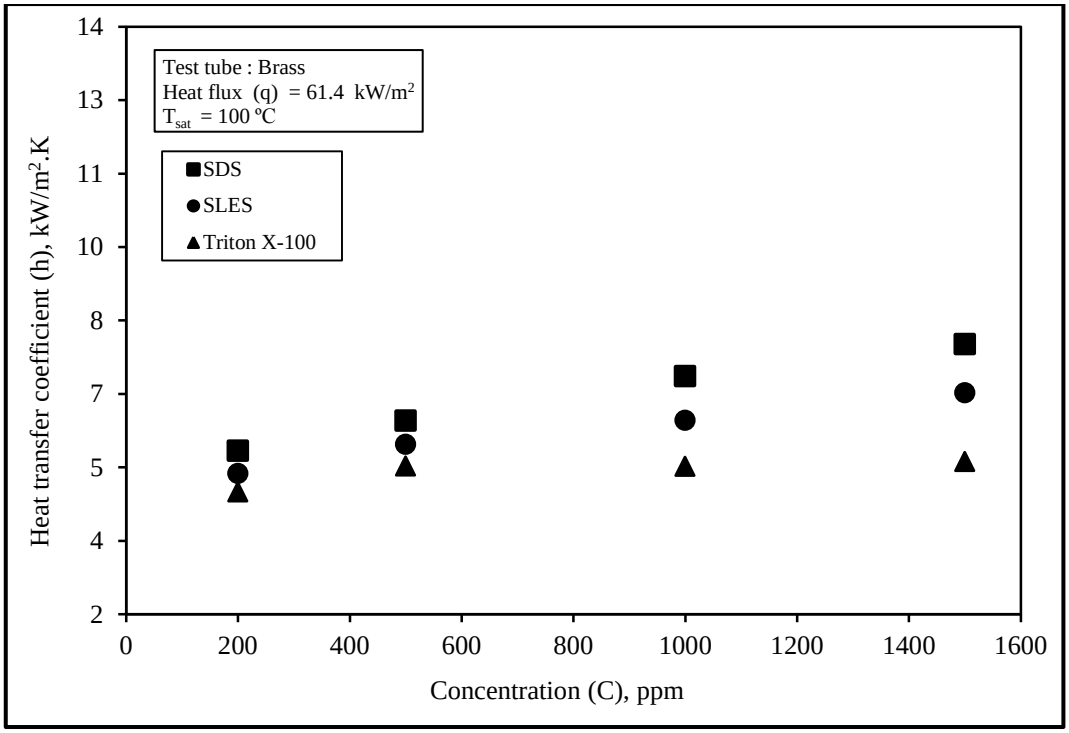


**Fig. 5.8b: Comparison between the three test surfactants for constant wall heat flux of 61.4 kW/m$^2$ using brass test tube**

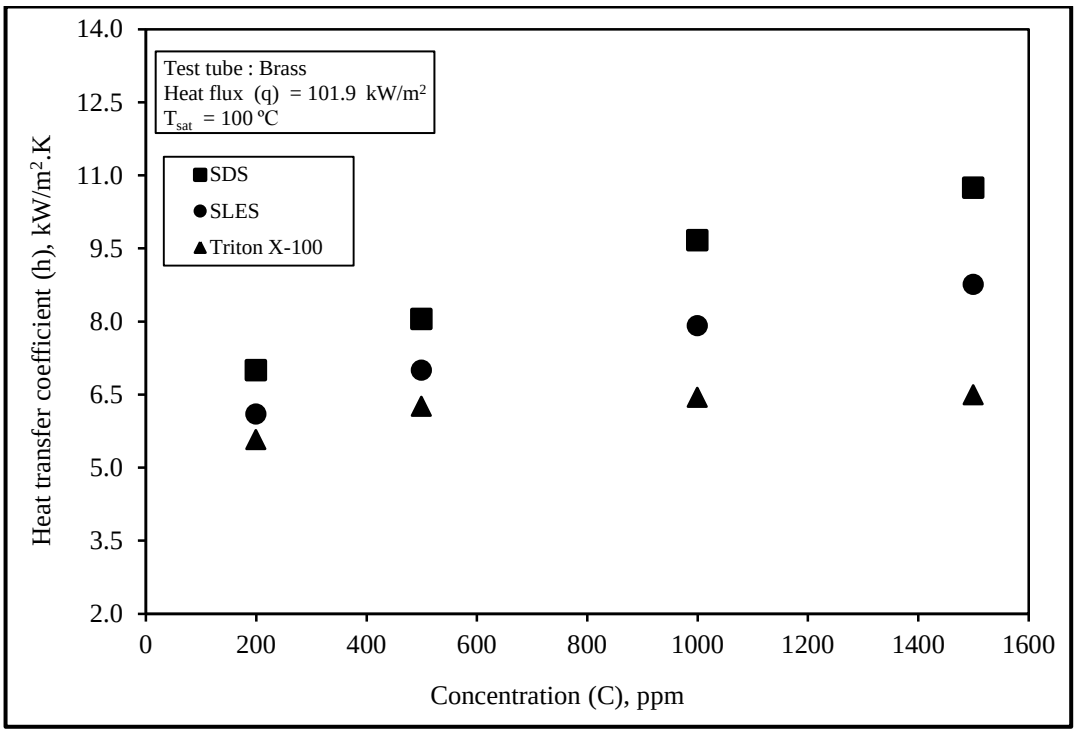


**Fig. 5.8c: Comparison between the three test surfactants for constant wall heat flux of 101.9 kW/m$^2$ using brass test tube**

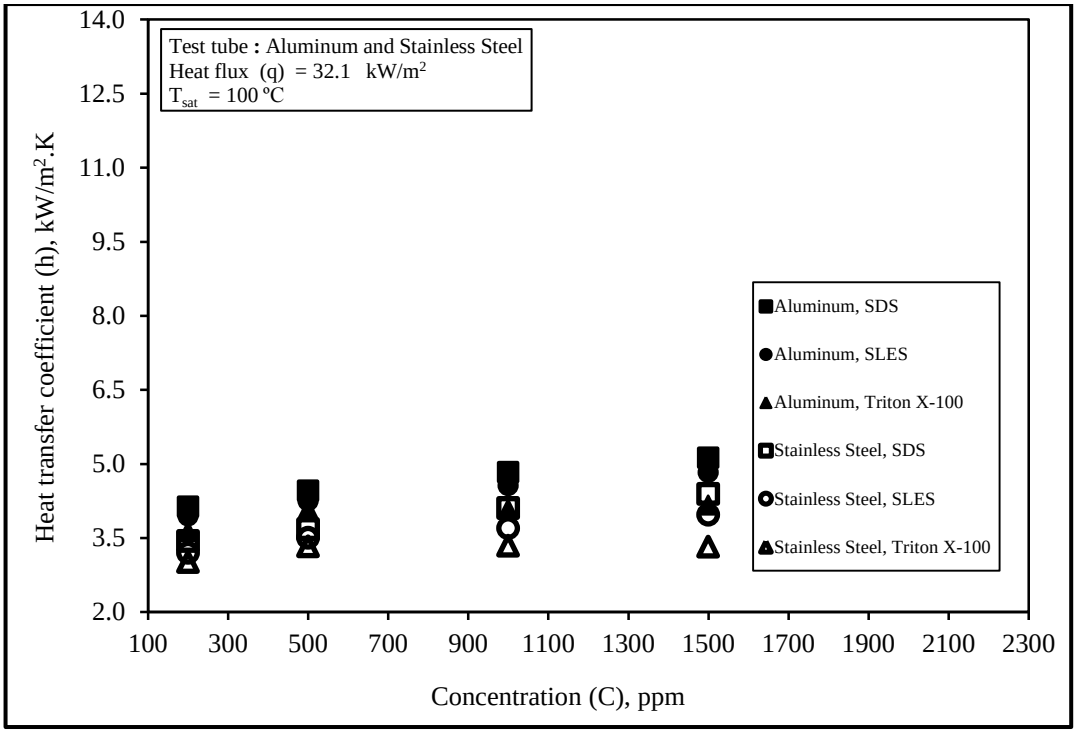


**Fig. 5.9a: Comparison between the three test surfactants for constant wall heat flux of 32.1kW/m$^2$ using aluminum and stainless steel test tubes**

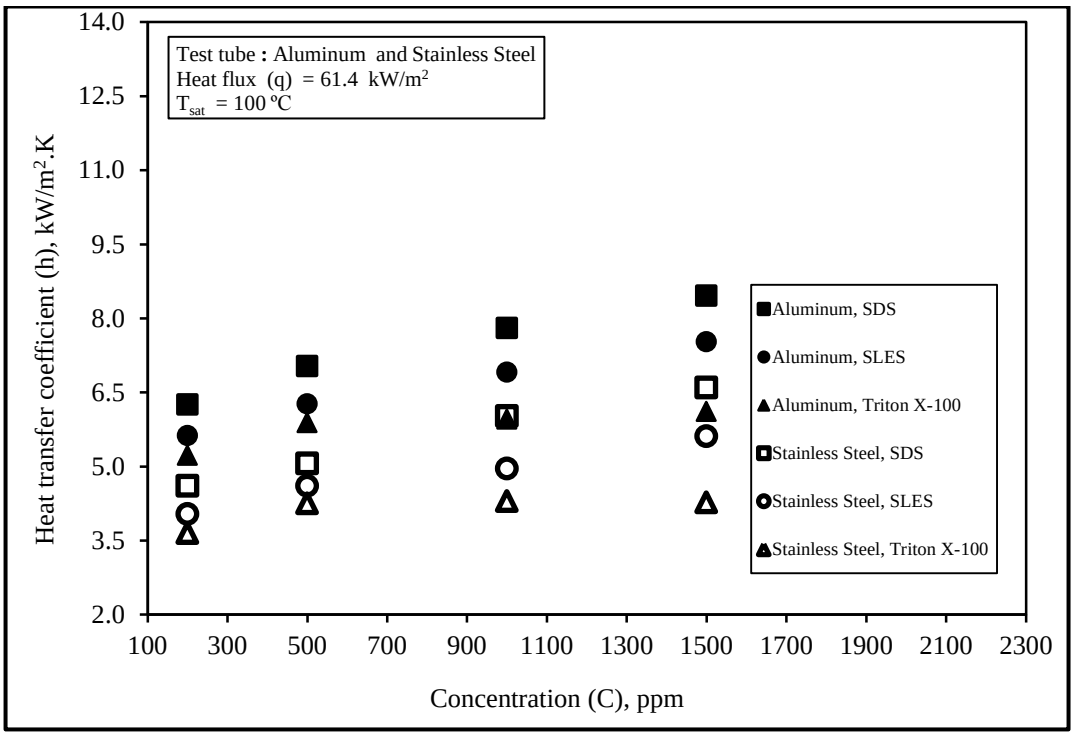


**Fig. 5.9b: Comparison between the three test surfactants for constant wall heat flux of 61.4 kW/m$^2$ using aluminum and stainless steel test tubes**

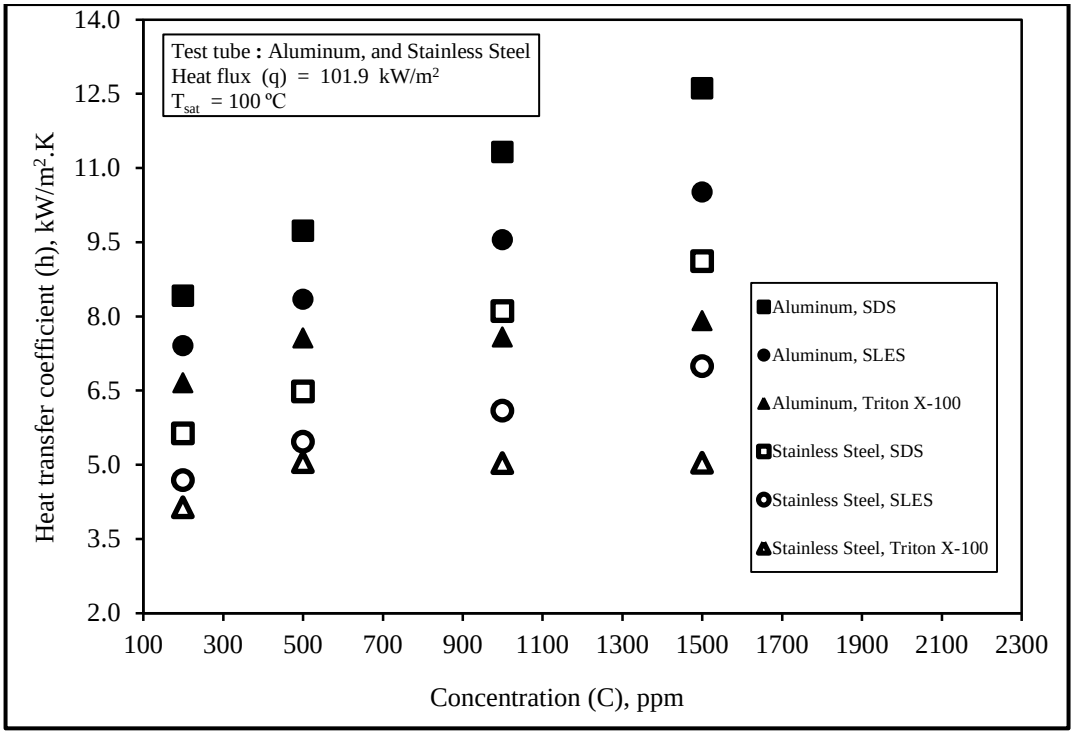


**Fig. 5.9c: Comparison between the three test surfactants for constant wall heat flux of 101.9 kW/m$^2$ using aluminum and stainless steel test tubes**

## 5.2. Comparison between the three test aqueous surfactant solutions

To further delineate, the enhancement in the pool boiling heat transfer coefficient, h*, as a result of employing aqueous surfactant solutions is shown in Figures 5.10 and 5.11. In these Figures h* is represented as a function of tube wall heat flux, q for the three test tubes S1, S2 and S3. It can be seen that for a given q, increasing the concentration of surfactant in its aqueous solution, increases the enhancement in nucleate boiling heat transfer process represented by h*. This behavior is observed for the three test surfactants SDS, SLES and Triton X-100 by different amounts. Also, it should be emphasized that for a given concentration of aqueous surfactant solution, increasing q,

increases the magnitude of $h^*$. This may be related to the definition of the enhancement in the pool boiling heat transfer coefficient, $h^*$ as:

$$h^* = h_{sur}/h_w = (q_{sur}/\Delta T_{sur})/(q_w/\Delta T_w) = \Delta T_w/\Delta T_{sur} \quad 5.1$$

With increasing q, more nucleation sites are activated and therefore more active cavities for initiating bubbles, there by increasing the nucleation site density as well as the bubble frequency. Also, from Eq. 5.1 increasing the heat flux, q decreases $\Delta T_{sur}$. This, in turn is reflected on the degree of enhancement. It is also indicated that the boiling heat transfer characteristics of SDS is superior to that of SLES and Triton X-100 for all investigated aqueous solution concentrations. This may be due to the fact that during nucleate boiling, the surfactant molecules diffuse towards the growing bubble interface from the adjacent sublayer. The surfactant concentration in this sublayer would tend to be very close to the bulk concentration. This concurs with literature in the sense that the dynamic surface tension at the interface directly proportional to the bubble dynamics during boiling. Consequently, a lower molecular weight surfactant molecule SDS diffuses faster than the higher molecular weight counterpart SLES and Triton X-100.

## 5.3. Effect of the wall heat flux on the enhancement of heat transfer coefficient, $h^*$

Figures 5.12 and 5.13 show the effect of increasing the wall heat flux on the variation of $h^*$ with the aqueous solution concentration, C. The results of surfactants SDS, SLES and Triton X-100 using test tubesS1, S2 and S3 are presented. It is indicated that for a given q, increasing the concentration of a given surfactant, increases $h^*$. This is true for all the test tubes. It is also observed that for a given surfactant aqueous solution concentration and a given test tube, increasing q; increases $h^*$.

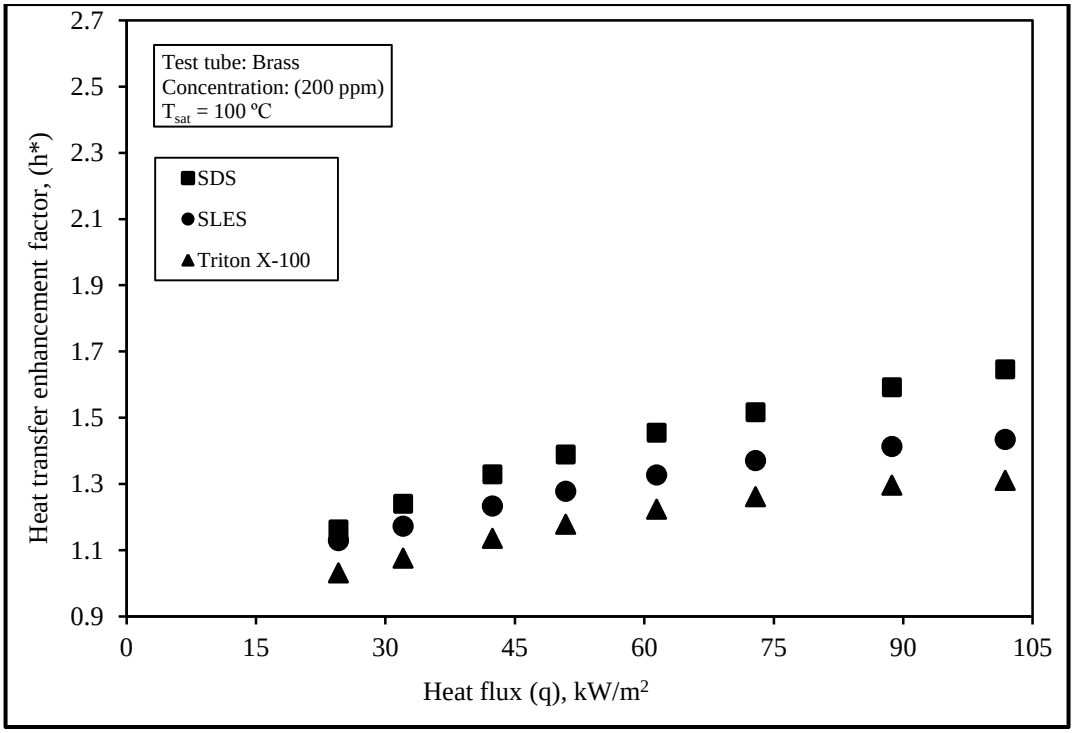


**Fig. 5.10a: Comparison between the three test surfactants at constant concentrations of 200 ppm using brass test tube**

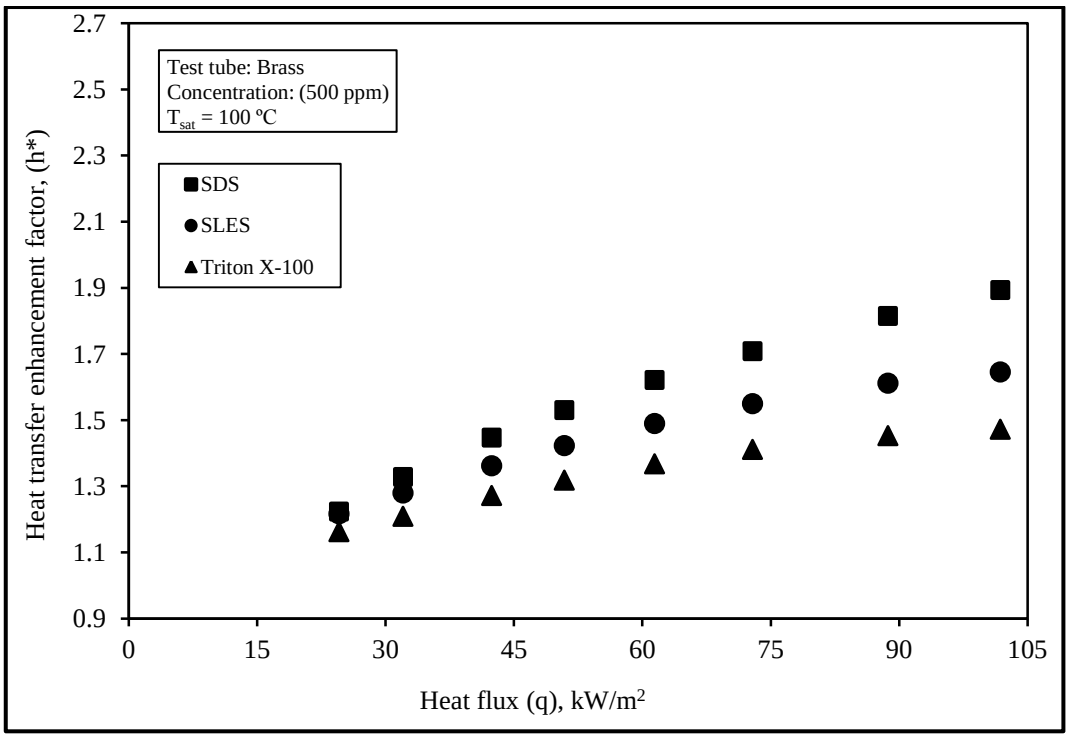


**Fig. 5.10b: Comparison between the three test surfactants at constant concentrations of 500 ppm using brass test tube**

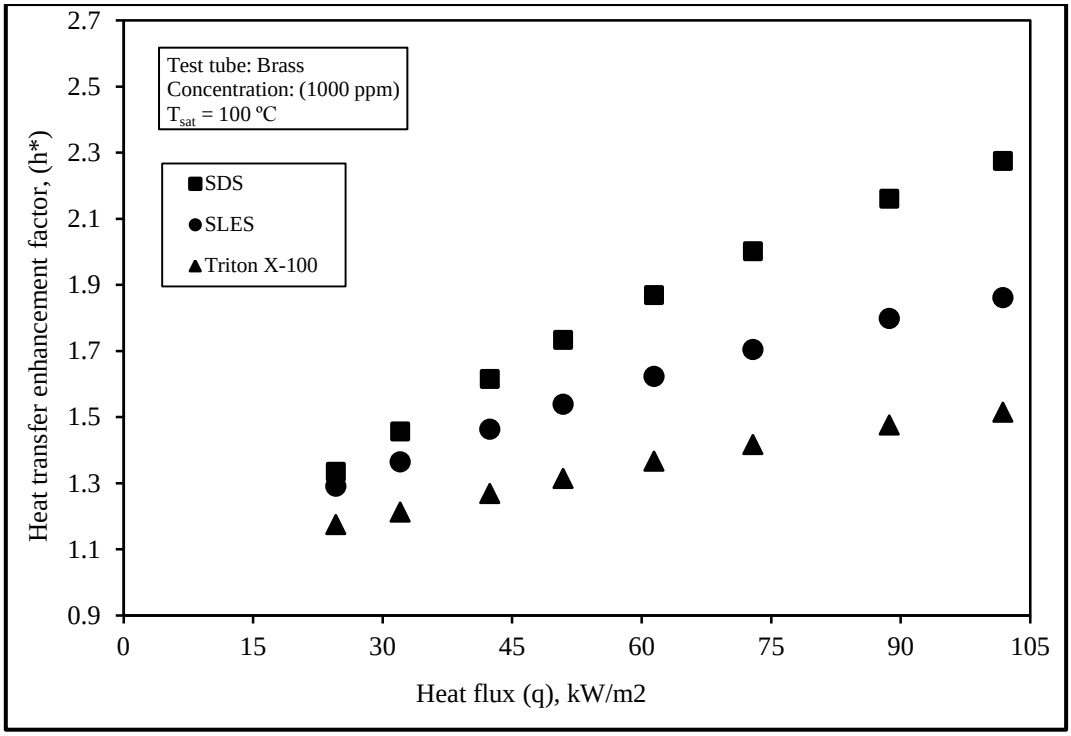


**Fig.5.10c: Comparison between the three test surfactants at constant concentrations of 1000 ppm using brass test tube**

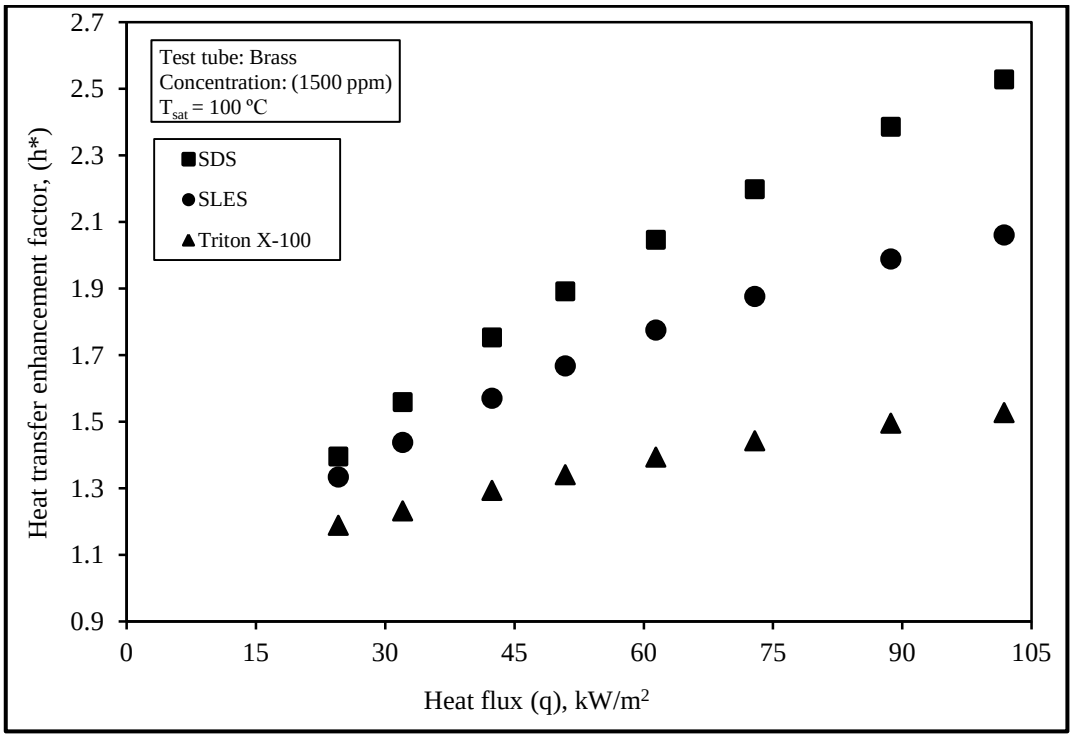


**Fig.5.10d: Comparison between the three test surfactants at constant concentrations of 1500 ppm using brass test tube**

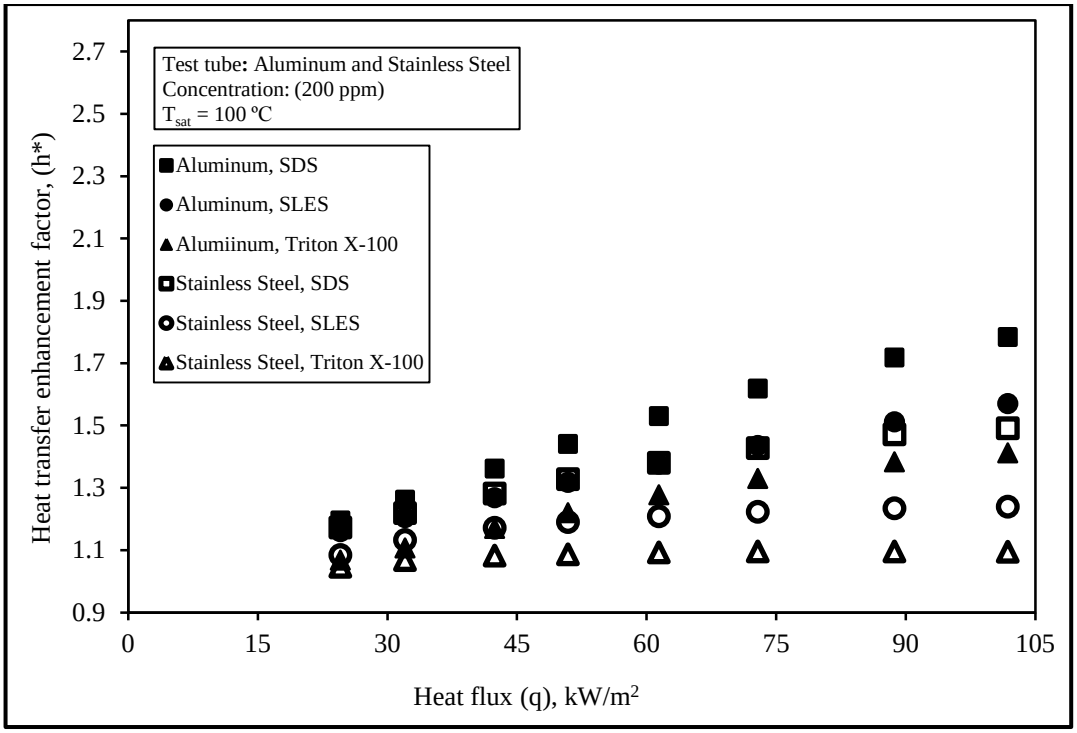


**Fig. 5.11a: Comparison between the three test surfactants at constant concentrations of 200 ppm using aluminum and stainless steel tubes**

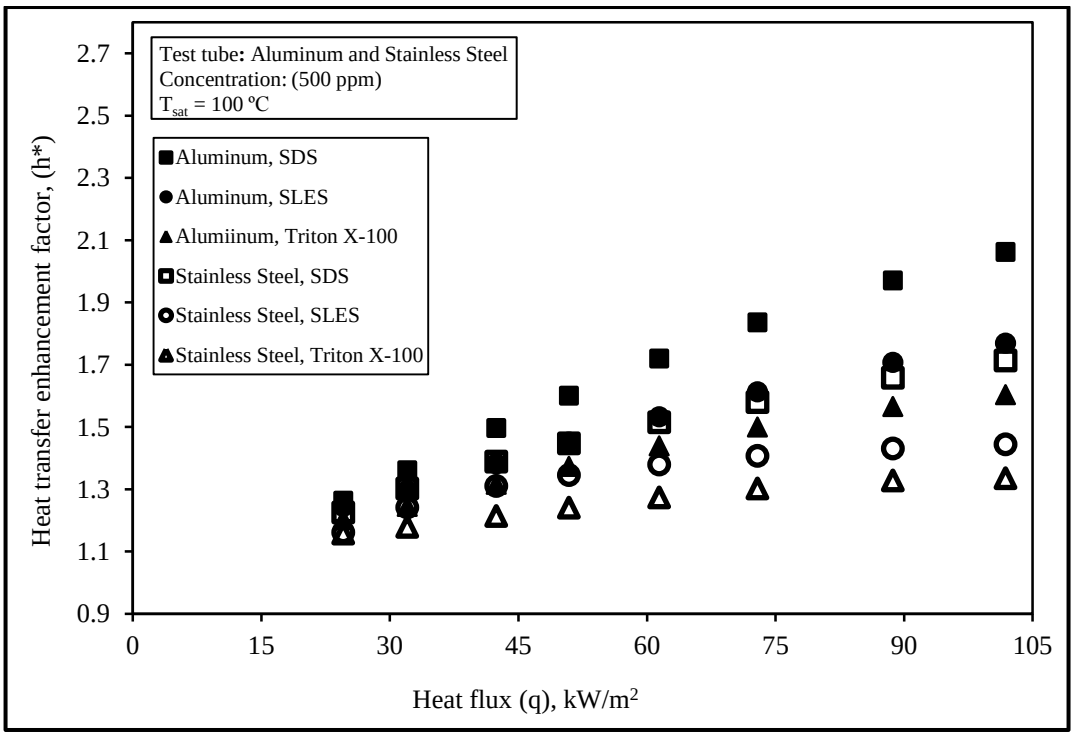


**Fig. 5.11b: Comparison between the three test surfactants at constant concentrations of 500 ppm using aluminum and stainless steel test tubes**

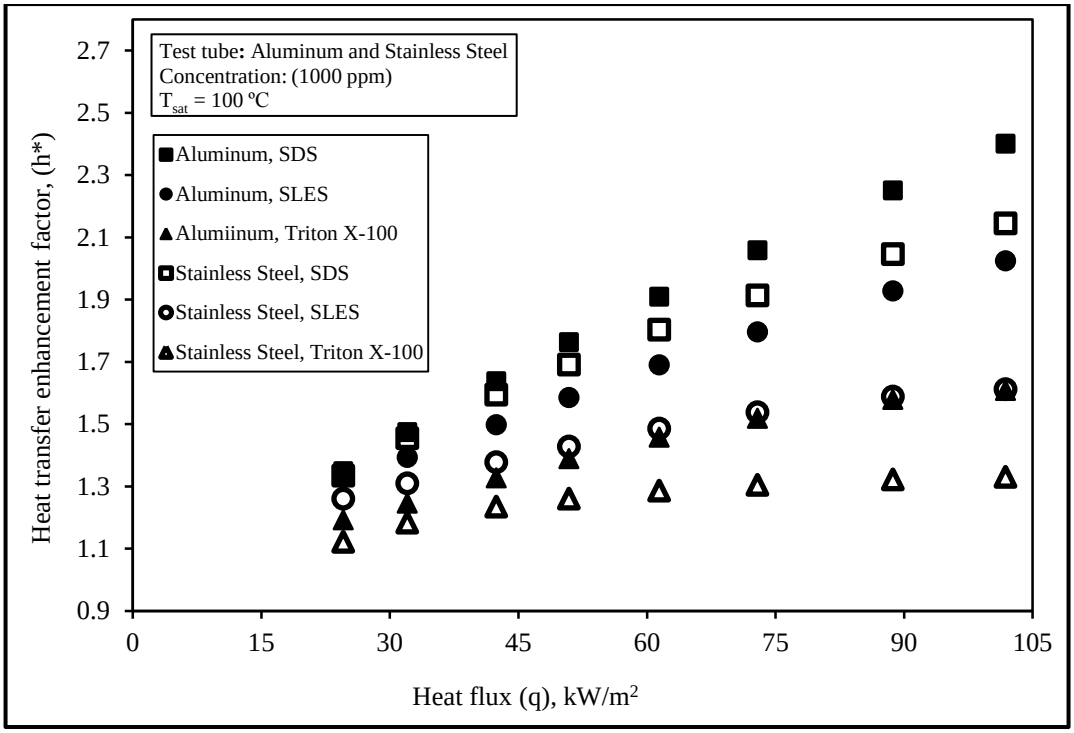


**Fig. 5.11c: Comparison between the three test surfactants at constant concentrations of 1000 ppm using aluminum and stainless steel tubes**

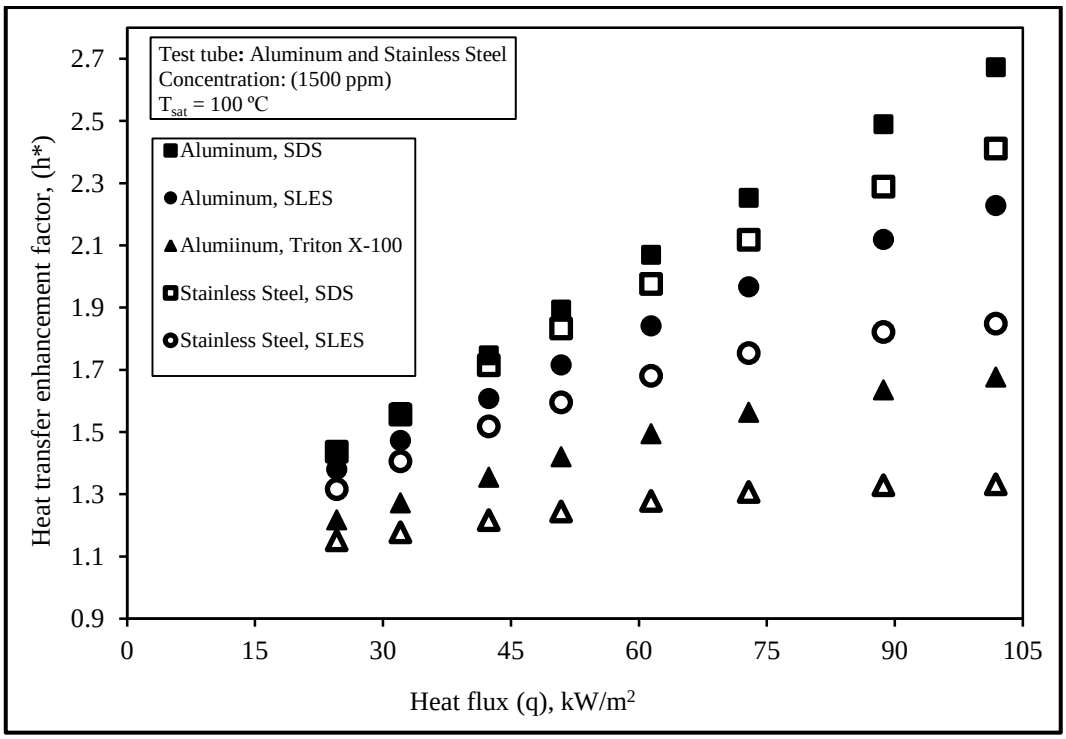


**Fig. 5.11d: Comparison between the three test surfactants at constant concentrations of 1500 ppm using aluminum and stainless steel tubes**

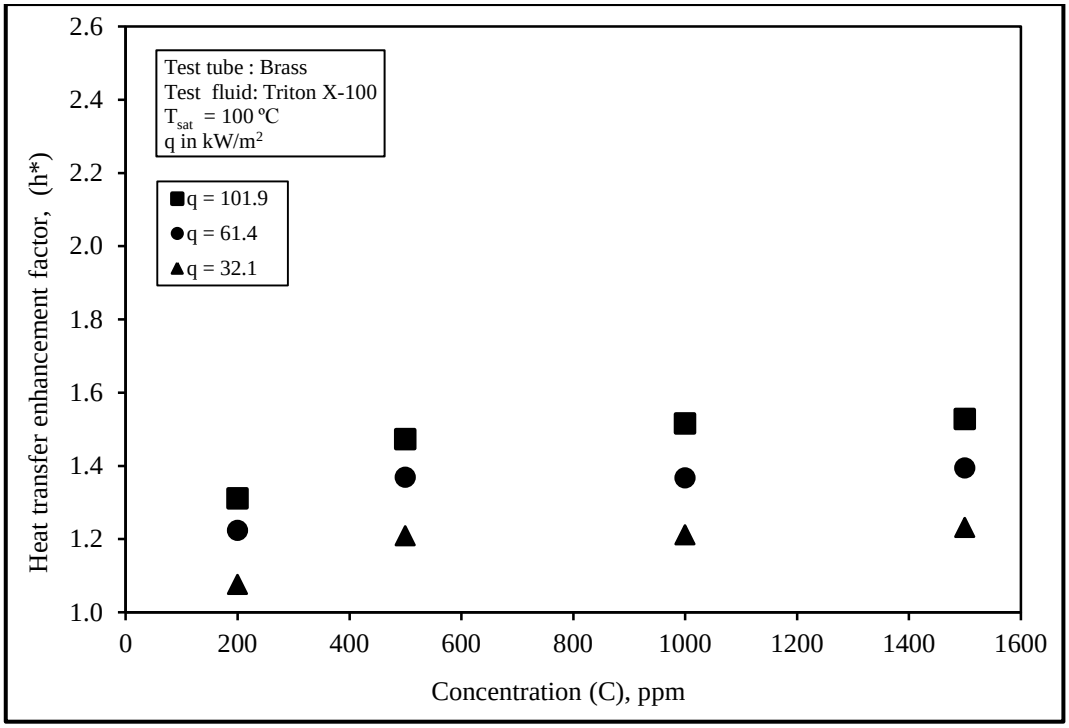


**Fig. 5.12a**: **Effect of the wall heat flux on the variation of h* with Triton X-100 aqueous solution concentration using brass test tube**

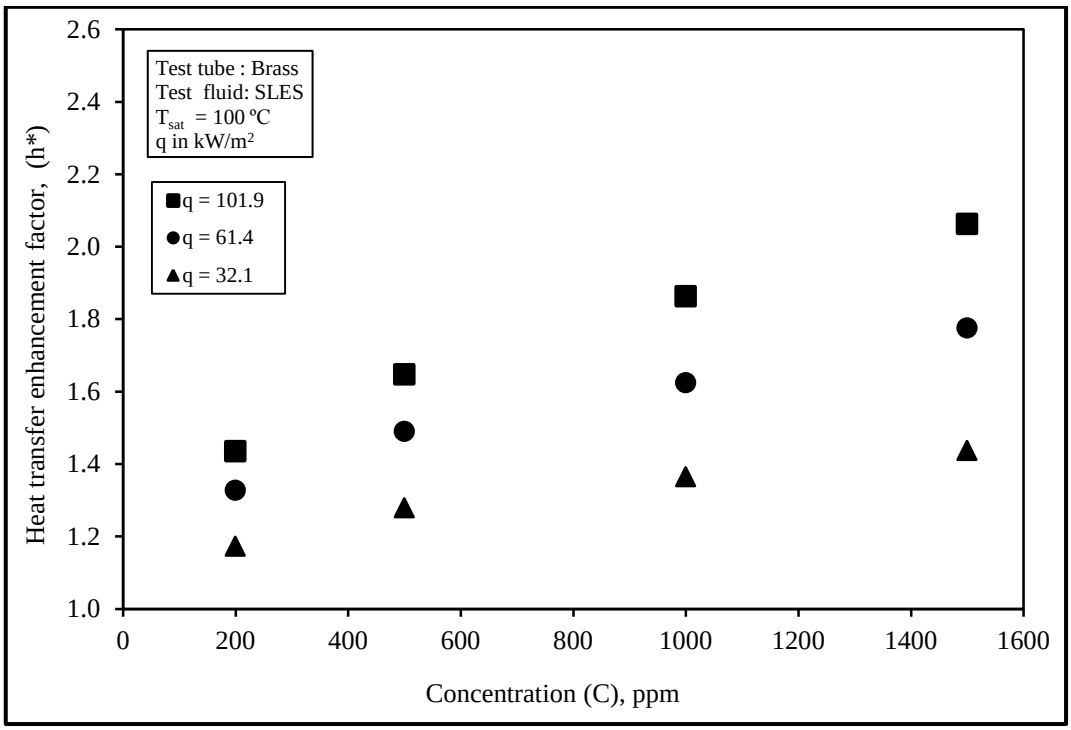


**Fig. 5.12b: Effect of the wall heat flux on the variation of h* with SLES aqueous solution concentration using brass test tube**

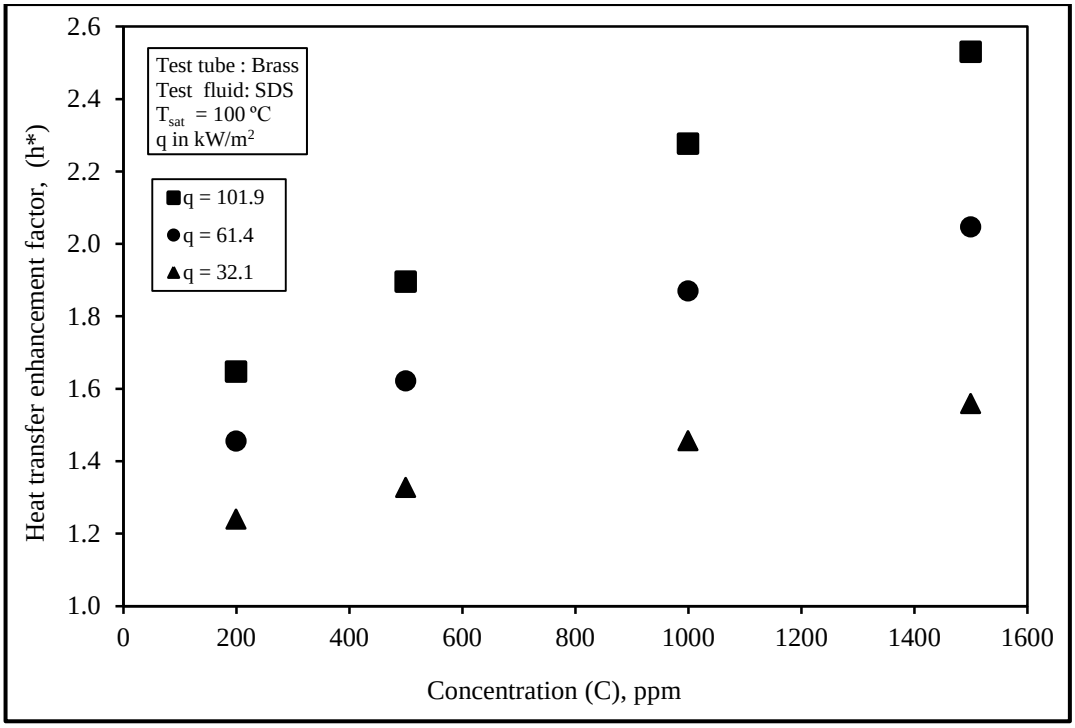


**Fig. 5.12c: Effect of the wall heat flux on the variation of h* with SDS aqueous solution concentration using brass test tube**

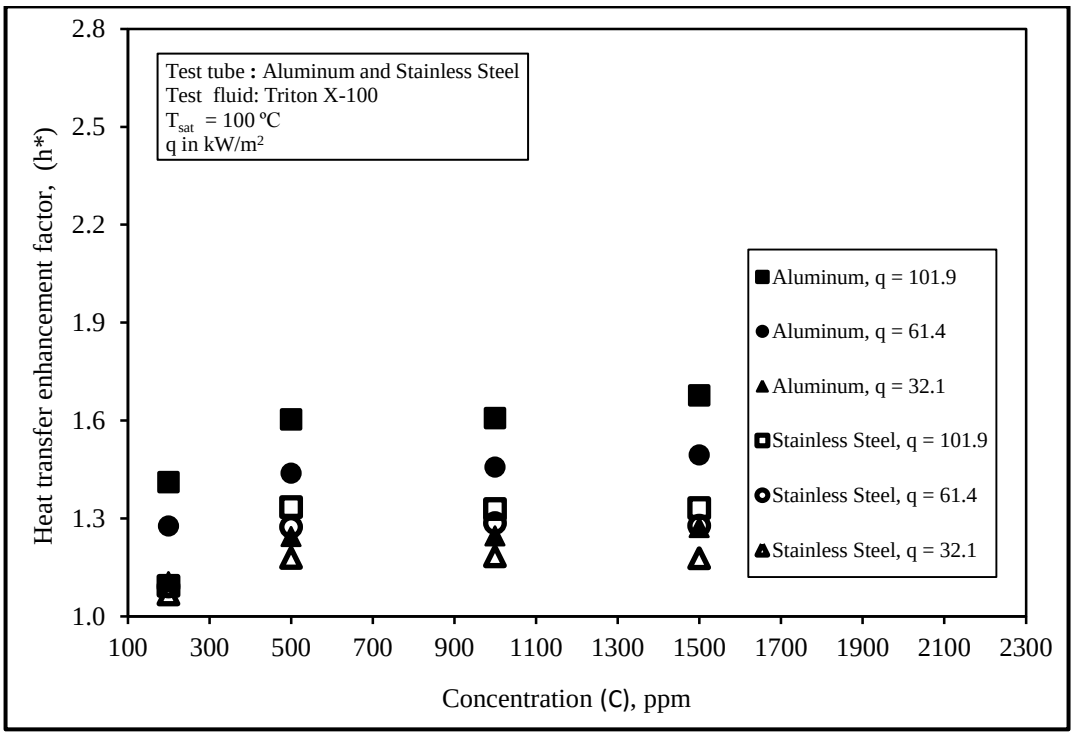


**Fig. 5.13a**: **Effect of the wall heat flux on the variation of h* with Triton X-100 aqueous solution concentration using aluminum and stainless steel tubes**

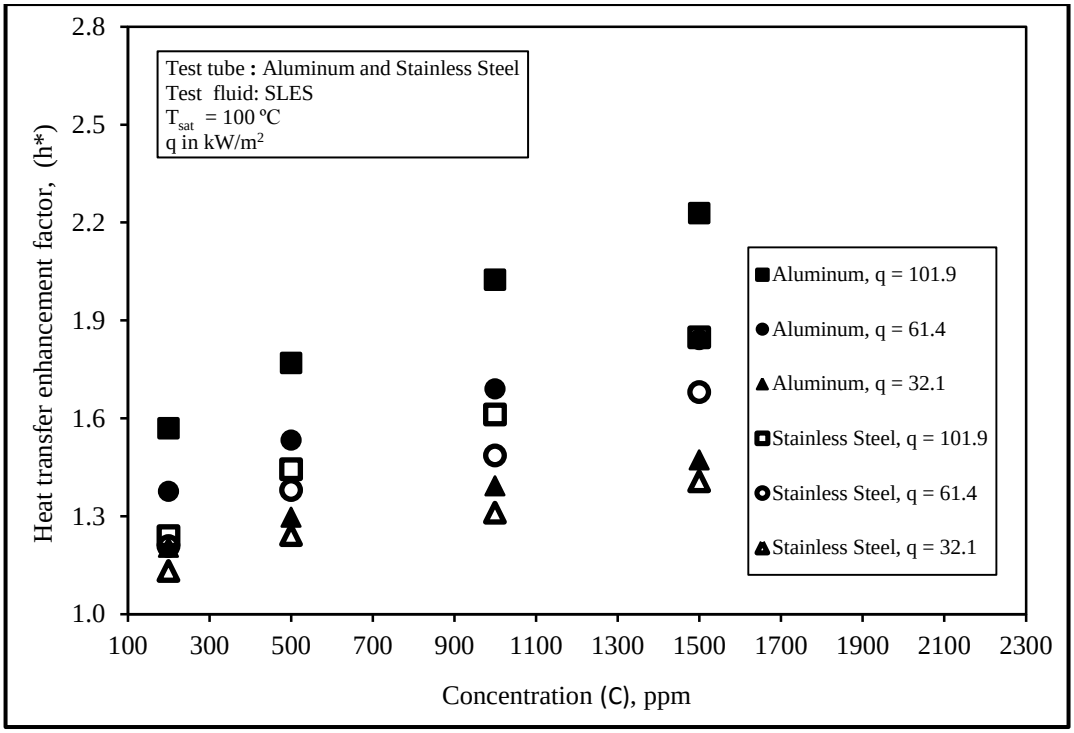


**Fig. 5.13b: Effect of the wall heat flux on the variation of h* with SLES aqueous solution concentration using aluminum and stainless steel tubes**

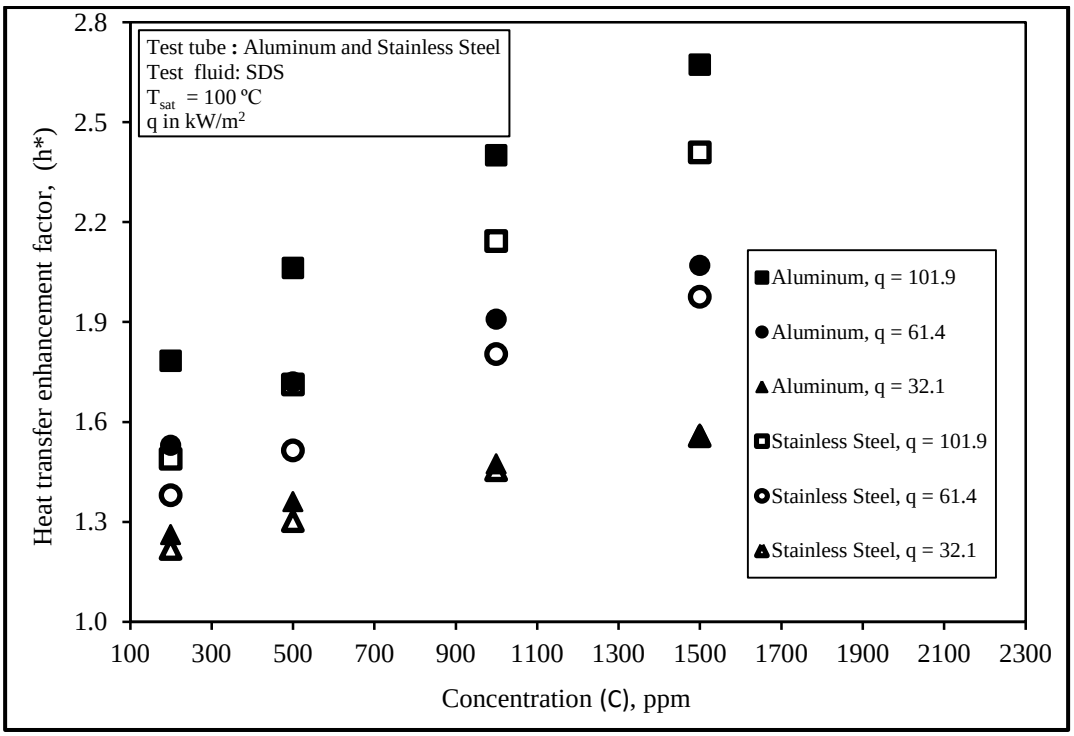


**Fig. 5.13c: Effect of the wall heat flux on the variation of h* with SDS aqueous solution concentration using aluminum and stainless steel tubes**

## 5.4. Effect of surfactant type on heat transfer enhancement factor $h^*$

Figures 5.14and 5.15 show the variation of $h^*$ with aqueous surfactant concentration at constant wall heat flux, q. A comparison is made between the results of SDS, SLES and Triton X-100 aqueous solutions. A closer inspection of the comparative results show that the heat transfer coefficient increases by about 160 % for SDS, 144 % for SLES and 123% for Triton X-100 over that for pure water at q equals 32.1 $kW/m^2$, using tube S1. The respective values at q equal 61.4$kW/m^2$ are 205 % for SDS, 178 % for SLES and 140 % for Triton X-100. At q equals 101.9$kW/m^2$, the respective values are 253% for SDS, 206% for SLES and 153 % for Triton X-100. The discrepancy in enhancement is attributed to the greater surface tension depression, and the better wetting characteristics of SDS solutions compared with those of SLES and Triton X-100. The results of the other test tube S2 are the heat transfer coefficient increases by about 156 % for SDS, 147 % for SLES and 127% for Triton X-100 over that for pure water at q equals 32.1$kW/m^2$. The respective values at q equals 61.4 $kW/m^2$ are 207 % for SDS, 184 % for SLES and 150 % for Triton X-100. At q equals 101.9 $kW/m^2$, the respective values are 267% for SDS, 223% for SLES and 168 % for Triton X-100. The results of the other test tube S3 show that the heat transfer coefficient increases by about 156 % for SDS, 141 % for SLES, and 118% for Triton X-100 over that for pure water at q equals 32.1 $kW/m^2$. The respective values at q equals 61.4 $kW/m^2$ are 198 % for SDS, 168 % for SLES and 128 % for Triton X-100. At q equals 101.9 $kW/m^2$, the respective values are 241% for SDS, 185% for SLES and 133 % for Triton X-100.

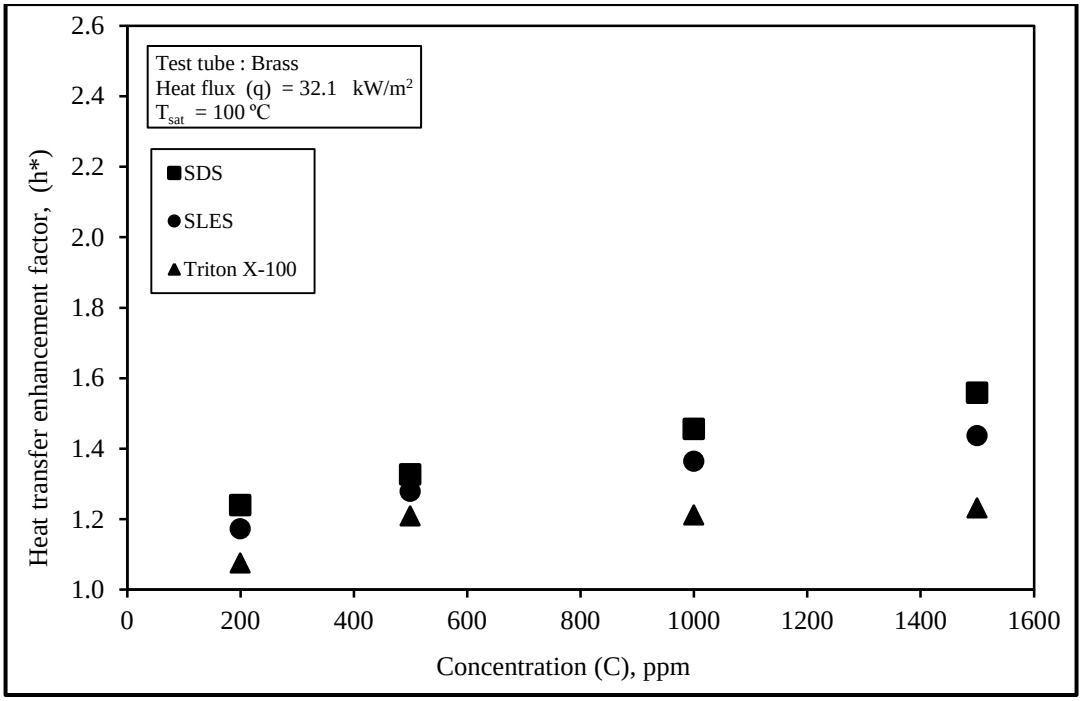


**Fig. 5.14a: Comparison between the three test surfactants for constant wall heat flux of 32.1 kW/m$^2$ using brass test tube**

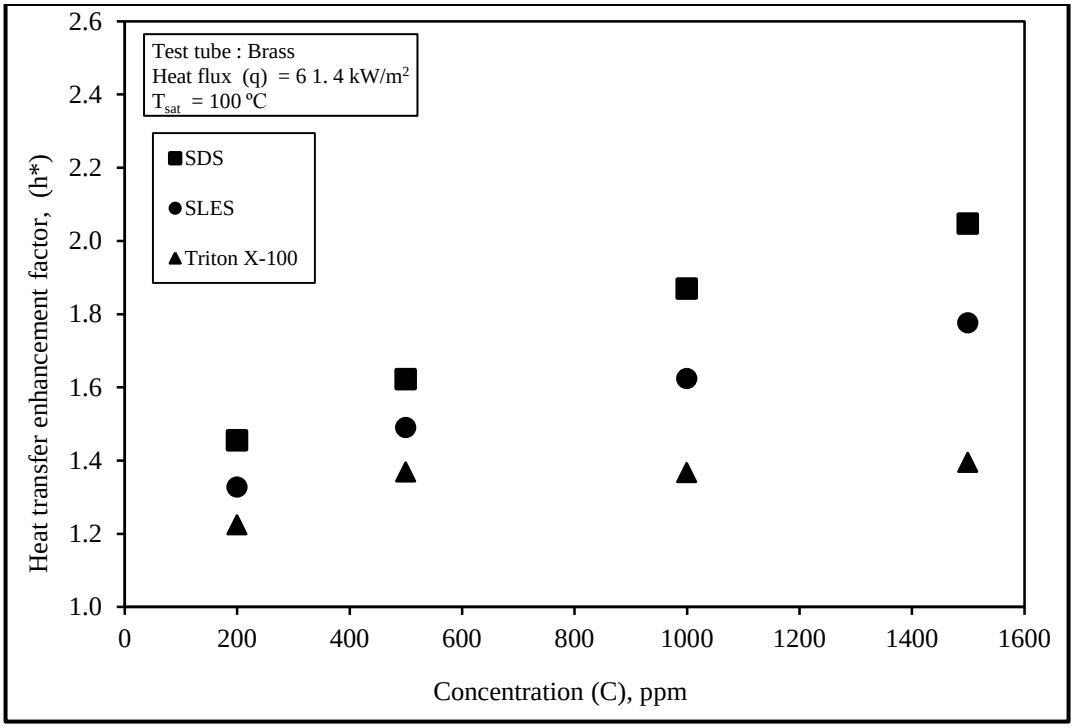


**Fig. 5.14b: Comparison between the three test surfactants for constant wall heat flux of 61.4 kW/m$^2$ using brass test tube**

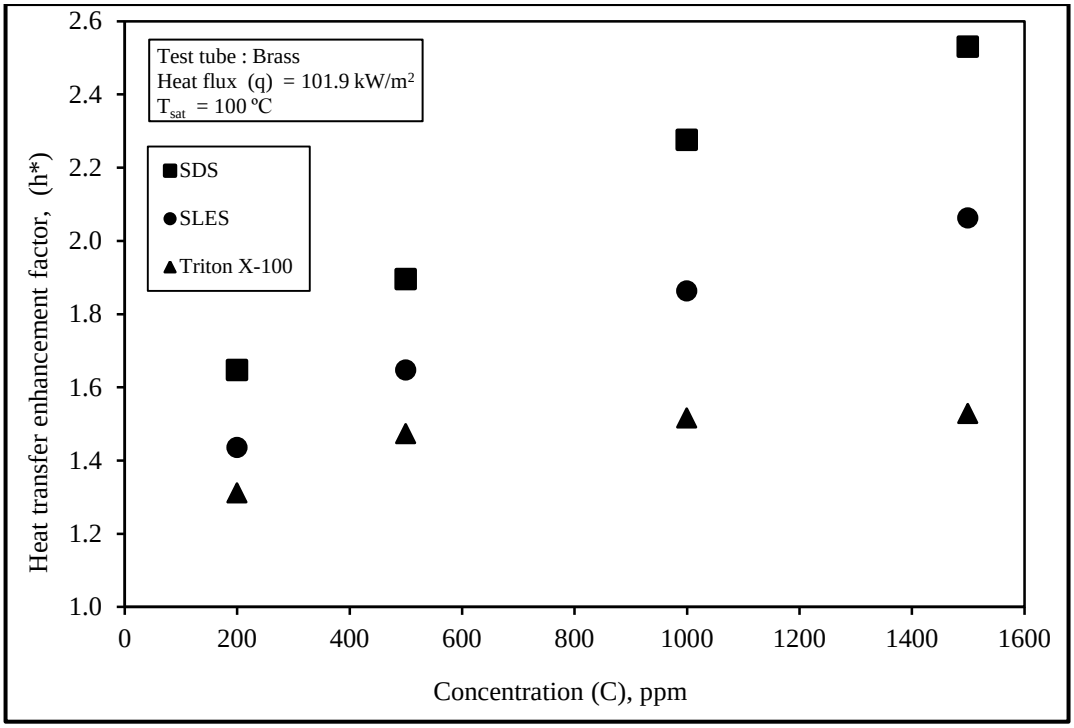


**Fig. 5.14c: Comparison between the three test surfactants for constant wall heat flux of 101.9 kW/m$^2$ using brass test tube**

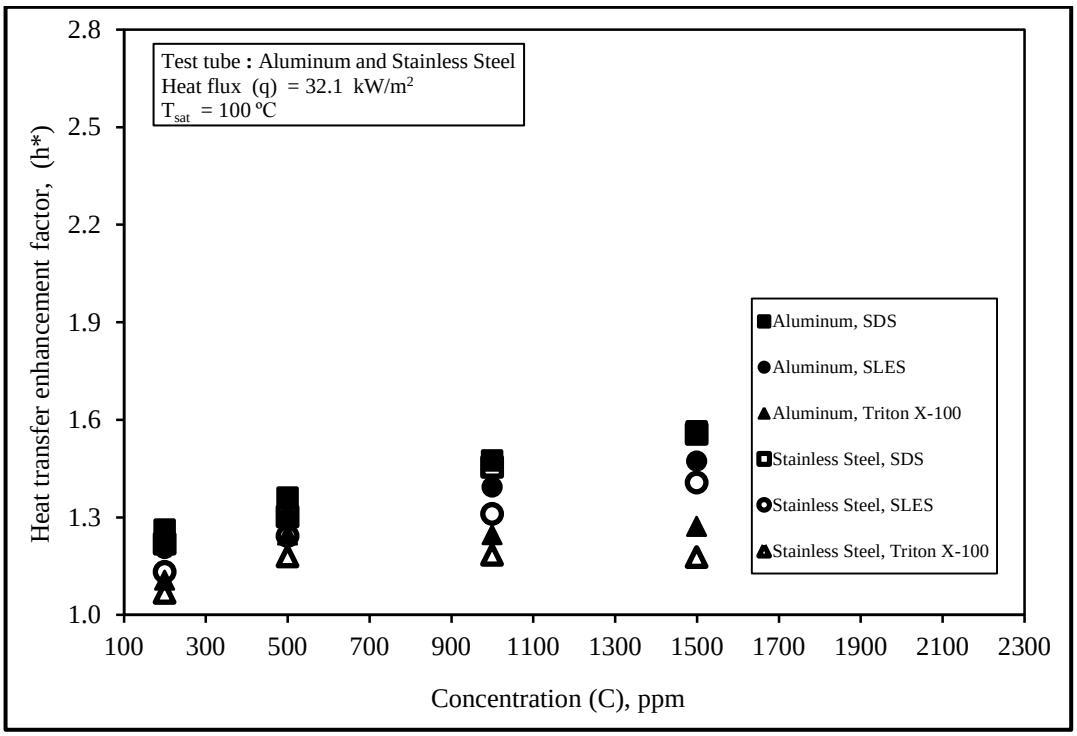


**Fig. 5.15a: Comparison between the three test surfactants for constant wall heat flux of 32.1 kW/m$^2$ using aluminum and stainless steel tubes**

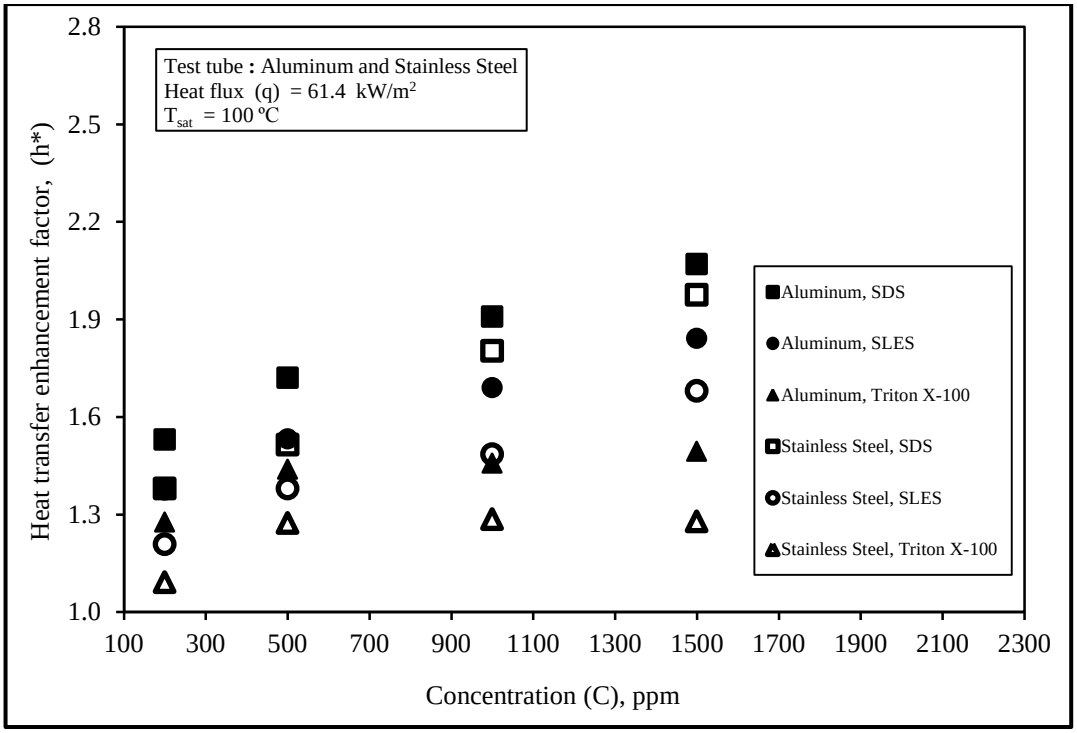


**Fig. 5.15b: Comparison between the three test surfactants for constant wall heat flux of 61.4 kW/m$^2$ using aluminum and stainless steel tubes**

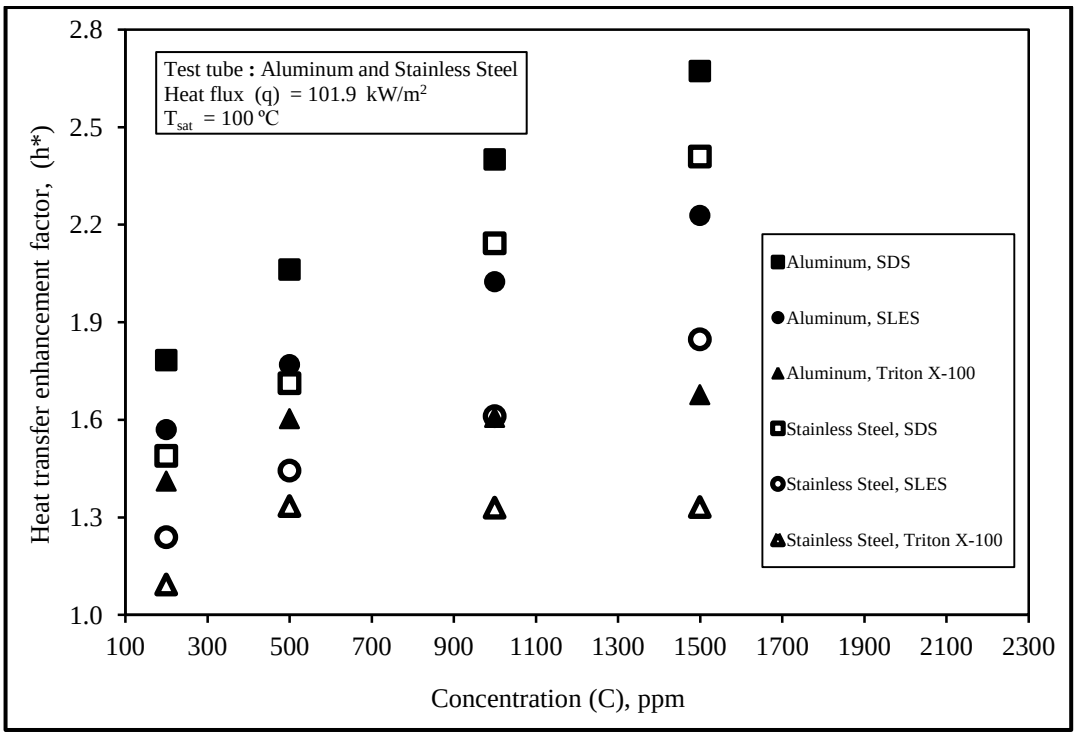


**Fig. 5.15c: Comparison between the three test surfactants for constant wall heat flux of 101.9 kW/m$^2$ using aluminum and stainless steel tubes**

## 5.5. Size distribution function, N(r) data

Figures 5.16 and 5.17 depict the size distribution function for the aqueous surfactant solutions, using test tubes S1, S2 and S3. From the semi- logarithmic representation of these Figures, it could be seen that the values of the active nucleation sites N/A increase as $r_c$ decreases. Also, it could be seen that N/A starts to increase with the addition of the surfactant to the test fluid, and increases sharply as the surfactant concentrations increase. The relation between the activated nucleation site density N/A and the minimum cavity radius $r_c$ for the three tested boiling surfaces with the three aqueous surfactant solutions SDS, SLES and Triton X-100 are summarized in Table 5.1.

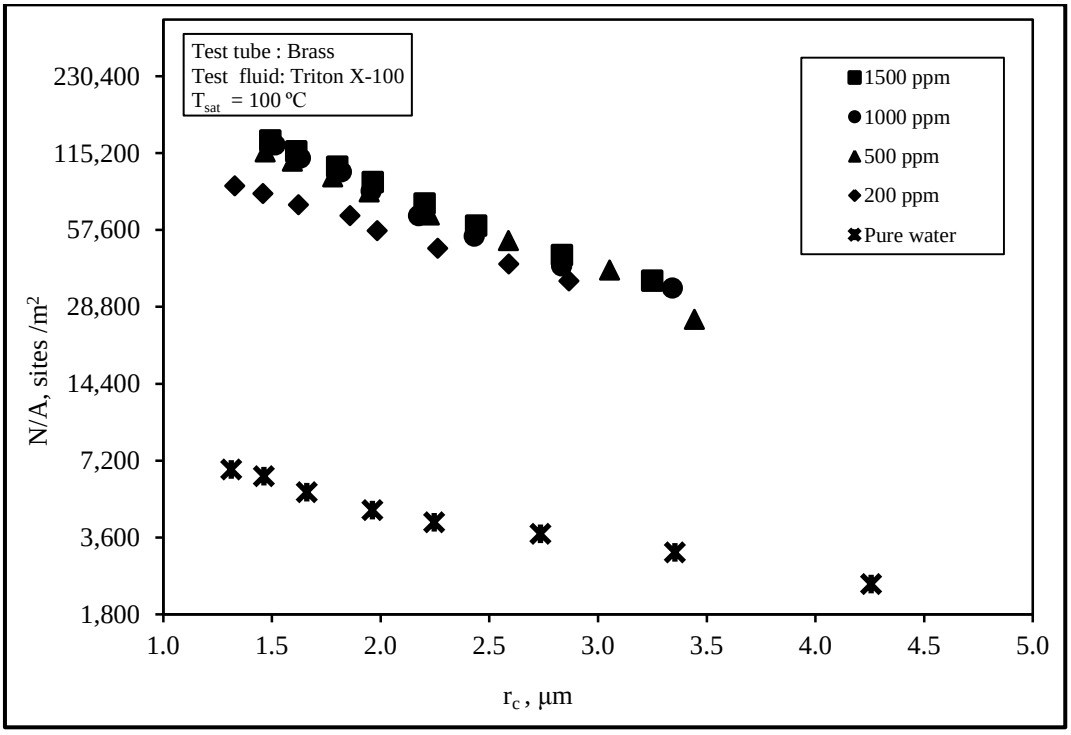


**Fig. 5.16a: Effect of Triton X-100 aqueous solution concentrations on the size distribution functions of brass test tube**

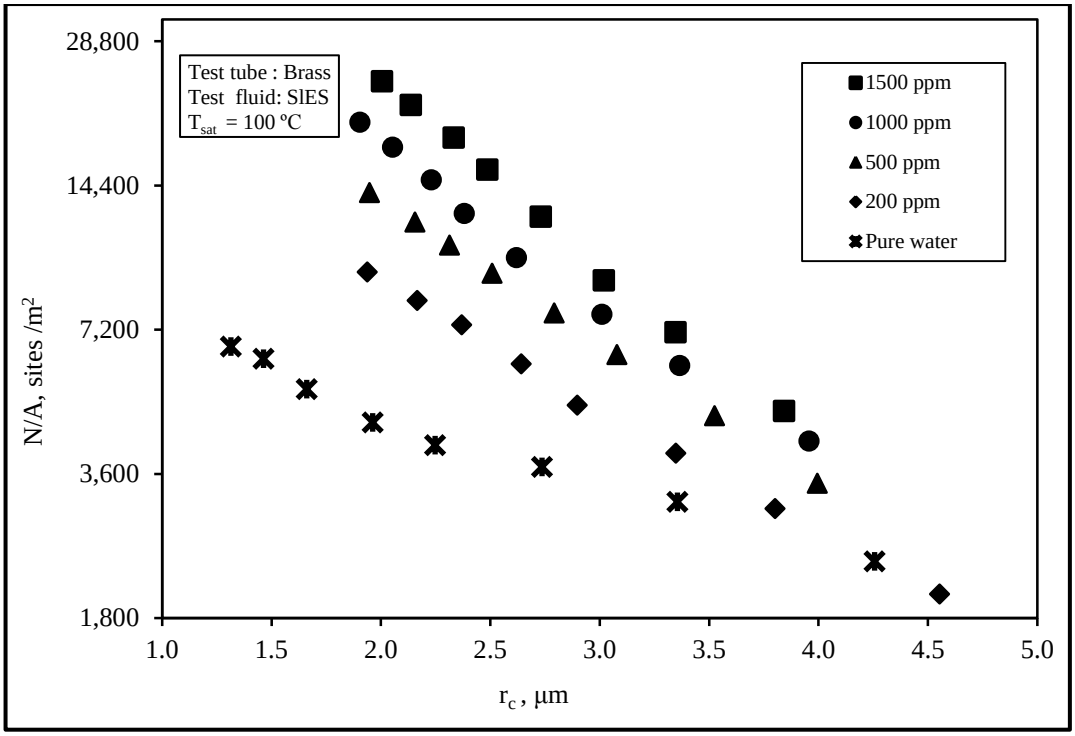


**Fig. 5.16b: Effect of SLES aqueous solution concentrations on the size distribution functions of brass test tube**

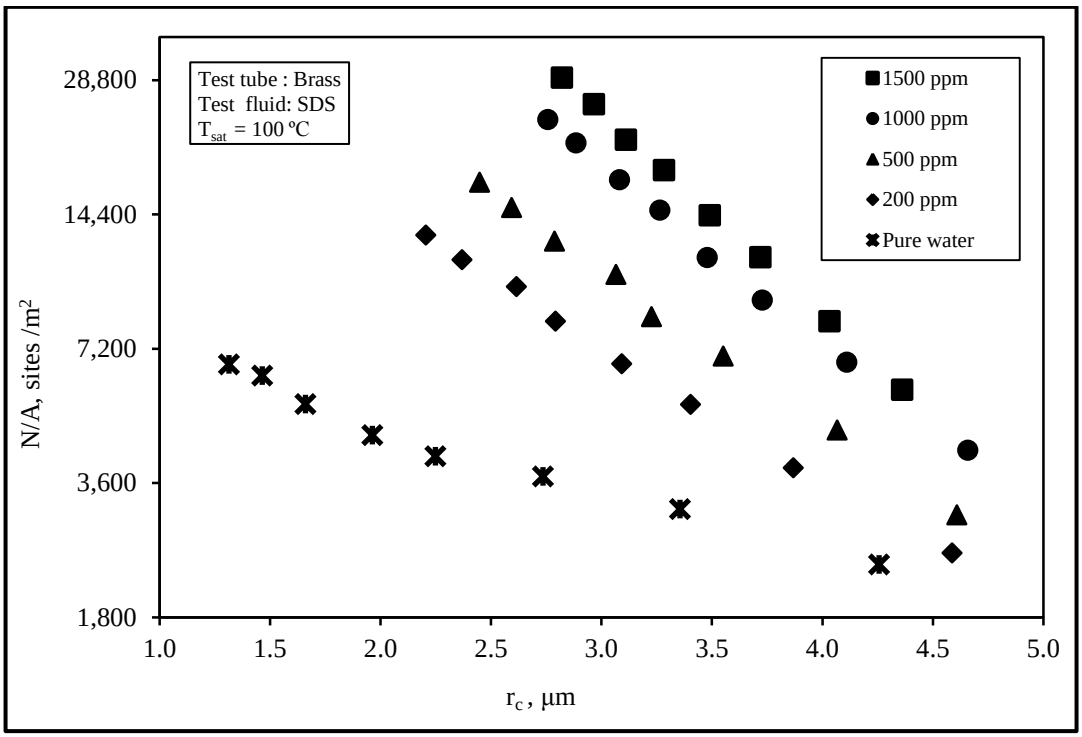


**Fig. 5.16c: Effect of SDS aqueous solution concentrations on the size distribution functions of brass test tube**

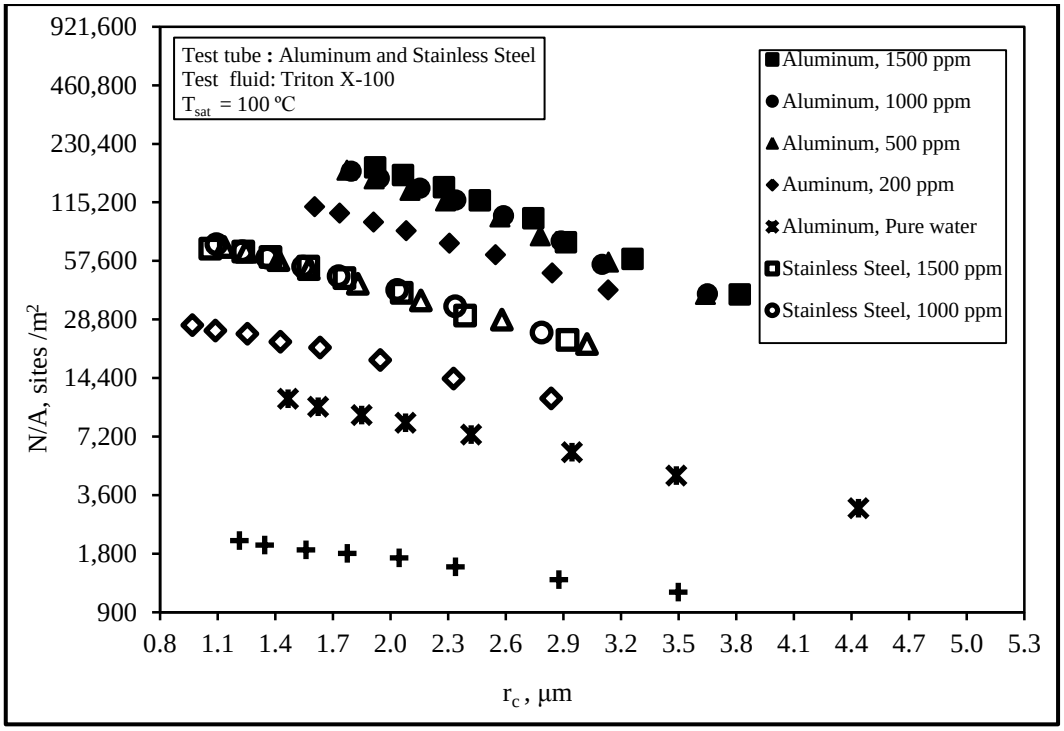


**Fig. 5.17a: Effect of Triton X-100 aqueous solution concentrations on the size distribution functions of aluminum and stainless steel test tubes**

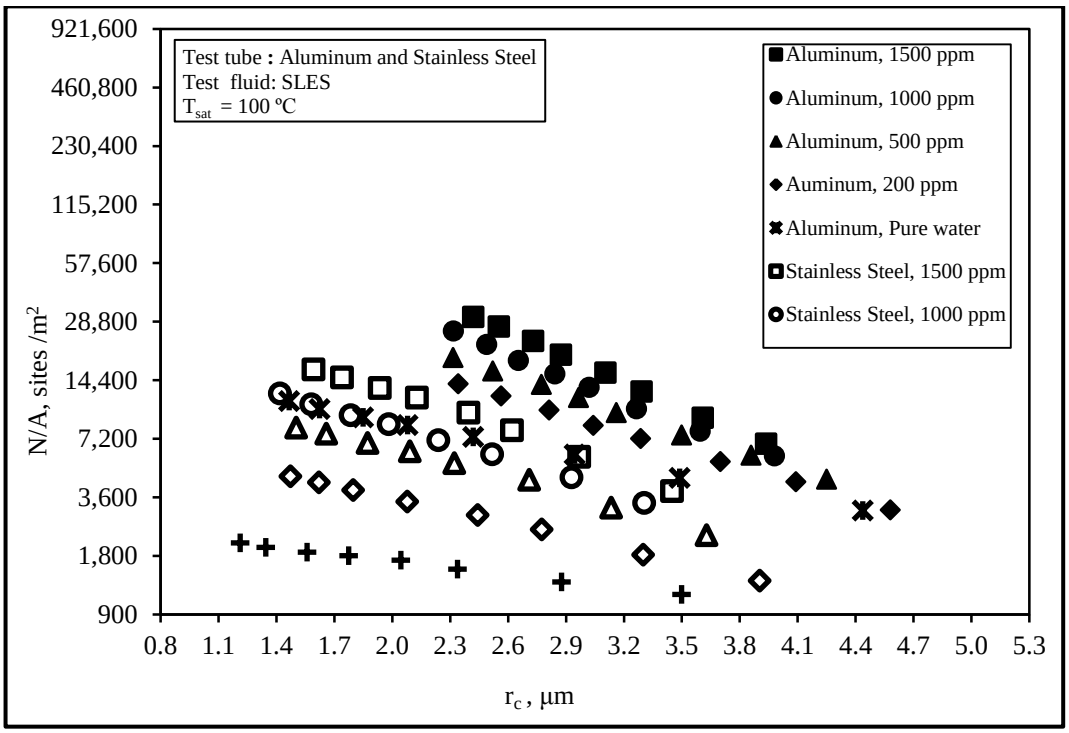


**Fig. 5.17b: Effect of SLES aqueous solution concentrations on the size distribution functions of aluminum and stainless steel test tubes**

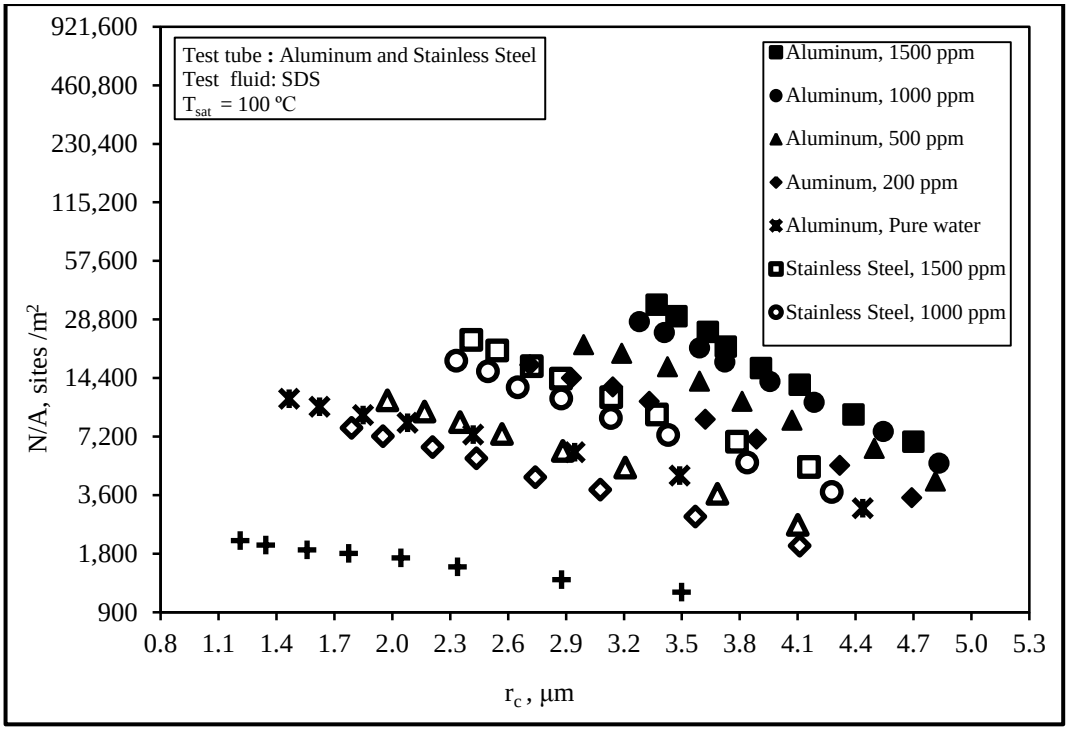


**Fig. 5.17c: Effect of SDS aqueous solution concentrations on the size distribution functions of aluminum and stainless steel test tubes**

From the semi-logarithmic representation of the above Figures, it is believed that the power function with constant exponent not to be able to express the present experimental data. So, it is found that by trail and error the interpolation lines in these diagrams may be expressed by the exponential function with a power term, Eq. 4.15. Appendix (C) gives the calculation of the three parametric distribution function constants ($\frac{N_{max}}{A}$, $r_{st}$ and m).

The experimental h-q relation may be described fairly well by curves calculated with the same three parametric distribution function constants, although only approximate expressions for the bubble frequency f and the bubble diameter $D_b$ are used in the calculation of N(r). On the other hand, the constants ($\frac{N_{max}}{A}$, $r_{st}$ and m) for the three aqueous surfactant solutions are given in table (5.2).

**Table 5.1: Form of the size distribution function N(r) for the tested surfaces**

| Test tube | Test fluid | Concentration, ppm | Form of N(r) |
|---|---|---|---|
| brass ,S1 | water | | $N/A = 9655.4\ \mathbf{e}^{-339.97r}$ |
| | Triton X-100 | 200 | $N/A = 181681.1\ \mathbf{e}^{-565.6\ r}$ |
| | | 500 | $N/A = 343152.71\mathbf{e}^{-731.86\ r}$ |
| | | 1000 | $N/A = 353046.91\ \mathbf{e}^{-732.81\ r}$ |
| | | 1500 | $N/A = 379106.33\ \mathbf{e}^{-735.94\ r}$ |
| | SLES | 200 | $N/A = 29740.16\ \mathbf{e}^{-596.81\ r}$ |
| | | 500 | $N/A = 52368.25\ \mathbf{e}^{-681.59\ r}$ |
| | | 1000 | $N/A = 78719.7\ \mathbf{e}^{-755.73\ r}$ |
| | | 1500 | $N/A = 138591.72\ \mathbf{e}^{-881.71\ r}$ |
| | SDS | 200 | $N/A = 59127.53\ \mathbf{e}^{-696.97r}$ |
| | | 500 | $N/A = 113994.94\ \mathbf{e}^{-786.58\ r}$ |
| | | 1000 | $N/A = 280024.67\ \mathbf{e}^{-905.67r}$ |
| | | 1500 | $N/A = 551268.36\ \mathbf{e}^{-1042.03\ r}$ |
| aluminum, S2 | water | | $N/A = 20834.26\ \mathbf{e}^{-431.88\ r}$ |
| | Triton X-100 | 200 | $N/A = 311058.67\ \mathbf{e}^{-642.79\ r}$ |
| | | 500 | $N/A = 709929.77\mathbf{e}^{-797.18\ r}$ |
| | | 1000 | $N/A = 765693.62\ \mathbf{e}^{-818.43\ r}$ |
| | | 1500 | $N/A = 863044.25\ \mathbf{e}^{-819.65\ r}$ |
| | SLES | 200 | $N/A = 65179.73\ \mathbf{e}^{-665.83\ r}$ |
| | | 500 | $N/A = 107693.71\ \mathbf{e}^{-752.37\ r}$ |
| | | 1000 | $N/A = 200791.82\ \mathbf{e}^{-897.42\ r}$ |
| | | 1500 | $N/A = 352464.84\ \mathbf{e}^{-1005.6\ r}$ |
| | SDS | 200 | $N/A = 148232.5\ \mathbf{e}^{-787.59\ r}$ |
| | | 500 | $N/A = 331269.34\ \mathbf{e}^{-892.86\ r}$ |
| | | 1000 | $N/A = 934075.99\ \mathbf{e}^{-1065.85\ r}$ |
| | | 1500 | $N/A = 2137464.3\ \mathbf{e}^{-1233.54\ r}$ |

| Test tube | Test fluid | Concentration, ppm | Form of N(r) |
|---|---|---|---|
| stainless steel, S3 | water | | $N/A = 2874.27\ \mathbf{e}^{-265.48\ r}$ |
| | Triton X-100 | 200 | $N/A = 42914.99\ \mathbf{e}^{-466.1\ r}$ |
| | | 500 | $N/A = 136079.23\mathbf{e}^{-609.56\ r}$ |
| | | 1000 | $N/A = 137185.3\ \mathbf{e}^{-607.55\ r}$ |
| | | 1500 | $N/A = 136118.94\ \mathbf{e}^{-613.55\ r}$ |
| | SLES | 200 | $N/A = 9834.48\ \mathbf{e}^{-507.3\ r}$ |
| | | 500 | $N/A = 21024.21\ \mathbf{e}^{-597.84\ r}$ |
| | | 1000 | $N/A = 31782.13\ \mathbf{e}^{-669.9\ r}$ |
| | | 1500 | $N/A = 59105.41\ \mathbf{e}^{-776.82\ r}$ |
| | SDS | 200 | $N/A = 32458.72\ \mathbf{e}^{-597.6\ r}$ |
| | | 500 | $N/A = 42054.53\ \mathbf{e}^{-674.11\ r}$ |
| | | 1000 | $N/A = 109374.33\ \mathbf{e}^{-790.65\ r}$ |
| | | 1500 | $N/A = 172830.79\ \mathbf{e}^{-857.36\ r}$ |

**Table 5.2a: Values of ($N_{max}/A$, $r_{st}$ and m) for brass test tube with the three aqueous surfactant solutions**

| Test tube | Test fluid | Concentration, ppm | $N_{max}/A$, sites/$m^2$ | $r_{st}$, µm | m |
|---|---|---|---|---|---|
| brass (S1) | water | | 9631.82 | 2.706 | 1 |
| | Triton X-100 | 200 | 181639.1 | 2.142 | 1 |
| | | 500 | 344003.66 | 1.747 | 0.998 |
| | | 1000 | 353045.75 | 1.743 | 1 |
| | | 1500 | 378117.24 | 1.741 | 1.002 |
| | SLES | 200 | 29023.82 | 1.691 | 1.018 |
| | | 500 | 52378.05 | 1.594 | 1 |
| | | 1000 | 78435.91 | 1.489 | 1.002 |
| | | 1500 | 167702.11 | 1.339 | 1.003 |
| | SDS | 200 | 58584.87 | 1.569 | 1.005 |
| | | 500 | 111794.5 | 1.471 | 1.008 |
| | | 1000 | 276827.17 | 1.381 | 1.004 |
| | | 1500 | 534463.19 | 1.262 | 1.009 |

**Table 5.2b: Values of ($N_{max}/A$, $r_{st}$ and m) for aluminum test tube with the three aqueous surfactant solutions**

| Test tube | Test fluid | Concentration, ppm | $N_{max}/A$, sites/$m^2$ | $r_{st}$, µm | m |
|---|---|---|---|---|---|
| Aluminum(S2) | water | | 20954.15 | 2.306 | 0.999 |
| | Triton X-100 | 200 | 311114.78 | 1.967 | 1 |
| | | 500 | 712229.1 | 1.694 | 0.998 |
| | | 1000 | 765766.22 | 1.655 | 1 |
| | | 1500 | 863016.66 | 1.668 | 1 |
| | SLES | 200 | 65257.82 | 1.664 | 1 |
| | | 500 | 107708.41 | 1.54 | 1 |
| | | 1000 | 200861.19 | 1.36 | 1 |
| | | 1500 | 349586.92 | 1.267 | 1.003 |
| | SDS | 200 | 146734.17 | 1.507 | 1.004 |
| | | 500 | 327058.75 | 1.42 | 1.004 |
| | | 1000 | 899470.75 | 1.283 | 1.01 |
| | | 1500 | 2034259.68 | 1.175 | 1.011 |

**Table 5.2c: Values of ($N_{max}/A$, $r_{st}$ and m) for stainless steel test tube with the three aqueous surfactant solutions**

| Test tube | Test fluid | Concentration, ppm | $N_{max}/A$, sites/$m^2$ | $r_{st}$, µm | m |
|---|---|---|---|---|---|
| Stainless Steel (S3) | water | | 2868.3 | 2.962 | 1.005 |
| | Triton X-100 | 200 | 42831.51 | 2.276 | 1.003 |
| | | 500 | 136198.7 | 1.942 | 0.999 |
| | | 1000 | 136789.25 | 1.938 | 1.003 |
| | | 1500 | 136142.3 | 1.926 | 1 |
| | SLES | 200 | 9731.58 | 1.793 | 1.009 |
| | | 500 | 20828.95 | 1.677 | 1 |
| | | 1000 | 31827.7 | 1.552 | 0.998 |
| | | 1500 | 59457.25 | 1.42 | 1.006 |
| | SDS | 200 | 23274.45 | 1.672 | 1.006 |
| | | 500 | 41520.33 | 1.581 | 1.003 |
| | | 1000 | 107804.18 | 1.458 | 1.008 |
| | | 1500 | 167603.42 | 1.392 | 1.013 |

## 5.6. Effect of aqueous surfactant solution type and its concentration on the size distribution function's constants

Figure 5.18 depicts the relation between the exponent m, deduced from the three-parametric distribution functions calculated from the heat transfer measurements of the three tested boiling surfaces using the three aqueous surfactant solutions (SDS, SLES and Triton X-100) and the concentration, C. It seems that the exponent m of the present results is not affected by the concentration, the aqueous surfactant solutions type and the material of the test tubes. It could be concluded that the exponent m may be considered as a constant equal to unity.

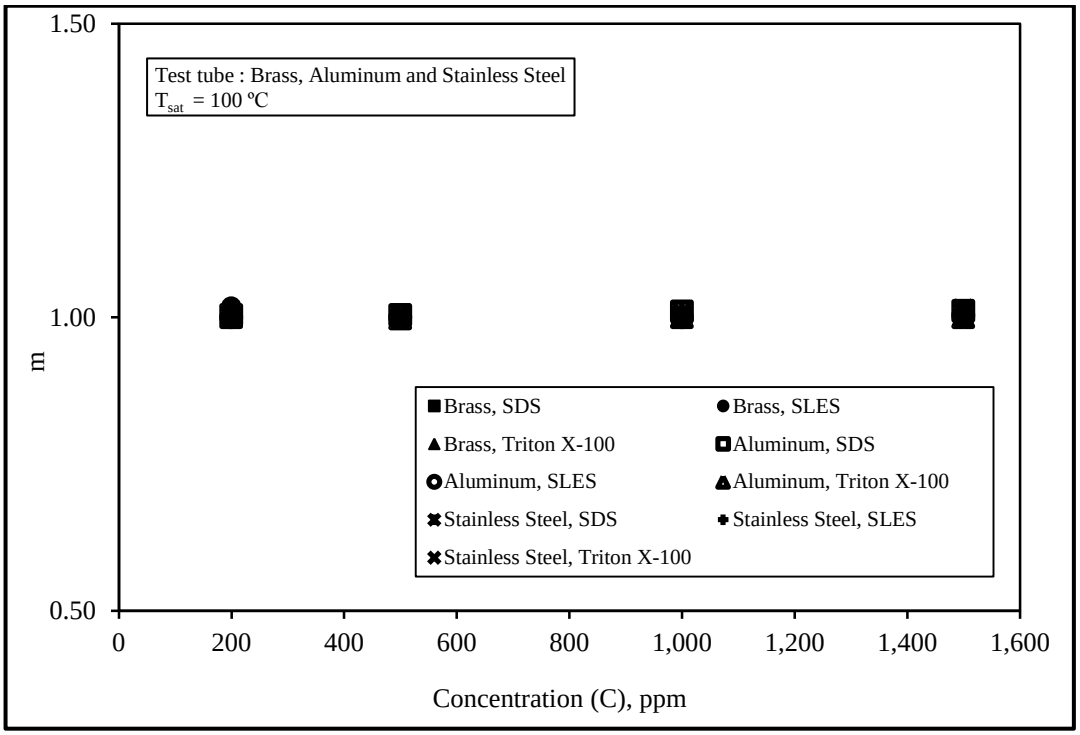


**Fig. 5.18: Effect of surfactant type on the variation of size distribution function exponent m with concentration for the three test tubes brass, aluminum and stainless steel**

Figures 5.19 and 5.20 depict the relation between the constant $r_{st}$ of the three tested boiling surfaces with the three aqueous surfactant solutions (SDS, SLES and Triton X-100) and the concentration, C. It is noted from the present results that the constant $r_{st}$ decreases with the increase of the concentration, C**.** On the other hand, the results of $r_{st}$ showed a similar trend for the three aqueous surfactant solutions. This behavior is similar for the three tested boiling surfaces S1, S2 and S3.

Figures 5.21 and 5.22 depict the relation between the constant $r_{st}$ of the three tested boiling surfaces with the three aqueous surfactant solutions (SDS, SLES and Triton X-100) and the concentration, C. It is noted from the present results that the active nucleation sites density $N_{max}/A$ increases with the increase of the concentration, C**.** On the other hand, the results of $N_{max}/A$ showed a similar trend for the three aqueous surfactant solutions. In addition, for the Triton X-100 the $N_{max}/A$ values are the highest, followed by SDS and then SLES. This behavior is similar for the three tested boiling surfacesS1, S2 and S3. This is reasoned to be due to the smaller contact angle associated with Triton X-100 aqueous solution. It could be observed from these Figures that the most surprising result is that there is no increase in $N_{max}/A$ for any level of concentration, C when using aqueous Triton X-100 solutions with concentrations more than 500 ppm. This is true for the three test tubes. This is related to the fact that the variation of surface tension with concentration for Triton X-100 is constant above solution concentration of 500 ppm as shown in Figure 4.10**.**

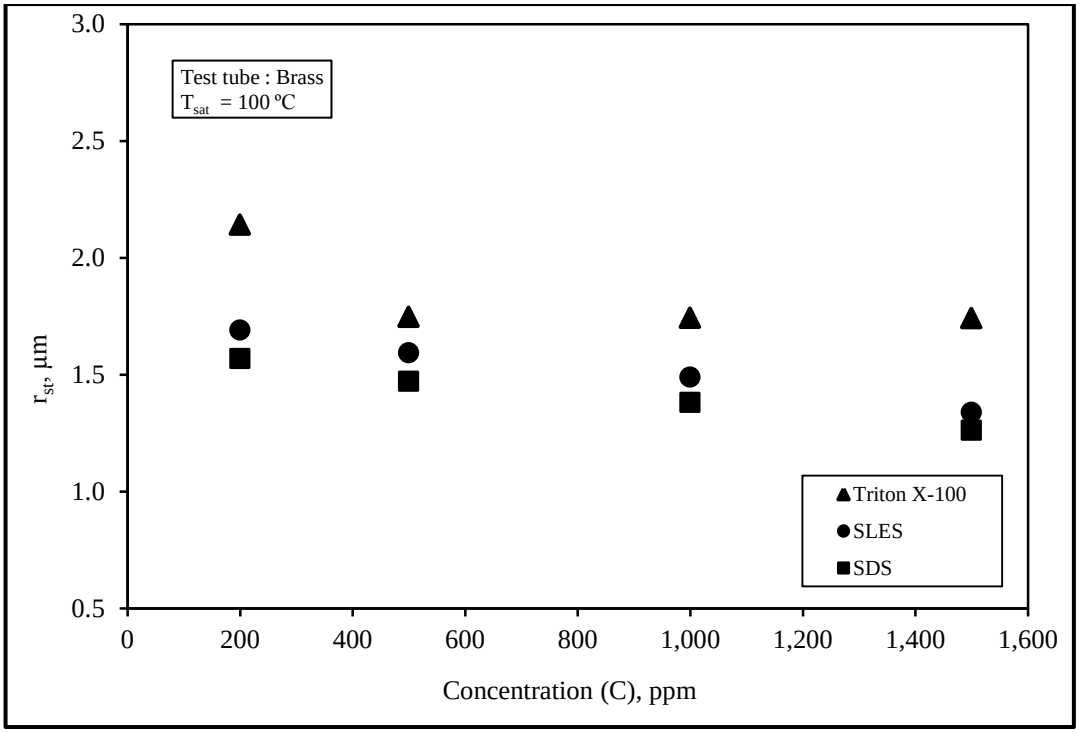


**Fig. 5.19: Effect of surfactant type on the variation of size distribution function constant $r_{st}$ with the concentration for brass test tube**

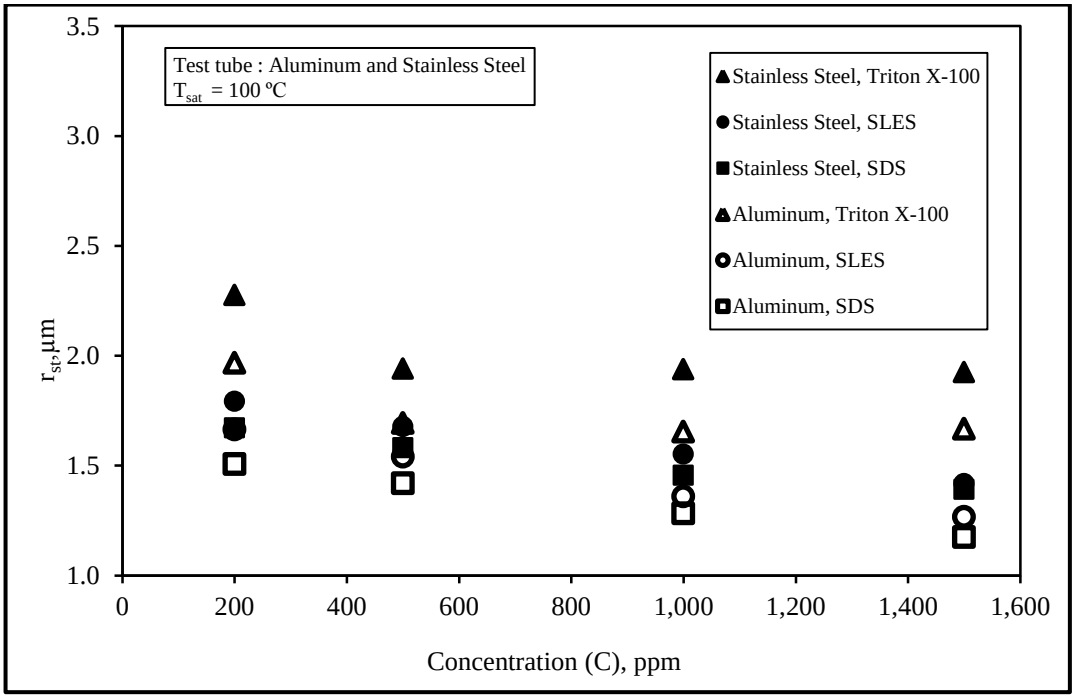


**Fig. 5.20: Effect of surfactant type on the variation of size distribution function constants $r_{st}$ with the concentration for aluminum and stainless steel tubes**

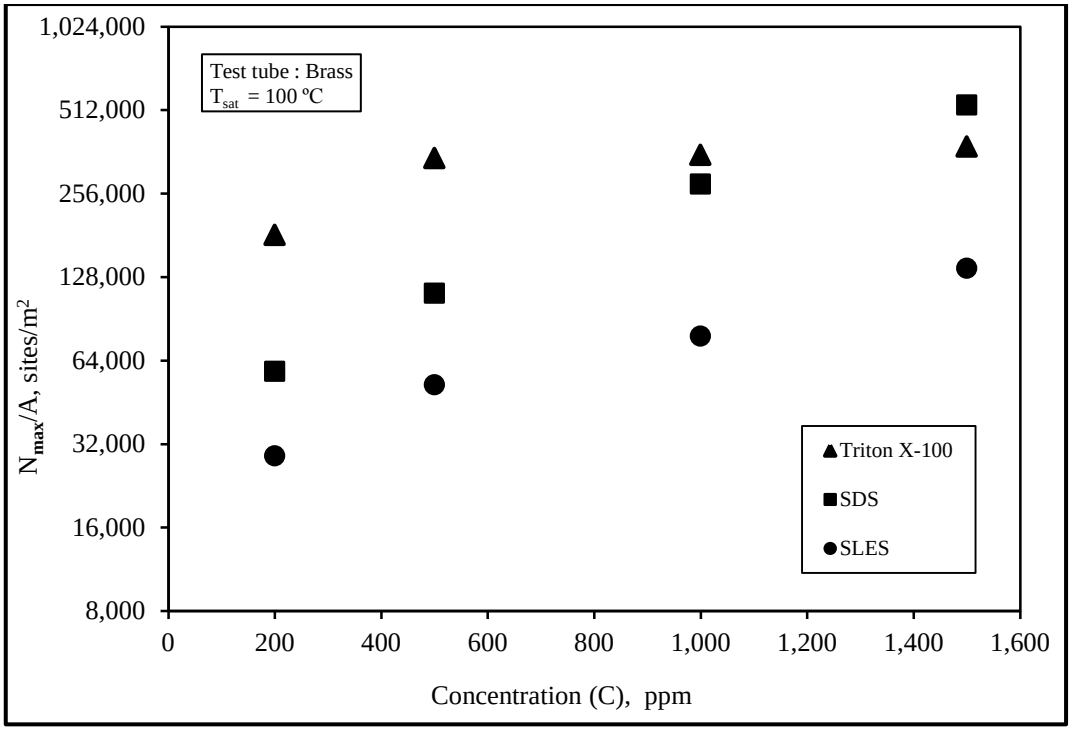


**Fig. 5.21: Effect of surfactant type on the variation of size distribution function constant $N_{max}/A$ with concentration for brass test tube**

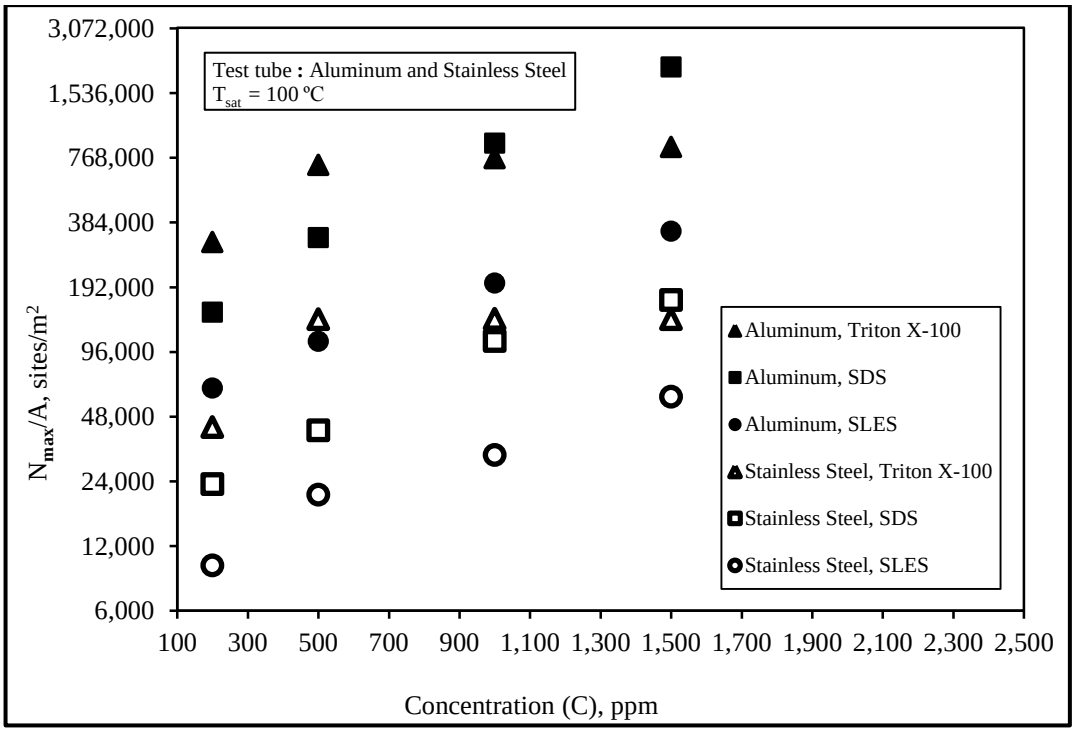


**Fig. 5.22: Effect of surfactant type on the variation of size distribution function constants $N_{max}/A$ with concentration, for aluminum and stainless steel tubes**

Figures 5.23 and 5.24 depicts the relation between the constant $N_{max}/A$ of the three tested boiling surfaces with the three aqueous surfactant solutions (SDS, SLES and Triton X-100) as a function of the constant $r_{st}$ in semi- logarithmic scales. It seems that all the results indicate that as the minimum cavity radius $r_{st}$ decreases, the activated nucleation site density $N_{max}/A$ is increased. On the other hand, the results of $r_{st}$ and $N_{max}/A$ showed a similar trend for the three aqueous surfactant solutions. In addition higher the $N_{max}/A$ values for the Triton X-100 are reached, followed by SDS and then SLES. This behavior is similar for the three tested boiling surfacesS1, S2 and S3with different amounts, depending on the contact angle, the departure diameter and departure frequency.

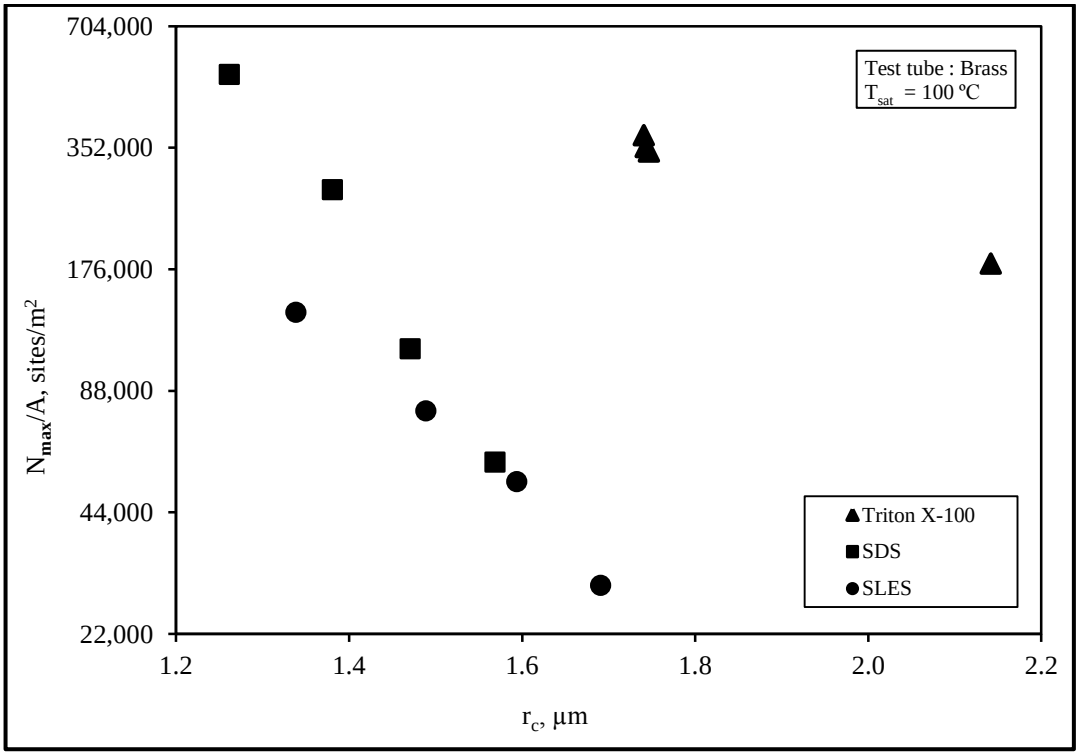


**Fig. 5.23: Variation of $N_{max}/A$ with $r_{st}$ for different aqueous solutions of SDS, SLES and Triton X-100 using brass test tube**

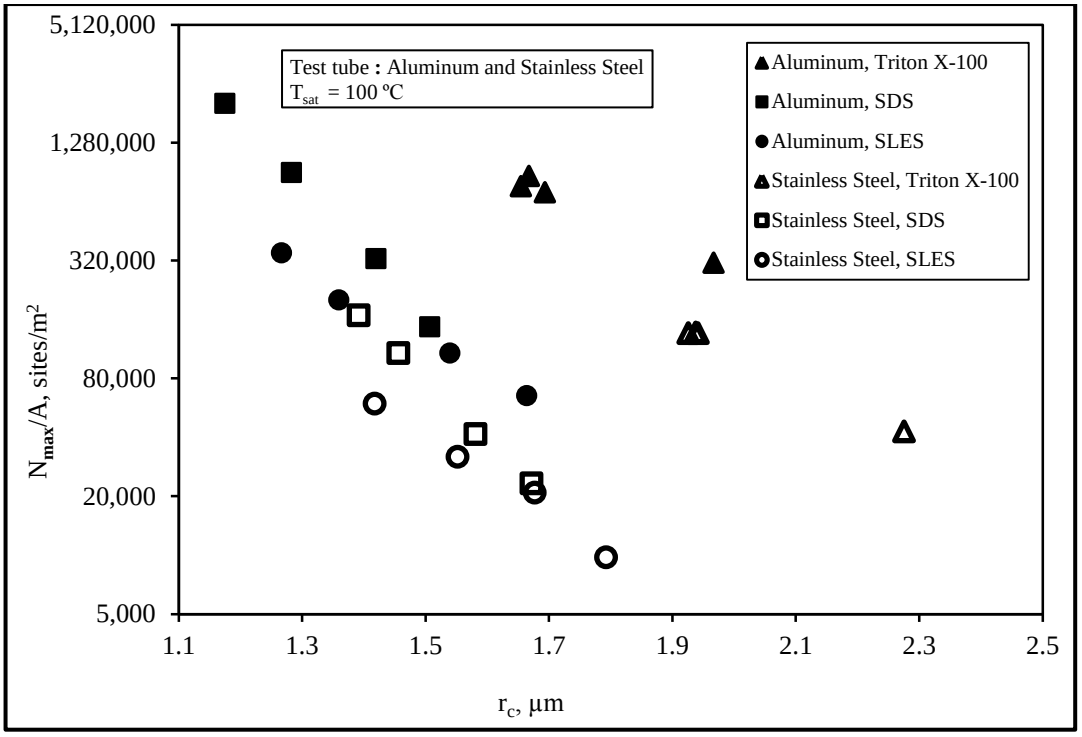


**Fig. 5.24: Variation of $N_{max}/A$ with $r_{st}$ for different aqueous solutions of SDS, SLES and Triton X-100 using aluminum and stainless steel tubes**

## 5.7. Effect of the concentrations of the aqueous surfactant solutions on the variation of N/A with q

Figures 5.25 and 5.26 depicts the relation between the active nucleation sites density N/A of the three tested boiling surfaces with the three aqueous surfactant solutions (SDS, SLES and Triton X-100) as a function of the heat flux q in semi- logarithmic scales. It is noted from the present results that the active nucleation sites density N/A increases with the increase of the heat flux q**.** On the other hand, the results of N/A showed a similar trend for the three aqueous surfactant solutions. In addition for the Triton X-100 the N/A values is the highest, followed by SDS and then SLES. This behavior is similar for the three tested boiling surfaces S1, S2 and S3.

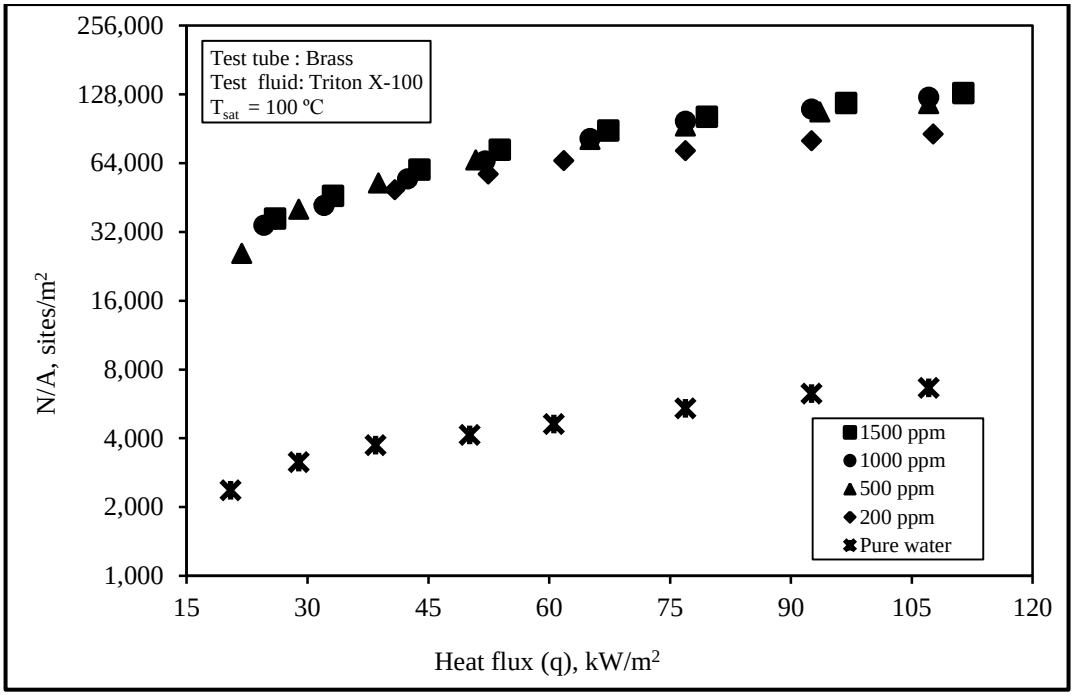


**Fig. 5.25a: Effect of aqueous Triton X-100 solution concentration on the variation of N/A with q for brass test tube**

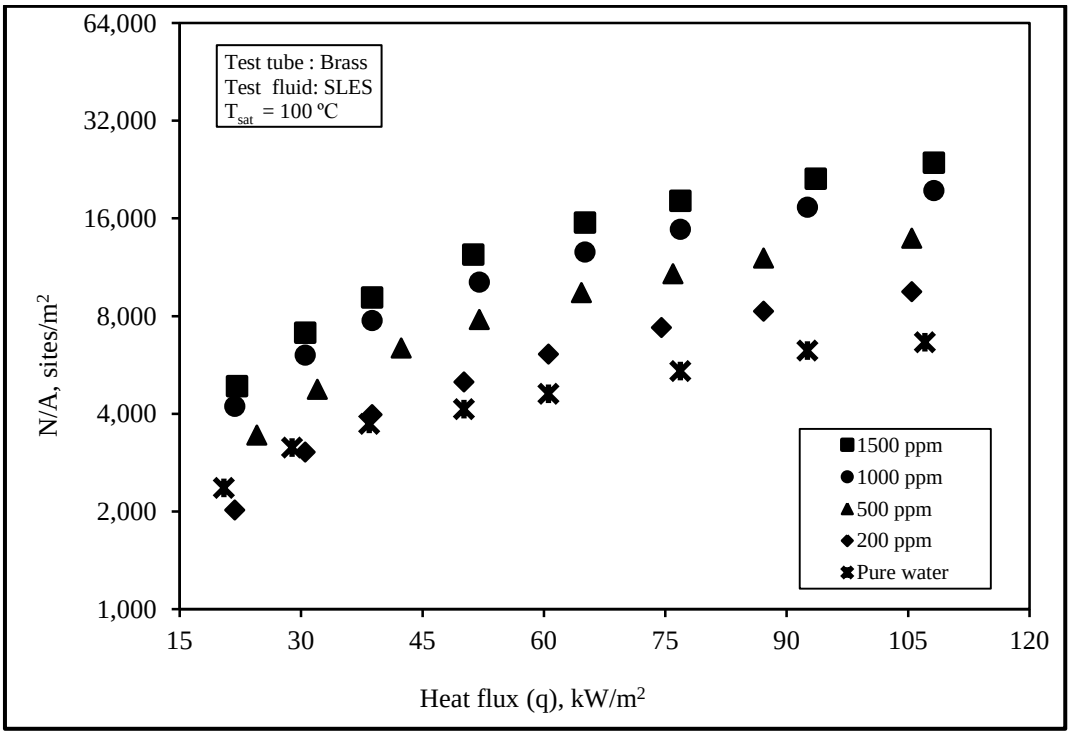


**Fig. 5.25b: Effect of aqueous SLES solution concentration on the variation of N/A with q for brass test tube**

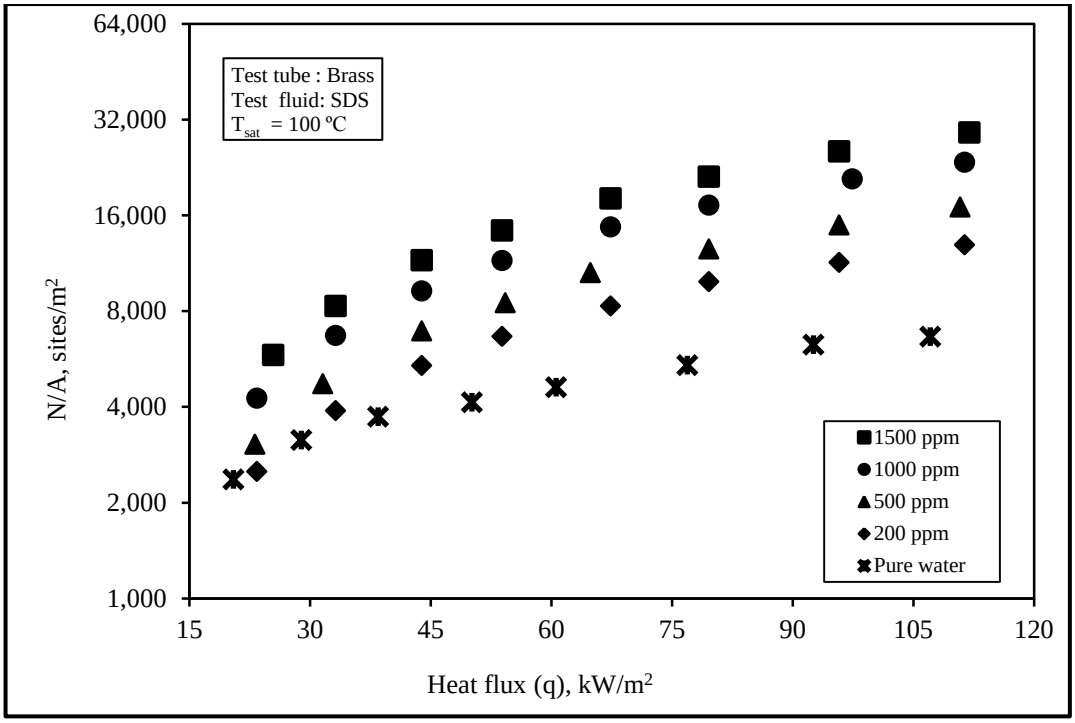


**Fig. 5.25c: Effect of aqueous SDS solution concentration on the variation of N/A with q for brass test tube**

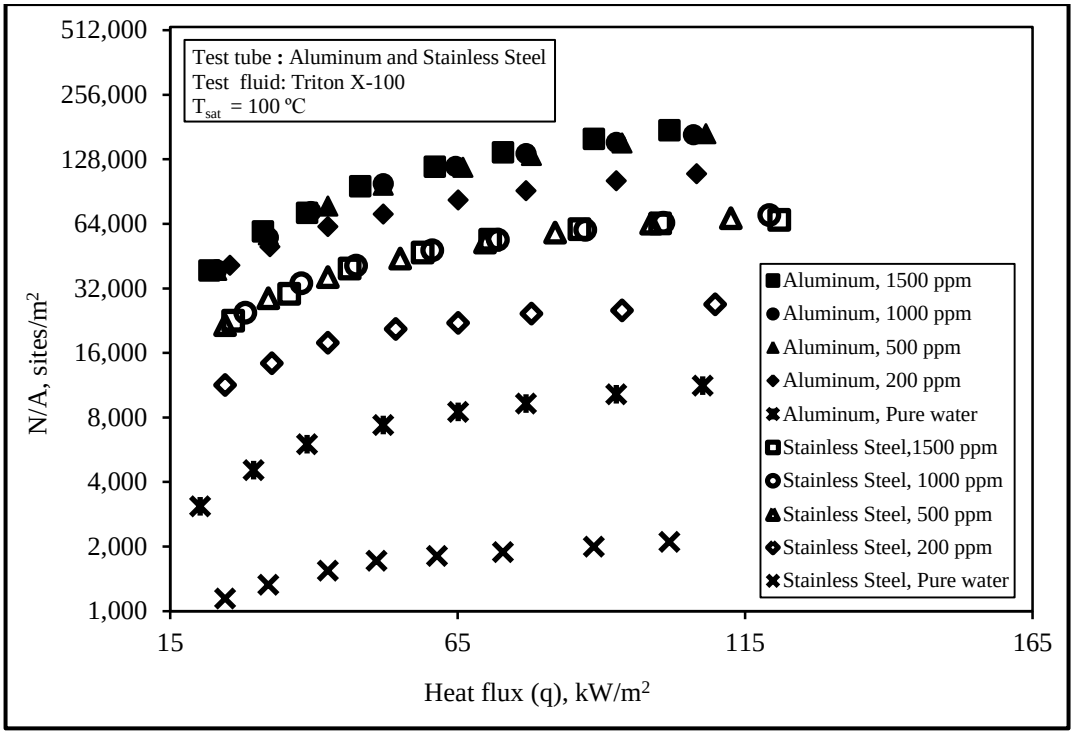


**Fig. 5.26a: Effect of aqueous Triton X-100 solution concentration on the variation of N/A with q for aluminum and stainless steel tubes**

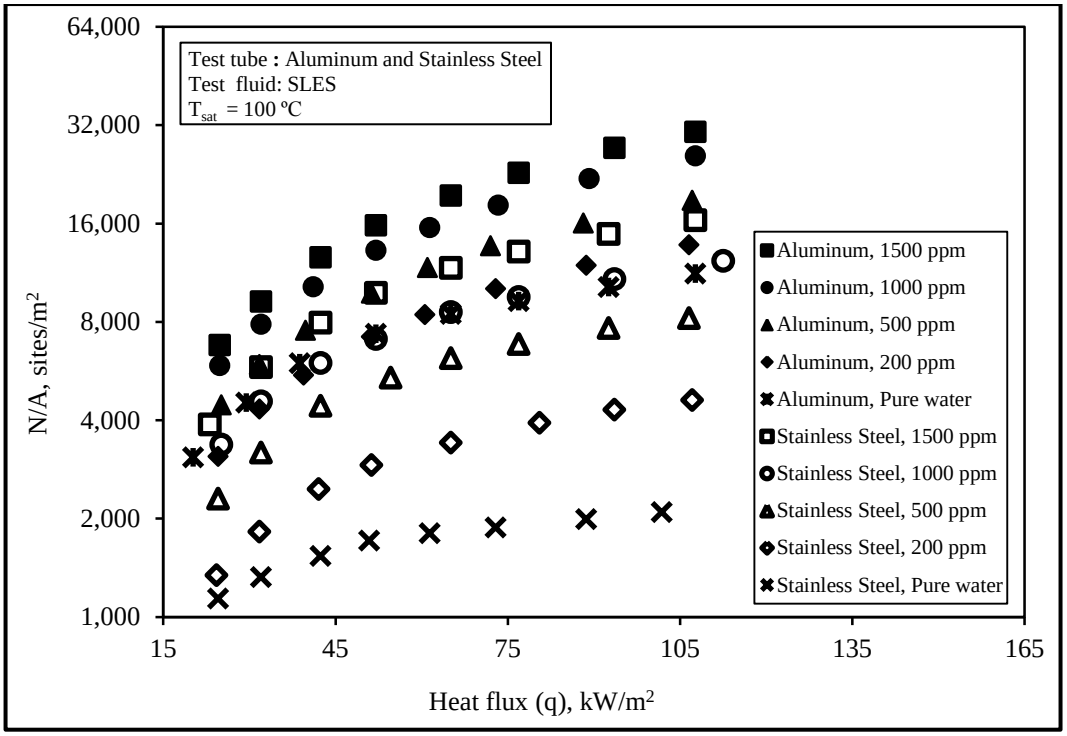


**Fig. 5.26b: Effect of aqueous SLES solution concentration on the variation of N/A with q for aluminum and stainless steel tubes**

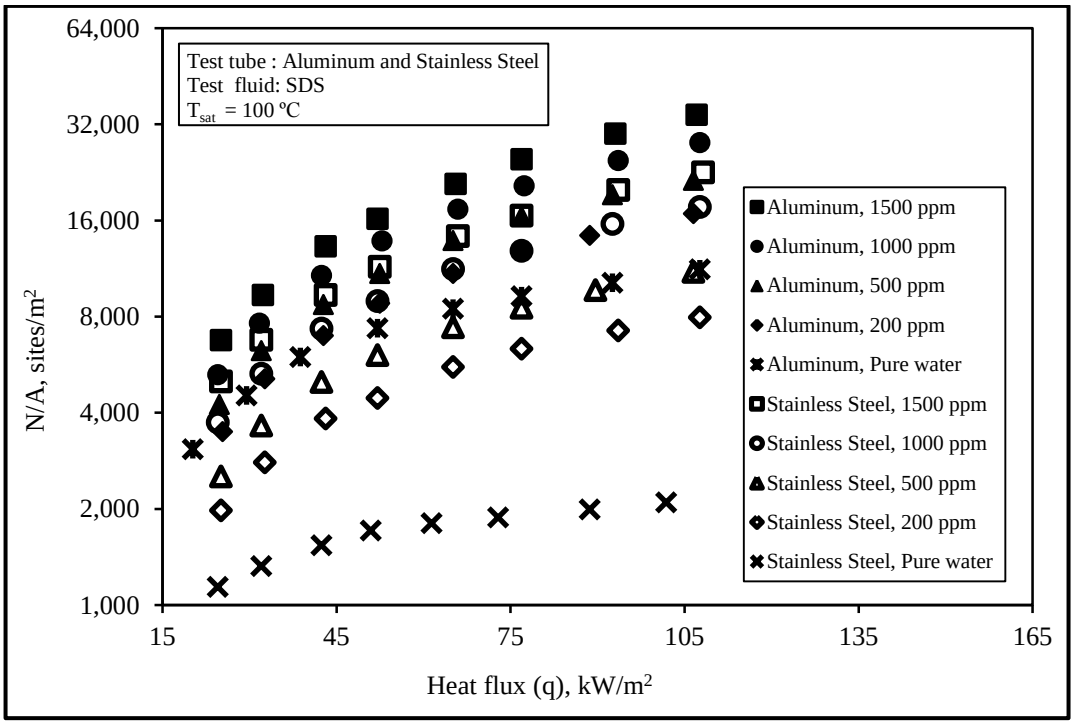


**Fig. 5.26c: Effect of aqueous SDS solution concentration on the variation of N/A with q for aluminum and stainless steel tubes**

## 5.8. Effect of test tube material on the pool boiling data

The influence of test tube material on the pool boiling data of aqueous surfactant solutions is discussed through the following Figures.

Figure 4.12 shows the influence of test tube material on the pool boiling data of pure distilled water. It is indicated that for a given tube wall heat flux q; the aluminum test tube introduces the lowest wall superheat, $T_w - T_{sat}$ followed by brass tube and then the stainless steel one. This means that the aluminum tube, S2 provides the same number of active nucleation site by smaller wall temperature, $T_w$. This is related to the better thermal conductivity of aluminum compared with brass and stainless steel tubes.

Figure 5.1 compares the pool boiling data of the three test tube materials S1, S2 and S3, using pure distilled water. It is seen that for a given tube material, increasing the wall heat flux, q increases the heat transfer coefficient, h. This is true for the three test materials. This is attributed to the fact that increasing q increases the number of nucleation sites which promotes h. Also, for a given q, aluminum tube, S2 introduces the highest h. This is related to the largest number of nucleation sites activated from it, due to its better thermal conductivity.

Figure 5.27 indicates the effect of tube material on the variation of h* with q, using aqueous SLES solution 1000 ppm. It is seen that for a given q, aluminum test tube gives the highest enhancement due to its better thermal properties in comparison with brass and stainless steel tubes.

Figure 5.28 ensures the same result, when using aqueous SDS and Triton X-100 solutions with the same concentration.

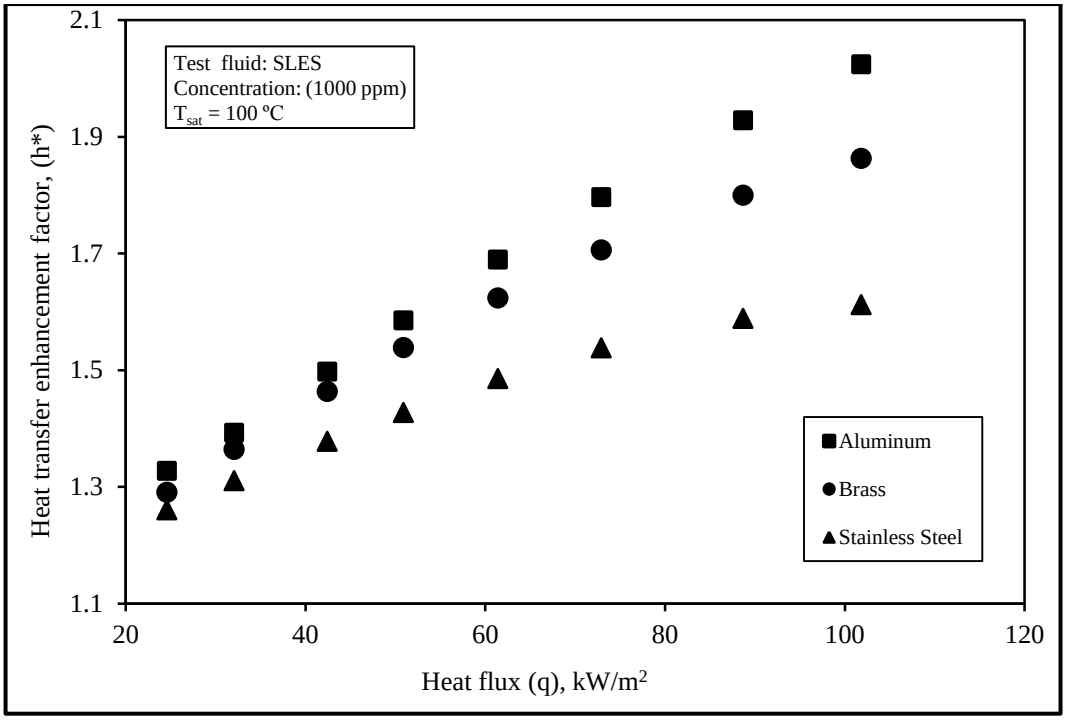


**Fig. 5.27: Comparison between the three test tubes at constant concentrations of 1000 ppm SLES**

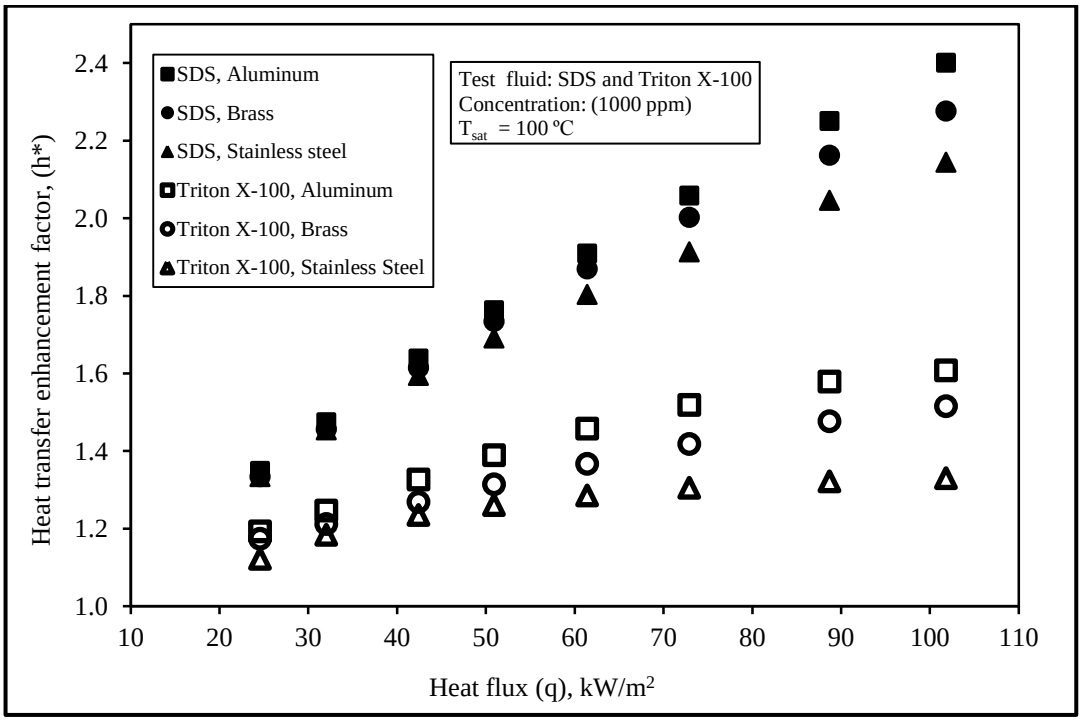


**Fig.5.28: Comparison between the three test tubes at constant concentrations of 1000 ppm SDS and Triton X-100**

Figure 5.29 show the influence of tube material on the variation of h* with the concentration, C of aqueous SLES solution at constant heat flux (= 101.9kW/$m^2$). The data ensure that aluminum test tube is the pioneer due to its better thermophsical properties. Also, the data presented in Figure 5.30. For SDS and Triton X-100 aqueous solutions ensure the same fact.

On the other side, Figure 5.31 reveals the influence of test tube material on the size distribution function of the active nucleation sites, using aqueous SLES solution with concentration 1000 ppm. It is indicated that aluminum test tube gives the highest N/A for any given value for $r_c$. So, h* for aluminum tube is always the pioneer. The data presented in Figure 5.32 ensure the same fact when using SDS and Triton X-100 aqueous solution.

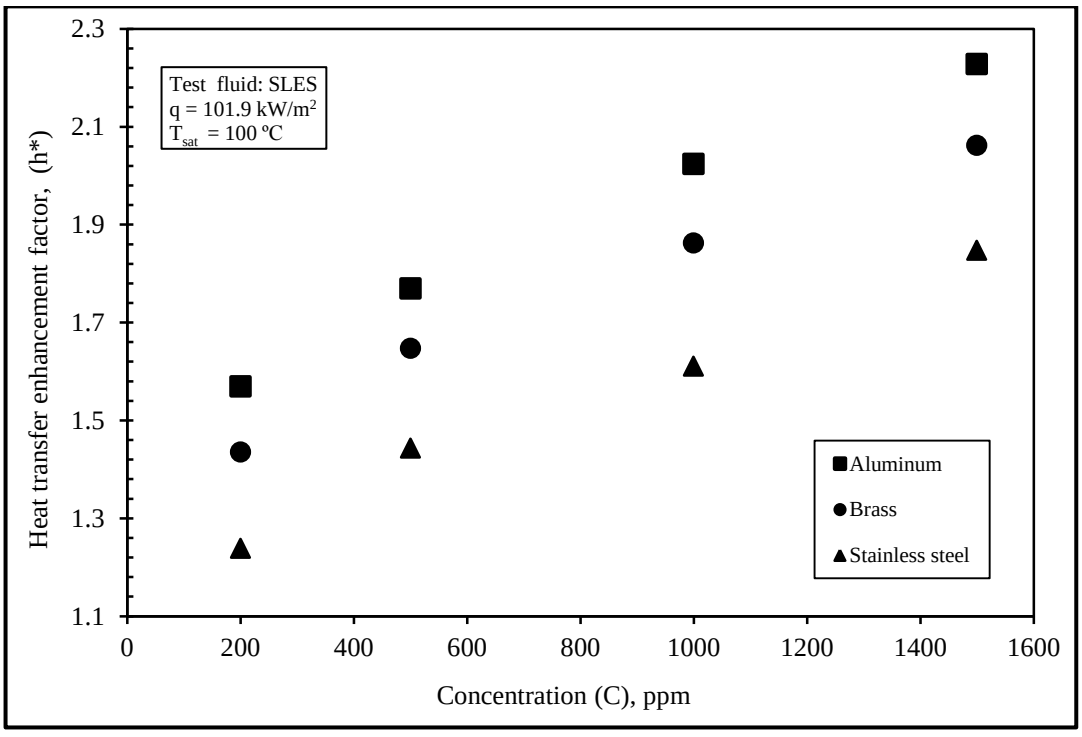


**Fig. 5.29: Effect of the wall heat flux 101.9 kW/$m^2$ on the variation of h* with SLES aqueous solution concentration for the three test tubes**

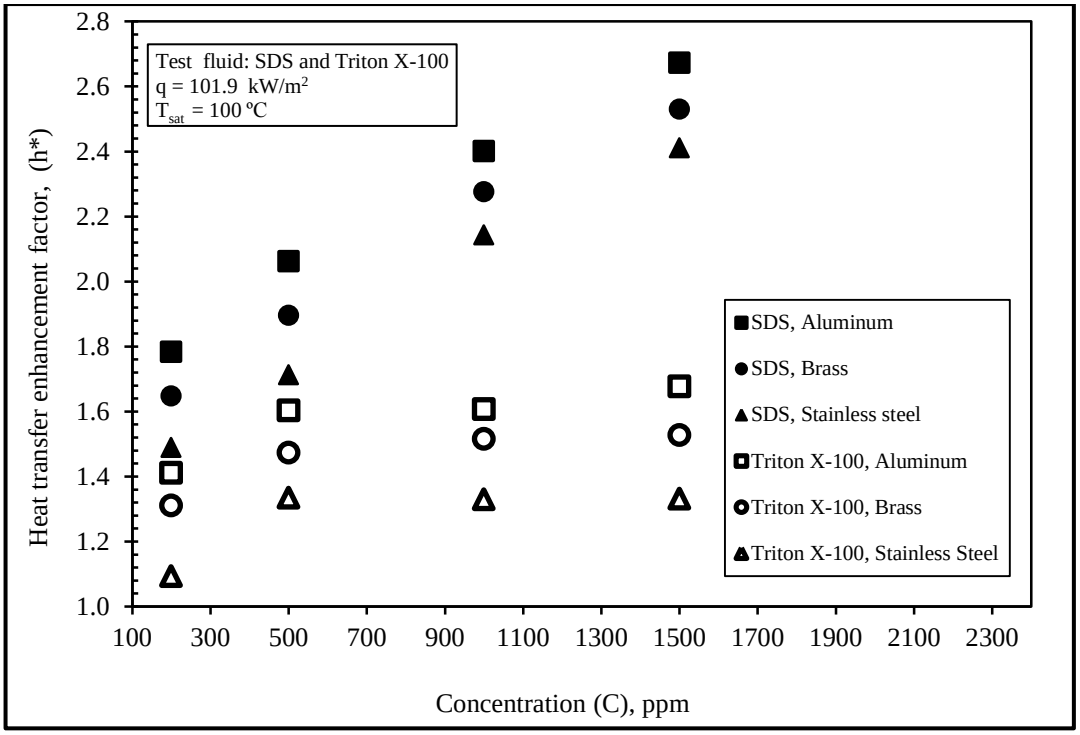


**Fig. 5.30: Effect of the wall heat flux 101.9 kW/m$^2$ on the variation of h* with SDS and Triton X-100 aqueous solutions concentration for the three test tubes**

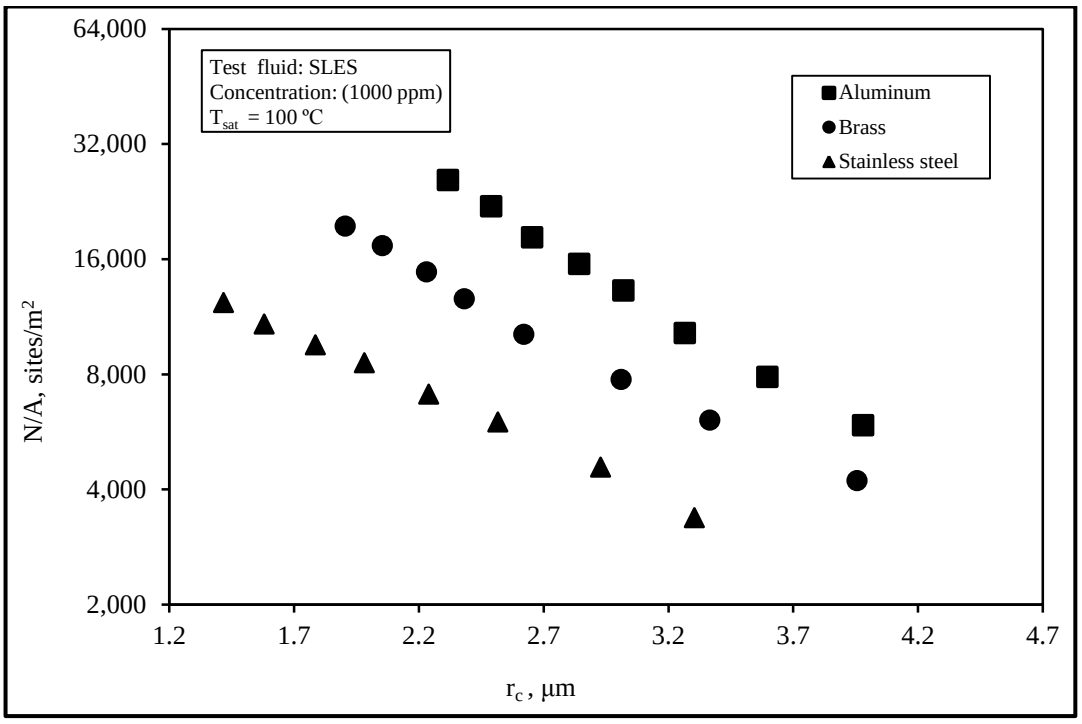


**Fig. 5.31: Effect of size distribution functions for three test tubes using constant concentration 1000 ppm of SLES aqueous solution**

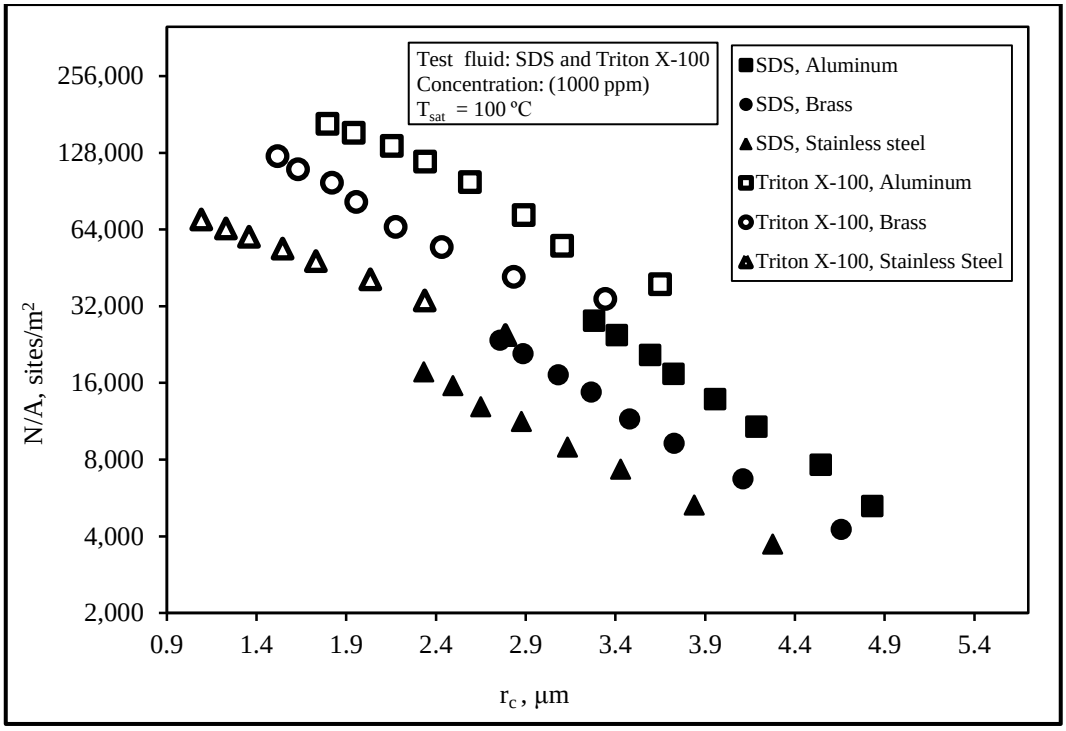


**Fig. 5.32: Effect of size distribution functions for three test tubes using constant concentration 1000 ppm of SDS and Triton X-100 aqueous solutions**

## 5.9. Effect of test tube material on the size distribution function's constants

In Figure 5.18, the effect of test tube material on the exponent m, with C, uses the three aqueous surfactant solutions (SDS, SLES and Triton X-100). It seems that the exponent m of the present results is not affected by the material of the test tubes, the aqueous surfactant solutions type and its concentrations. It could be concluded that the exponent m may be considered as a constant equal to unity.

In Figure 5.33, the effect of test tube material on the variation of $r_{st}$ with C is shown, using aqueous SLES solution. It is shown that for any given concentration; $r_{st}$ value for aluminum tube is the highest. This fact ensures that aluminum tube introduces higher N/A and h*. On the

contrary, Figure 5.34 indicates that $r_{st}$ values for stainless steel tube with Triton X-100, followed by brass and then aluminum tubes.

In addition, Figure 5.35 shows the variation of the constant $N_{max}/A$ with C using aqueous SLES solution. A comparison is made between the three test tube materials. It is clear that for any given concentration; $N_{max}/A$ value for aluminum test tube is the highest. This fact agrees with the data of Figure 5.33.

Also, Figure 5.36 ensures the data present in Figure 5.34, in the sense that stainless steel tube with Triton X-100, using any given concentration; introduces the highest $N_{max}/A$ values.

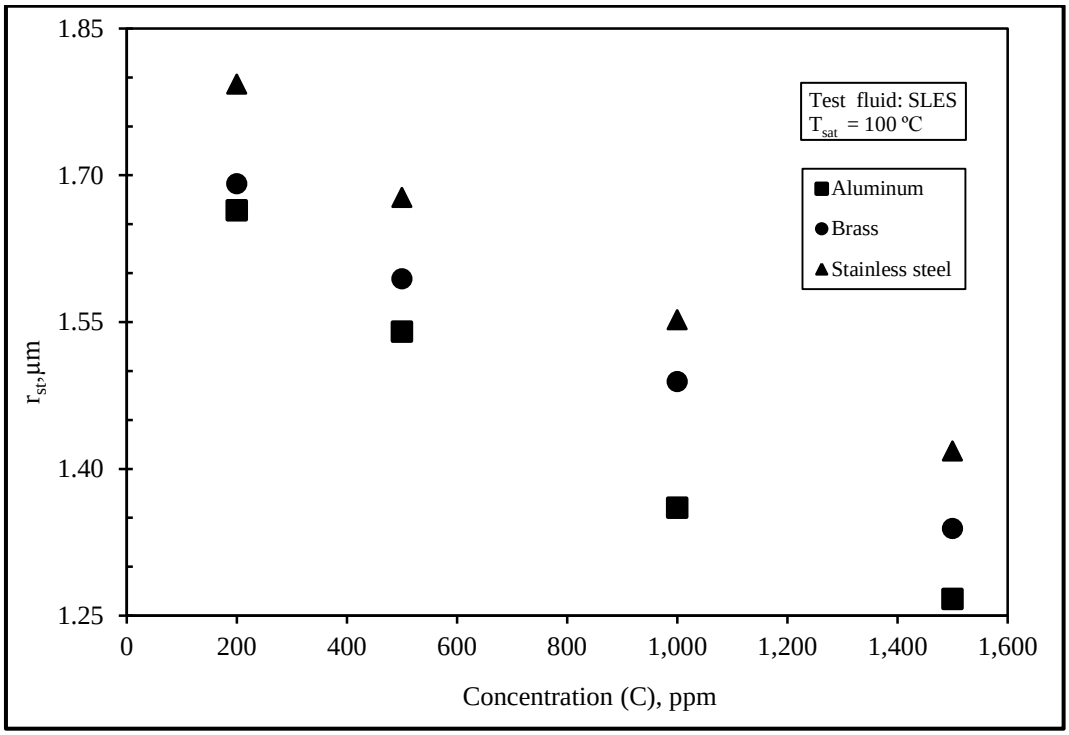


**Fig. 5.33: Effect of SLES on the variation of size distribution function constant $r_{st}$ with the concentration for the three test tubes**

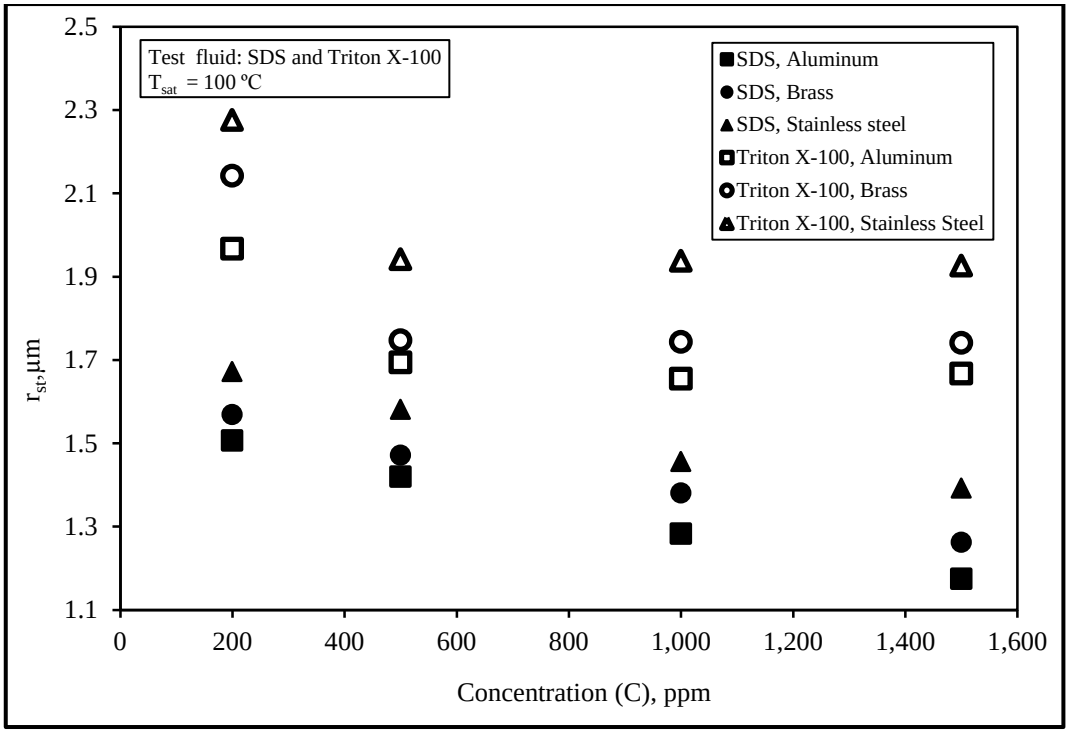


**Fig. 5.34: Effect of SDS and Triton X-100 on the variation of size distribution function constant $r_{st}$ with the concentration for the three test tubes**

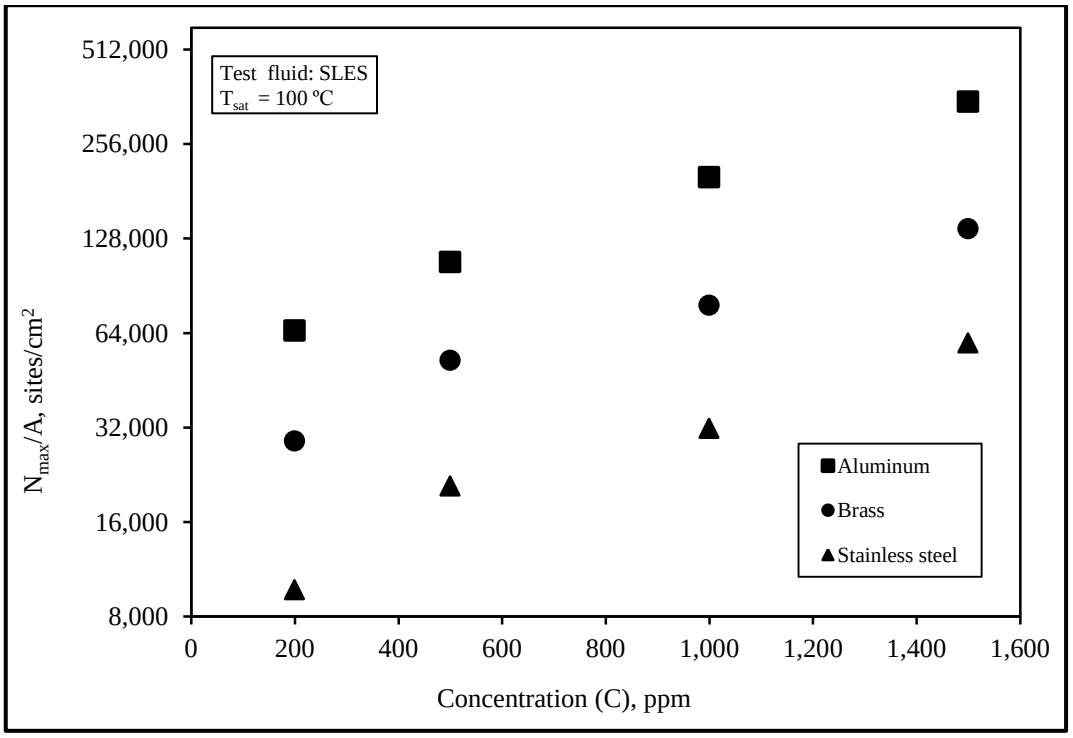


**Fig. 5.35: Effect of SLES on the variation of size distribution function constant $N_{max}/A$ with the concentration for the three test tubes**

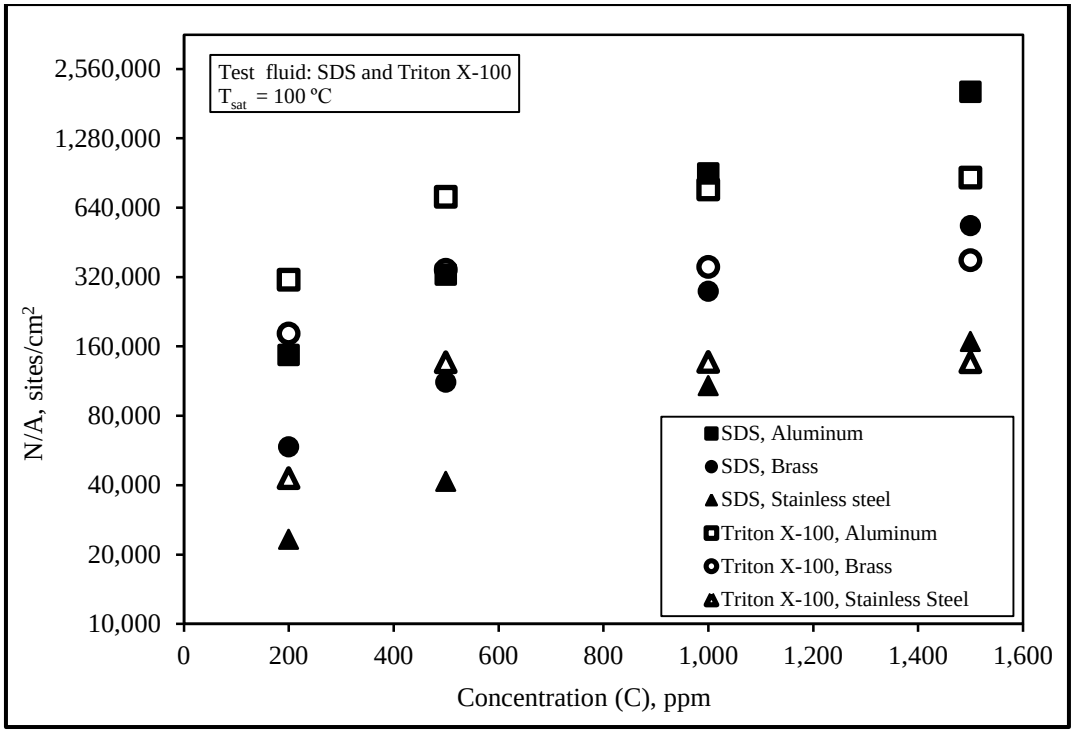


**Fig. 5.36: Effect of SDS and Triton X-100 on the variation of size distribution function constant N/A with the concentration for the three test tubes**

## 5.10. Correlation of the wall heat flux with ΔT and N/A

The present experimental data confirm that there is a substantial influence of wall heat flux, q, type of surfactant and concentration of aqueous surfactant solution, C on the degree of superheat, ΔT and the nucleation site density, N/A. ΔT is the driving force which is responsible for the initiation of vapor bubbles so as to control N/A. It is found that higher N/A causes higher heat transfer coefficients. The modeling efforts to data necessitate knowledge of how the bubble frequency, bubble departure diameter and N/A vary with q and ΔT. Different dependencies of q on ΔT and N/A are found that they can be correlated using the following formula;

$$q = y.\ \Delta T^{a}.(N/A)^{b} \qquad 5\text{-}2$$

Previous published data, such as those of Tien [78] and Zuber [79], support that ‘a’ lies somewhere between 1.0 and 1.8, while ‘b’ is

between 0.3 and 0.5. The exact values of these exponents in the power law relation, Eq. 5.2 proceeds to be an interesting subject. The present experimental data assure that the constant ‘c’ and the exponents ‘a’ and ‘b’ in Eq. 5.2 are functions of thermophysical properties of the boiling aqueous surfactant solution, concentration of the aqueous solution, type of surfactant and test tube material. For that situation, Eq. 5.2 accommodated to associate all the relevant parameters, to be applicable for all pool boiling conditions.

Based on the present experimental data, the constants of the Eq. 5.2 for the three test tubes with different concentrations of the three aqueous surfactant solutions are in Table 5.3.

**Table 5.3: Values of constants(y, a and b) for the three test tubes with the three aqueous surfactant solutions**

| Test tube | Test fluid | Concentration, ppm | y | a | b |
|---|---|---|---|---|---|
| Brass , S1 | water | | 337.35993 | 1.233649 | 0.204095 |
| | Triton X-100 | 200 | 3.432146 | 1.14060 | 0.615652 |
| | | 500 | 22.47057 | 1.21104 | 0.433143 |
| | | 1000 | 43.32210 | 1.36533 | 0.341371 |
| | | 1500 | 55.85512 | 1.41258 | 0.308902 |
| | SLES | 200 | 332.70010 | 1.601563 | 0.132754 |
| | | 500 | 199.77615 | 1.683012 | 0.181926 |
| | | 1000 | 143.36106 | 1.72794 | 0.218682 |
| | | 1500 | 69.68407 | 1.783599 | 0.289976 |
| | SDS | 200 | 230.22948 | 1.974865 | 0.085330 |
| | | 500 | 125.41611 | 2.066899 | 0.150957 |
| | | 1000 | 53.95856 | 2.540887 | 0.155961 |
| | | 1500 | 42.82638 | 3.140567 | 0.069439 |

| Test tube | Test fluid | Concentration, ppm | y | a | b |
|---|---|---|---|---|---|
| Aluminum, S2 | water | | 274.48728 | 1.26357 | 0.21983 |
| | Triton X-100 | 200 | 3.75814 | 1.31166 | 0.573176 |
| | | 500 | 15.24739 | 1.28813 | 0.454778 |
| | | 1000 | 25.99852 | 1.32290 | 0.403156 |
| | | 1500 | 34.42610 | 1.46974 | 0.351217 |
| | SLES | 200 | 92.06963 | 1.54959 | 0.309684 |
| | | 500 | 76.08011 | 1.69510 | 0.301741 |
| | | 1000 | 44.59073 | 2.01571 | 0.292866 |
| | | 1500 | 39.67995 | 2.19331 | 0.278483 |
| | SDS | 200 | 64.61089 | 1.74441 | 0.310633 |
| | | 500 | 50.31347 | 2.33965 | 0.211940 |
| | | 1000 | 21.14324 | 3.182666 | 0.14615 |
| | | 1500 | 11.19348 | 4.223313 | 0.028302 |
| Stainless Steel, S3 | water | | 793.87724 | 1.29796 | 0.075775 |
| | Triton X-100 | 200 | 348.84749 | 1.26704 | 0.159175 |
| | | 500 | 188.46231 | 1.28666 | 0.217447 |
| | | 1000 | 134.30348 | 1.25905 | 0.256730 |
| | | 1500 | 92.03092 | 1.20990 | 0.303964 |
| | SLES | 200 | 351.67825 | 1.26216 | 0.212395 |
| | | 500 | 197.41259 | 1.24807 | 0.288637 |
| | | 1000 | 97.36922 | 1.23257 | 0.372001 |
| | | 1500 | 61.74230 | 1.24684 | 0.427977 |
| | SDS | 200 | 200.46395 | 1.31732 | 0.270163 |
| | | 500 | 225.13379 | 1.602181 | 0.182288 |
| | | 1000 | 236.3473 | 2.593056 | -0.04919 |
| | | 1500 | 279.1606 | 3.131828 | -0.16653 |

Based on the present experimental data, the correlation of heat flux q with ΔT and N/A. Take the following form;

### 5.10.1. Correlation for brass test tube with the three aqueous surfactant solutions

#### i. Brass with Triton X-100

$$q = y.\ \Delta T^{a}.(N/A)^{b}$$

where,

$$y = -0.00002024C^{2} + 0.0744C - 10.316$$

$$a = -0.00000011C^{2} + 0.000406C + 1.0546$$

$$b = 3.808(C)^{-0.3466}$$

#### ii. Brass with SLES

$$y = -125.1*\ln(C) + 991.04$$

$$a = 0.0866*\ln(C) + 1.142$$

$$b = 0.0001147C + 0.11401$$

#### iii. Brass with SDS

$$y = 24{,}576.4(C)^{-0.8713}$$

$$a = 0.0000004C^{2} + 0.000169C + 1.907$$

$$b = -0.0000002C^{2} + 0.00034C + 0.02776$$

### 5.10.2. Correlation for aluminum test tube with the three aqueous surfactant solutions

#### i. Aluminum with Triton X-100

$$y = 0.0000102C^{2} + 0.0404C - 3.425$$

$$a = 0.0000002C^{2} + 0.000238C + 1.352$$

$$b = 1.978(C)^{\mathbf{-0.2343}}$$

**ii. Aluminum with SLES**

$y = 0.000031C^2 - 0.095C + 111.8$

$a = -0.000000115C^2 + 0.000719C + 1.396$

$b = -0.00000004C^2 - 0.0000172C + 0.313$

**iii. Aluminum with SDS**

$y = 0.0000208C^2 - 0.078C + 80.97$

$a = 0.000000133C^2 + 0.00165C + 1.43$

$b = 0.000000016C^2 - 0.00023C + 0.346$

### 5.10.3. Correlation for stainless steel test tube with the three aqueous surfactant solutions

**i. Stainless Steel with Triton X-100**

$y = 10241.28(C)^{-0.638}$

$a = -0.00000008C^2 + 0.000088C + 1.256$

$b = 0.0307(C)^{0.3115}$

**ii. Stainless Steel with SLES**

$y = 0.0002188C^2 - 0.59C + 452.21$

$a = 0.000000046C^2 - 0.000091C + 1.28$

$b = -0.000000083C^2 + 0.0003C + 0.16$

**iii. Stainless Steel with SDS**

$y = 0.0000161C^2 + 0.0284C + 198.28$

$a = -0.000000155C^2 + 0.00174C + 0.911$

$b = 0.000000078C^2 - 0.0004834C + 0.377$

## 5.11. Verification of the new correlation (Eq.5.2) with the present experimental data

In order to examine the validity of the new correlation to be applied in pool boiling data of aqueous surfactant solutions, Figures 5.37 through 5.39 introduce verification for the new correlation with the present experimental data.

Figure 5.37 shows presentation of the new correlation. The experimental data of aluminum test tube, S1, is using the different concentrations of the three test surfactants (SDS, SLES and Triton X-100). Good agreement is noticed between the correlation and the experimental data. Also, it is noticed that the experimental data of Triton X-100 with concentrations above 500 ppm are collected together. This is because above this concentration; there is no enhancement in the heat transfer coefficient.

Figure 5.38 shows a comparison between the correlation and the experimental data of brass test tube, S2 using the different concentrations of the three test aqueous solutions. The diagrams of this Figure indicate good agreement between the correlation and the experimental data.

Figure 5.39 indicates the same comparison for the stainless steel test tube, S3. Also, good agreement is noticed between the correlation and the present experimental data.

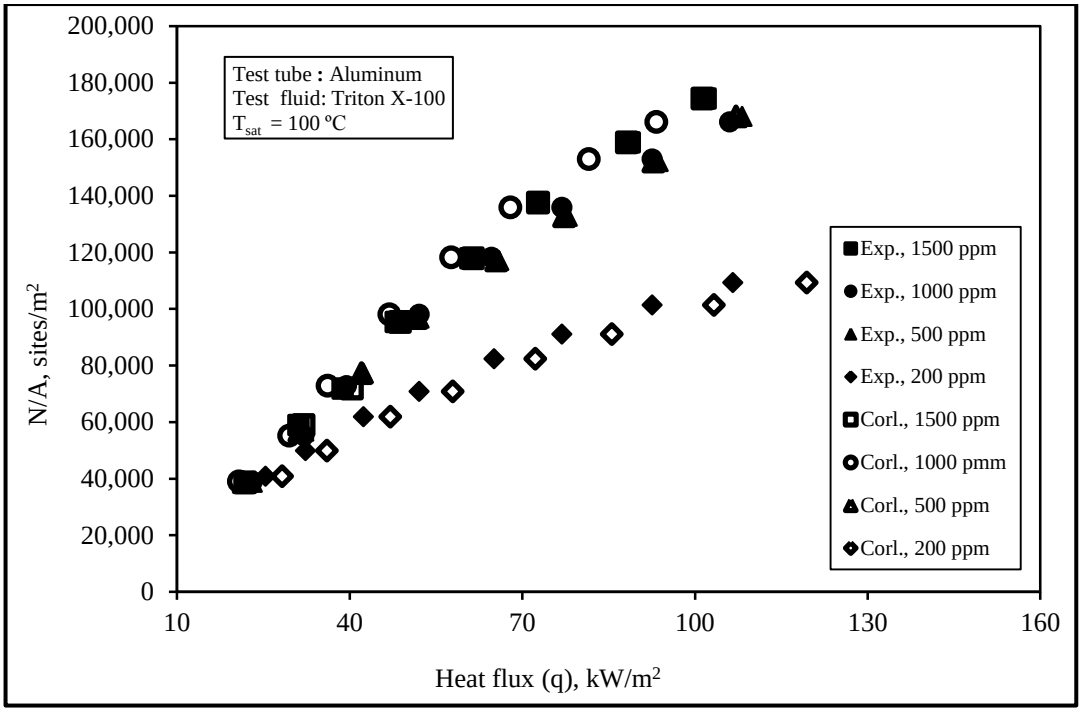


**Fig. 5.37a: Verification of the new correlation with the experimental data of aluminum test tube using Triton X-100 aqueous solution**

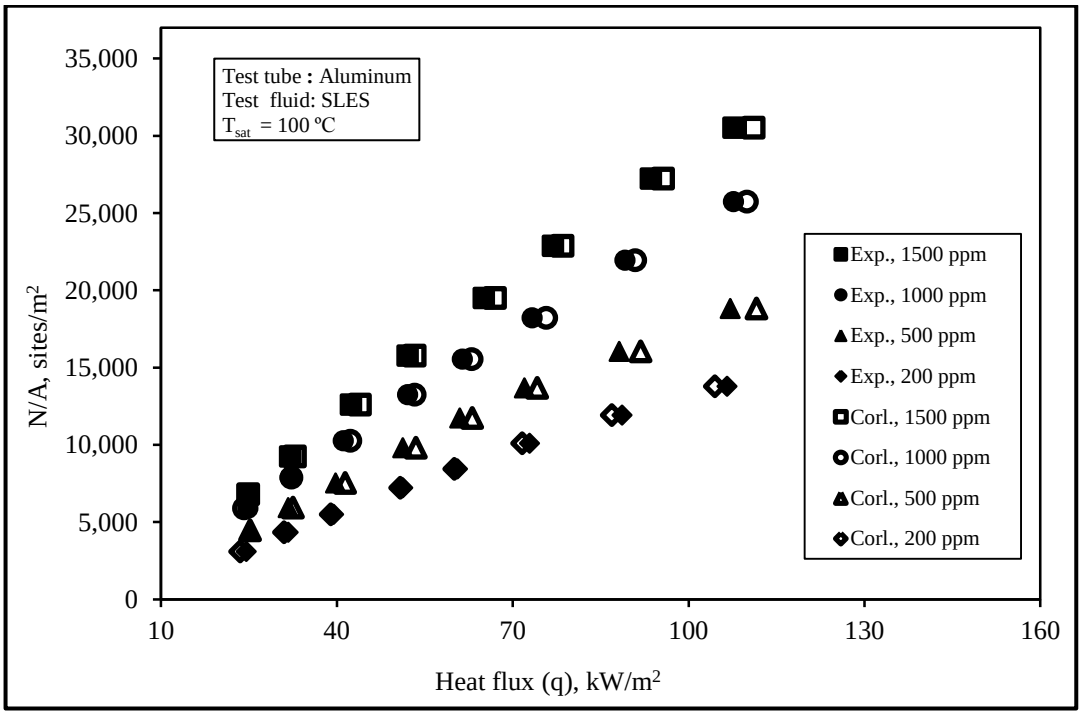


**Fig. 5.37b: Verification of the new correlation with the experimental data of aluminum test tube using SLES aqueous solution**

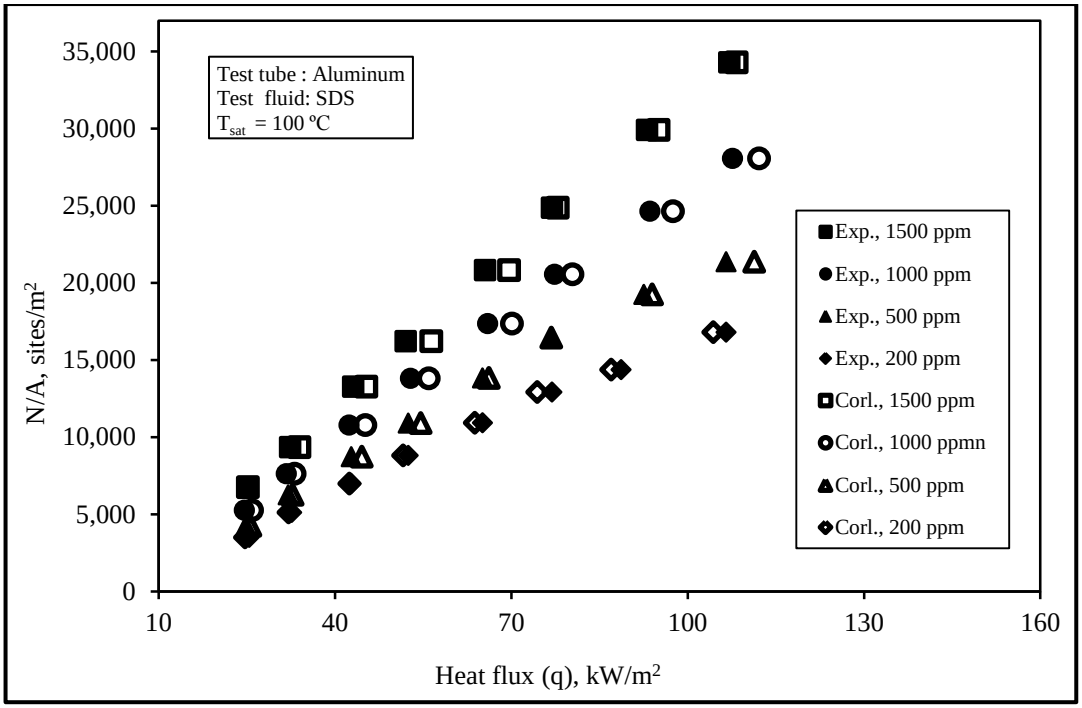


**Fig. 5.37c: Verification of the new correlation with the experimental data of aluminum test tube using SDS aqueous solution**

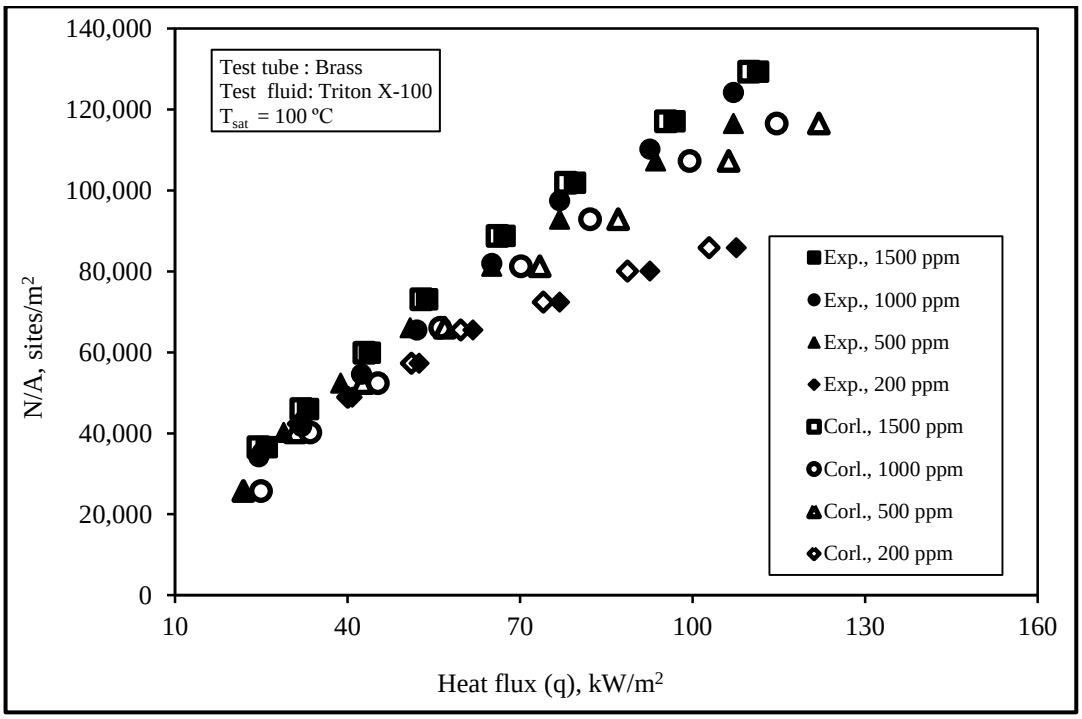


**Fig. 5.38a: Verification of the new correlation with the experimental data of brass test tube using Triton X-100 aqueous solution**

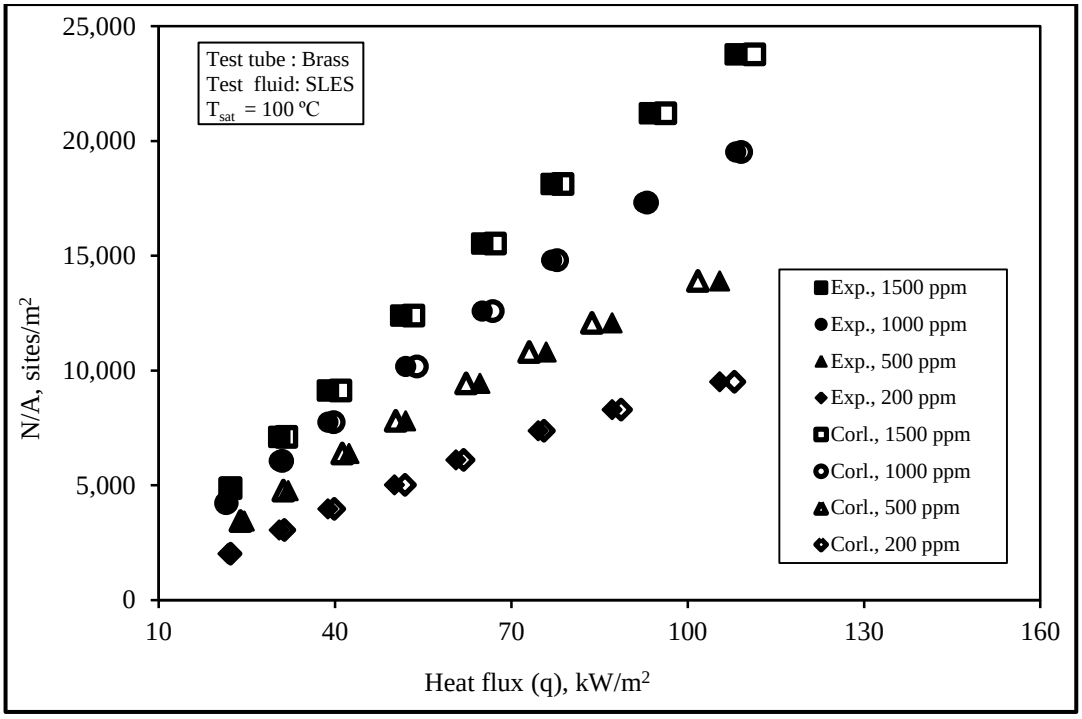


**Fig. 5.38b: Verification of the new correlation with the experimental data of brass test tube using SLES aqueous solution**

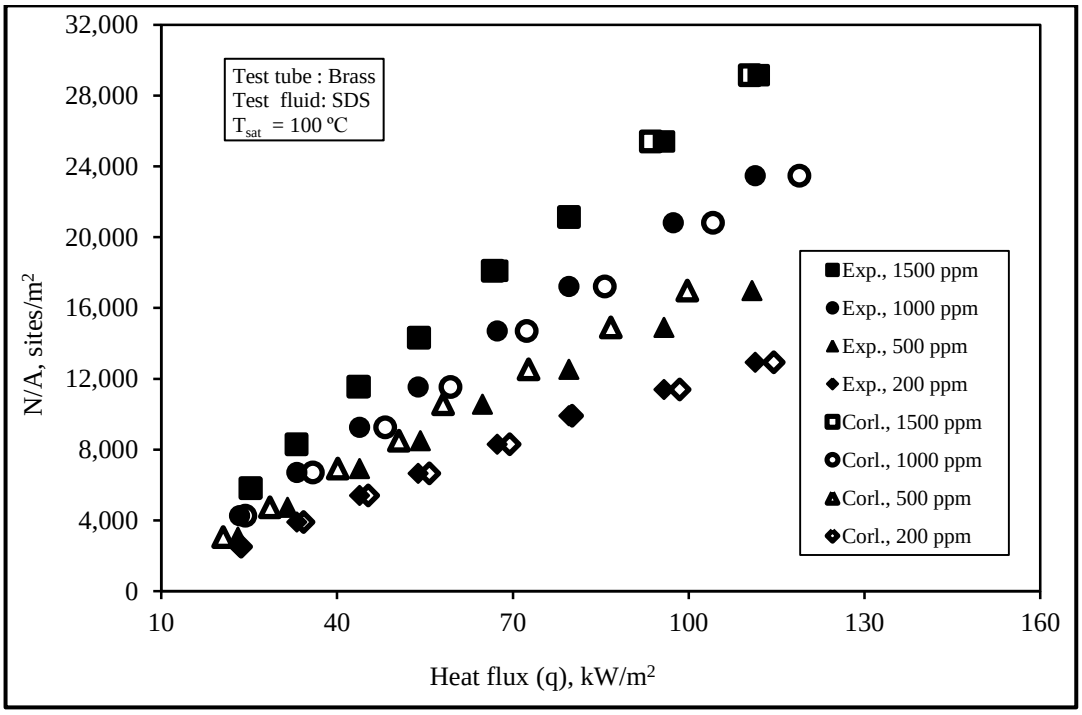


**Fig. 5.38c: Verification of the new correlation with the experimental data of brass test tube using SDS aqueous solution**

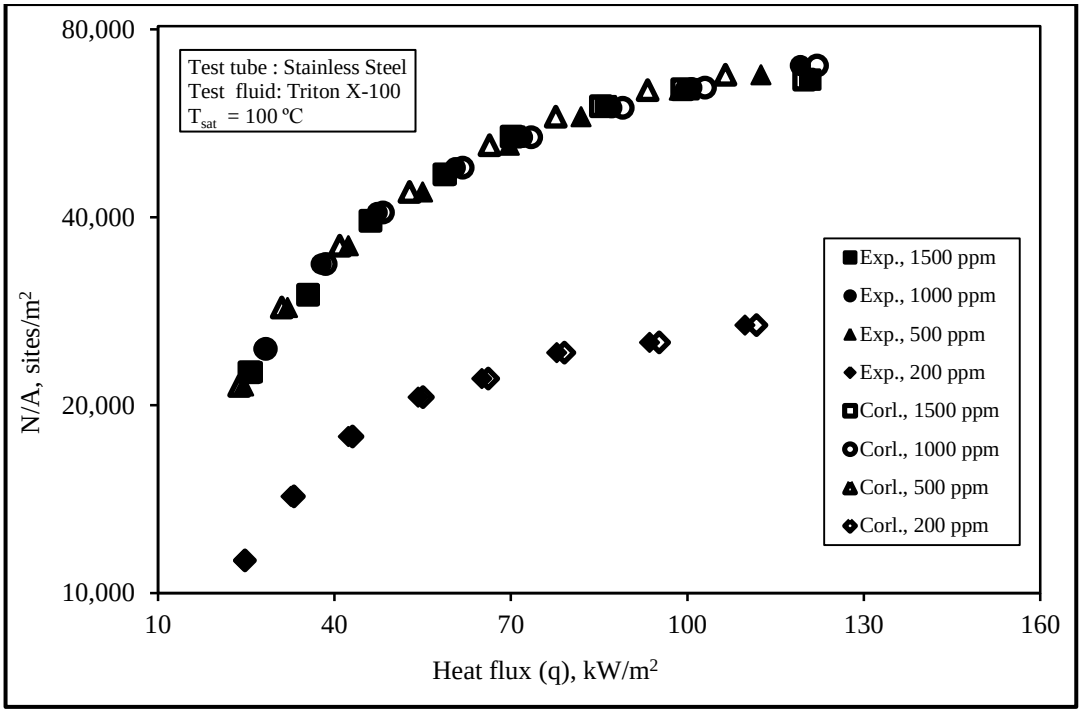


**Fig. 5.39a: Verification of the new correlation with the experimental data of stainless steel test tube using Triton X-100 aqueous solution**

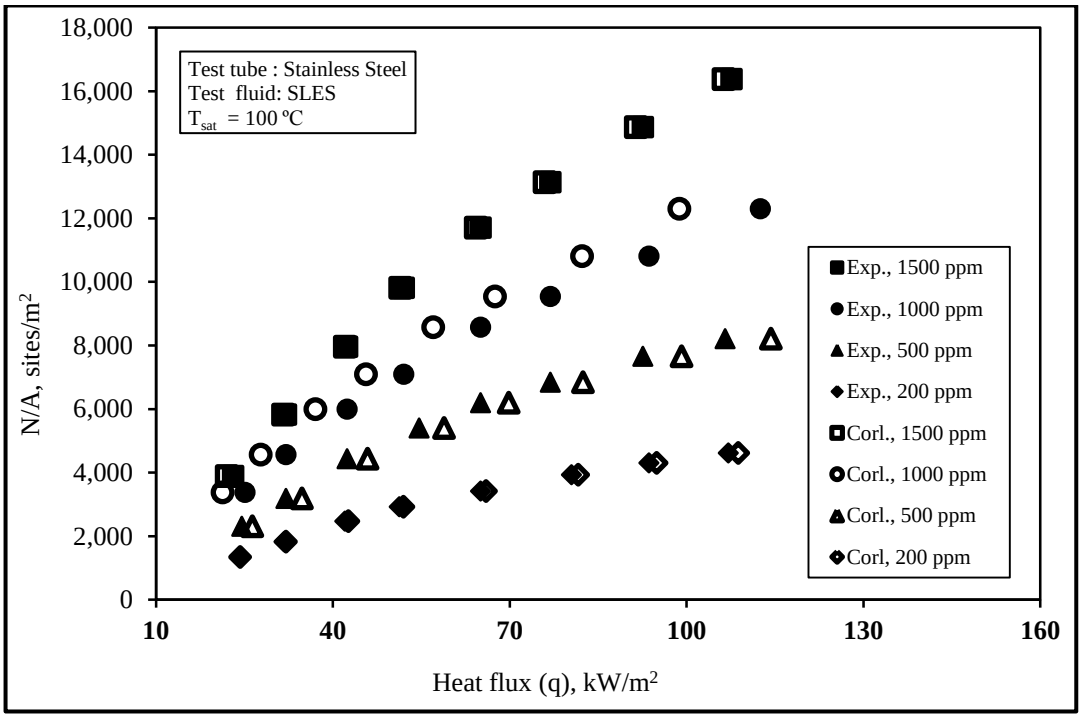


**Fig. 5.39b: Verification of the new correlation with the experimental data of stainless steel test tube using SLES aqueous solution**

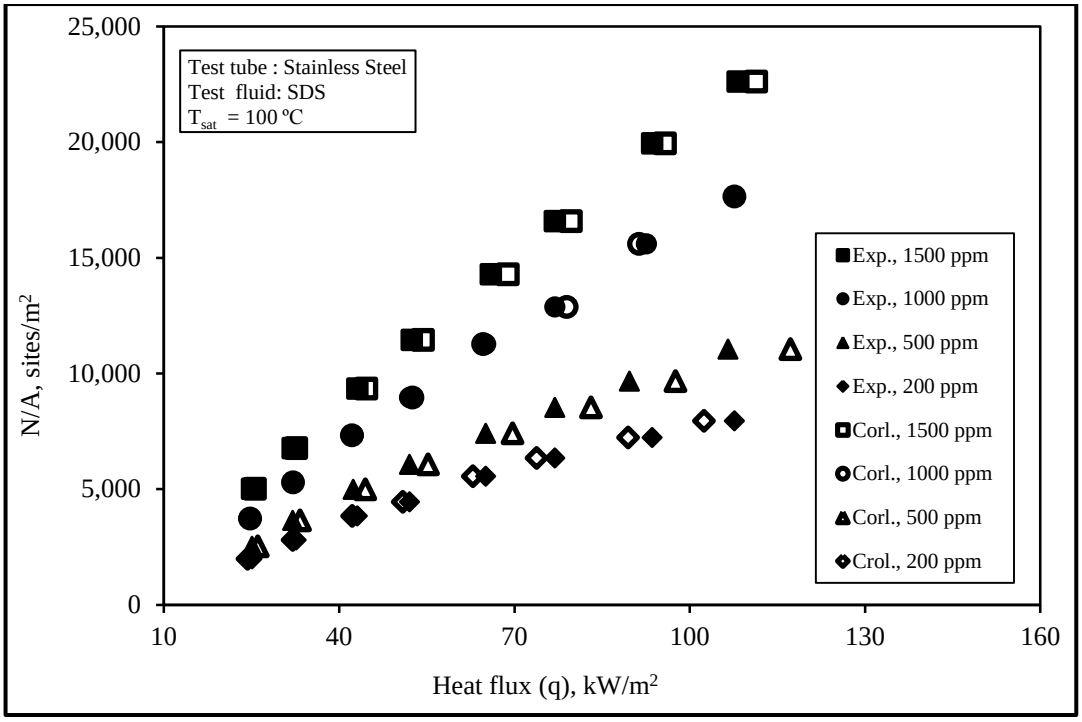


**Fig. 5.39c: Verification of the new correlation with the experimental data of stainless steel test tube using SDS aqueous solution**

## 5.12. Comparison between the present experimental data with the available published data

Figure 5.40 reveals a comparison between the present experimental data of aluminum test tube, S1 using aqueous SDS solutions with concentrations 200 ppm and 500 ppm those of Ref. [48]. Fair agreement is noticed between the two situations. The discrepancy between the present data and those of Ref. [48], may be related to the fact that the data of Ref. [48] is obtained from aluminum plate, so, the configuration of the test boiling surface is different from the present one.

On the other hand, Figure 5.41 introduces the same comparison for aqueous Triton X-100 solution with concentration 500 ppm. Fair agreement is noticed between the present and published data. The reason for the noticed discrepancy is related to the different in boiling surface configuration.

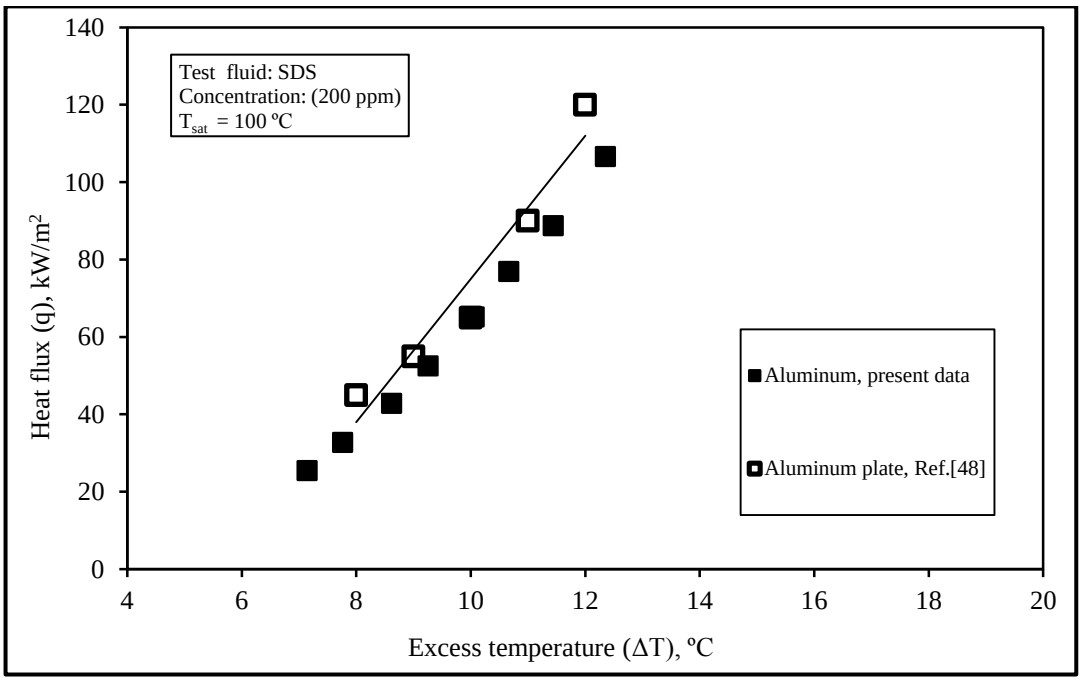


**Fig. 5.40a: Comparison between the present experimental data for SDS solution at 200 ppm concentration with the data of Ref. [48]**

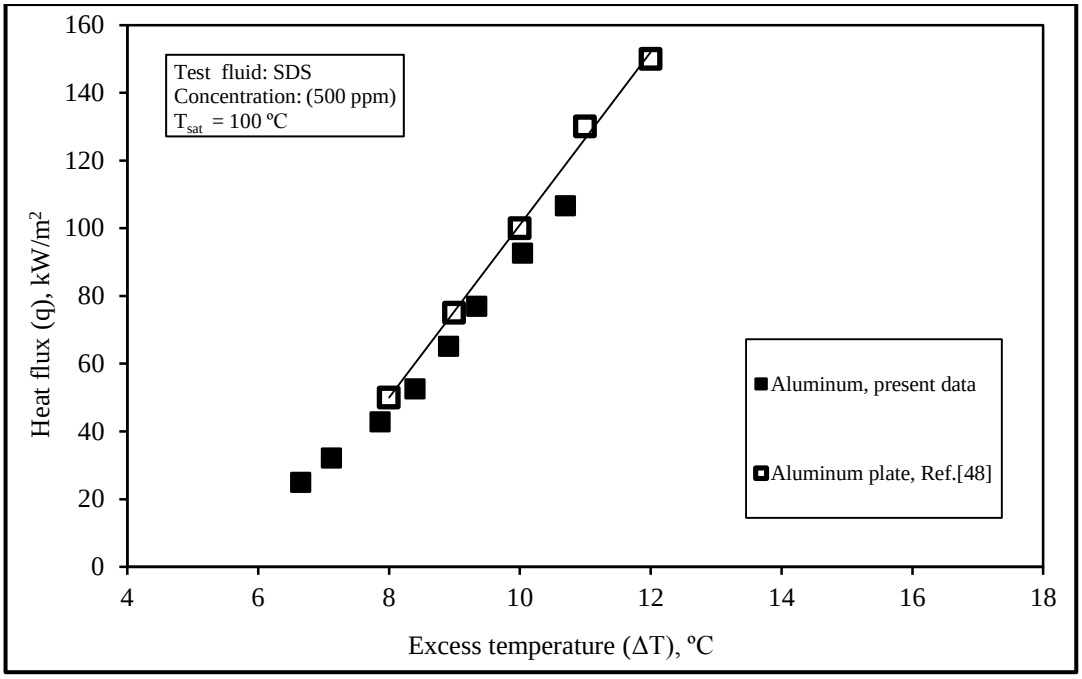


**Fig. 5.40b: Comparison between the present experimental data for SDS solution at 500 ppm concentration with the data of Ref. [48]**

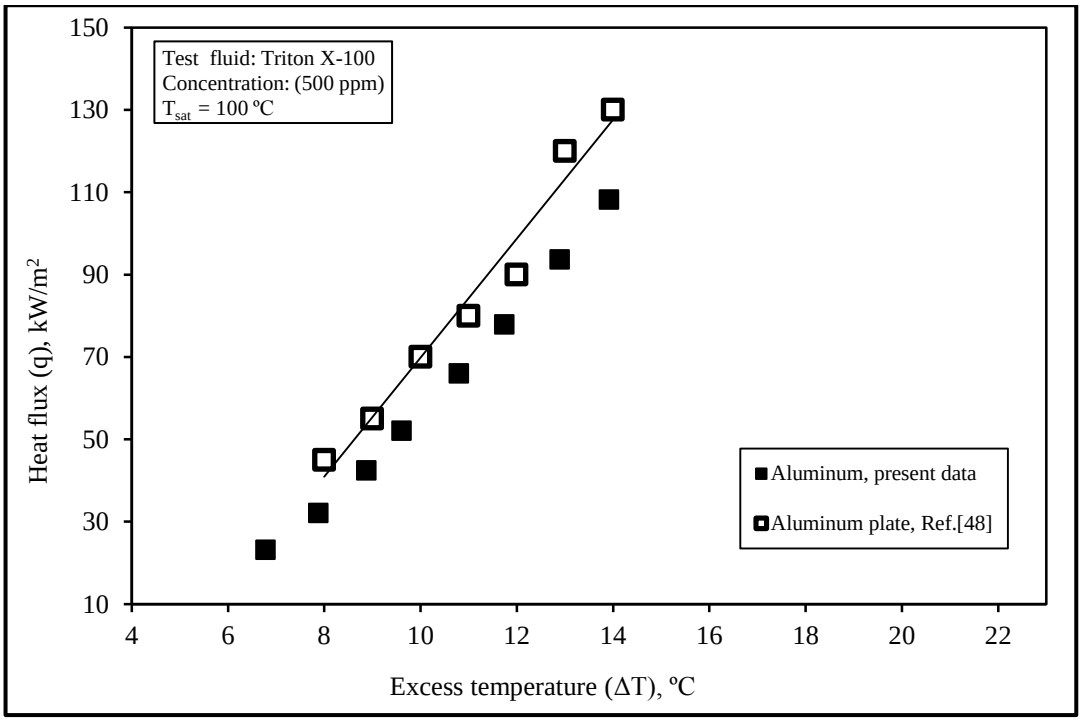


**Fig. 5.41: Comparison between the present experimental data for Triton X-100 solution at 500 ppm concentration with the data of Ref. [48]**